TECHNISCHE UNIVERSITÄT DARMSTADT

ROLE OF INTERDOMAIN AND INTERSUBUNIT CONTACTS FOR NMDA RECEPTOR FUNCTION

Vom Fachbereich Biologie der Technischen Universität Darmstadt

zur

Erlangung des akademischen Grades eines Doctor rerum naturalium

genehmigte Dissertation von

Dipl Bioinf. Ceyhun Tamer

aus Offenbach am Main

Berichterstatter (1. Referent): Prof.Dr. Bodo Laube

Mitberichterstatter (2. Referent): Prof.Dr. Kay Hamacher

Tag der Einreichung: 29. Juni 2012

Tag der mündlichen Prüfung: 31. August 2012

Darmstadt 2012

(D 17)

„Our greatest weakness lies in giving up. The most certain way to succeed is always to try just one more time.“

Thomas A. Edison

Table of contents **3**

CHAPTER 1
GENERAL INTRODUCTION

Ionotropic receptors mediate cell-cell communication

Communication between cells is generally achieved via signal molecules or ions. Nerve cells are specialized cells that contact other cells through so-called ‚synapses'. A synapse is formed by a presynaptic terminal where signal molecules, i.e. neurotransmitters, are released and a post-synaptic terminal where the neurotransmitters bind to specialized, membrane-bound proteins. These proteins are classified according to their respective biochemical reaction, i) metabotropic receptors, which induce secondary signal mechanisms that trigger a range of intracellular events, and ii) ionotropic receptors, which, upon ligand binding, open a channel that allows ions such as Na^+, K^+ or Cl^- to flow along their electrochemical gradient. In contrast, so-called ion channels are proteins that are activated e.g. by voltage changes, pH changes or mechanical stretch. Ion channels and ionotropic receptors are membrane-associated, oligomeric proteins and the ion channel pore is located in the membrane-domain. But only ionotropic receptors have an extracellular domain (ECD) where ligands can bind. Binding of a ligand to the ECD induces rearrangements in the protein that lead to the opening of the inherent ion channel (Mayer, 2006). Such receptors are involved in fast signal transmission as their operating time scale is in the range of a few milliseconds compared to seconds or minutes in metabotropic receptors (Kandel, 2000). Ionotropic receptors or their evolutionary ancestor proteins can be found throughout all life forms, e.g. bacteria, plants, insects, fish, birds, amphibians, reptiles and mammals. Their significance for cell-cell communication becomes apparent when mutations in the respective genes cause so-called channelopathies. Channelopathies are disorders or pathophysiological conditions that are caused by a mutation in an ion channel or ionotropic receptor. Examples for channelopathies caused by mutations in ionotropic receptors are, hyperekplexia or startle disease (Shiang et al., 1993), different forms of epilepsy (Steinlein et al., 1995, De Fusco et al., 2000, Baulac et al., 2001, Wallace et al., 2001, Endele et al., 2010), congenital myasthenic syndrome (Engel et al., 1993) or mental retardation (Endele et al., 2010). Additionally, ionotropic receptors are implicated in numerous neurological diseases such as, Alzheimer's, Parkinson's or Huntington's (Dingledine et al., 1999, Wu et al., 2006). In order to develop

treatment for such disorders it is essential to gain insight into the structure and function of these proteins.

Ligand-gated ion channels (LGICs), a subtype of ionotropic receptors

LGICs belong to the class of ionotropic receptors and are comprised of three superfamilies, the pentameric Cys-loop receptors, the tetrameric ionotropic glutamate receptors (iGluRs) and the trimeric ATP-gated channels (P2X receptors). Receptors are generally classified according to a specific ligand that activates the respective receptor type. However, all these receptors have a common basic structure of an extracellular domain (ECD), a transmembrane domain (TMD) and an intra-/extracellular C-terminal domain (CTD). Families within the Cys-loop receptor superfamily are nicotinic acetylcholine receptors (nAchRs), glycine receptors (GlyRs), γ-amino butyric acid type A receptors ($GABA_A$Rs) and serotonin type 3 receptors (5-HT_3 receptors). These receptors form pentameric complexes, the binding pocket for ligands is located in the interface between the ECDs of two neighboring subunits, the transmembrane domain of each subunit is formed by four transmembrane helices (TM1-TM4) and the TM2s in the pentamer are lining the ion channel pore and the CTD lies extracellular. Interestingly, nAChRs and 5-HT_3 receptors are cationic channels and lead to depolarization of the post-synaptic potential, whereas GlyRs and $GABA_A$Rs are anionic channels and lead to hyperpolarization. Cys-loop receptors represent an interesting pharmacological target as anesthetics, steroids and benzodiazepines act via modulation of $GABA_A$ or glycine receptor function (Thurmon et al., 1996a, Maksay et al., 2001, Thio et al., 2003, Garcia et al., 2010).

The *N*-methyl-D-aspartate receptors (NMDARs), (RS)-2-amino-3-(3-hydroxy-5-methyl-4-isoxazolyl)propionic acid receptors (AMPARs) and kainate receptors (KARs) form three distinct subfamilies in the family of iGluRs. Commonly, iGluRs can be activated by glutamate, however, the efficiency of activation depends on the subunit composition of the receptor (Dingledine et al., 1999). In contrast to Cys-loop receptors, the respective subunits assemble to form tetrameric complexes (Sobolevsky et al., 2009). Ligand-binding occurs in the ECD but not between, but within subunits. The TMD is organized by three transmembrane domains (TM1, TM3 and TM4), the M2 domain is a re-rentrant loop that is not spanning the membrane. The CTD is located on the intracellular side of the membrane (Madden, 2002). IGluRs convey the majority of excitatory neurotransmission in the mammalian central

nervous system and as such they are also implicated in the glutamate-induced excitotoxicity (Dingledine et al., 1999). Excessive activation of iGluRs by glutamate leads to overexcitation of the cell, which drives the cell into apoptosis. This basic principle underlies many neurodegenerative disorders, e.g. Alzheimer's, Parkinson's, Huntington's and multiple sclerosis (Dingledine et al., 1999).

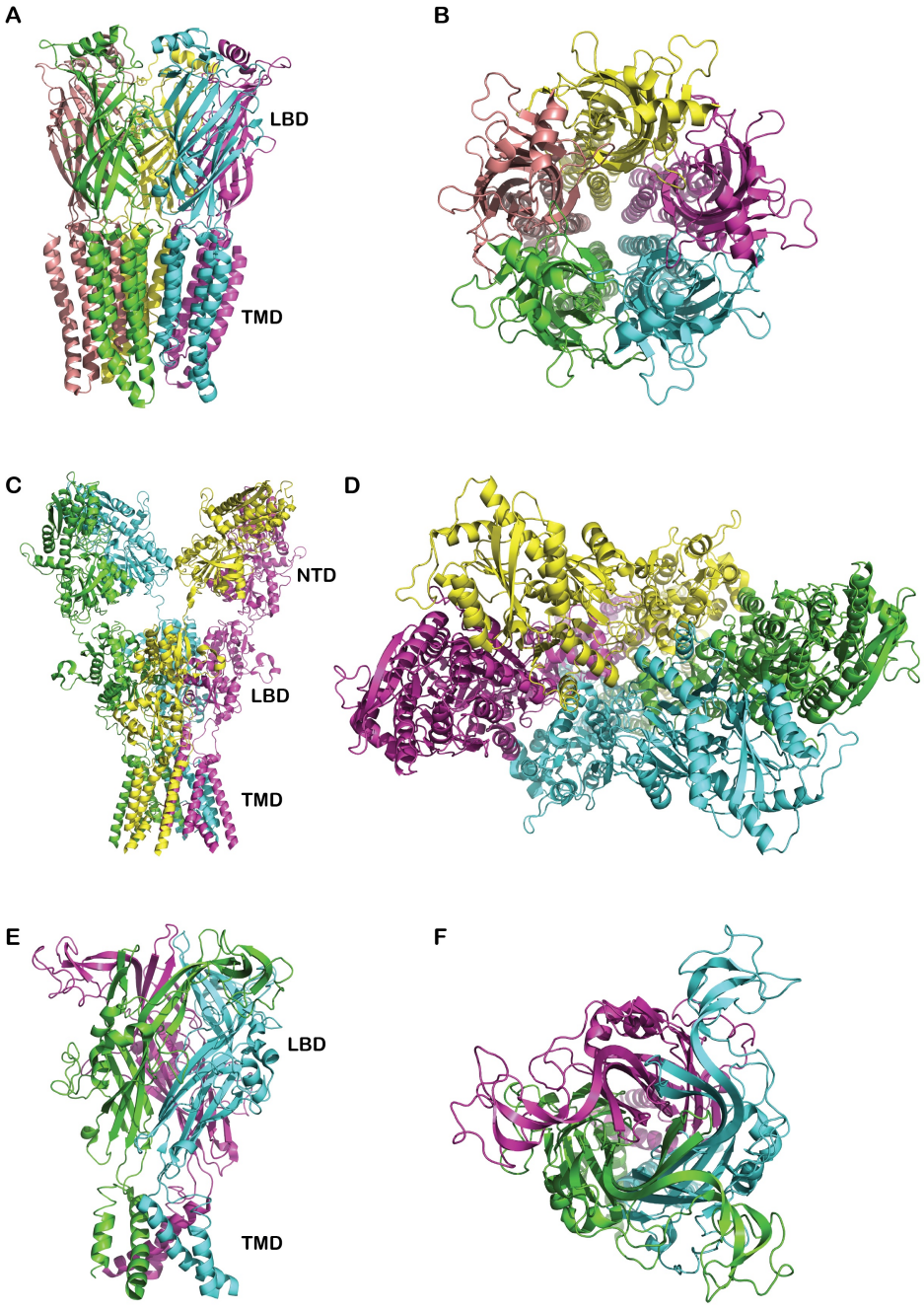

Fig. 1. Overview of the three superfamilies in LGICs. Cartoon representation of examples for Cys-loop receptors, iGluRs and P2X receptors. Each subunit is colored differently for a better overview. **(A-B)** Side/Top view of the pentameric GluCl crystal structure (PDB ID: 3RHW, Hibbs et al., 2011), which is an invertebrate Cys-loop receptor and is depicted here as a model for vertebrate Cys-loop receptors, **(C-D)** Crystal structure of the tetrameric GluA2-type AMPA receptor (PDB ID: 3KG2, Sobolevsky et al., 2009), **(E-F)** Crystal structure of the trimeric ATP-gated P2X4 receptor (PDB ID: 3I5D, Kawate et al., 2009).
LBD ligand-binding domain, NTD N-terminal domain, TMD transmembrane domain.

ATP-gated P2X receptors are cationic channels and have only two transmembrane domains (TM1, TM2), the N- and C-termini are intracellular located and the extracellular loop between TM1 and TM2 of two subunits form the ATP-binding site (Kawate et al., 2009). In contrast to Cys-loop and iGluRs, the P2X receptors form trimeric complexes. P2X receptors are implicated in a variety of physiological processes, such as synaptic transmission, inflammation, sensing of taste and pain (Kawate et al., 2009).

Although, all the ligand-gated ion channels serve the function of ligand-inducible ion channels that conduct ions along their respective electrochemical gradient, the molecular structure and overall organization of the receptors differ greatly. In the future it will be interesting to compare the structure and function relationship between the superfamilies in order to identify basic principles of receptor function. However, first the structure and function relationship within the superfamilies need to be analyzed. The work presented here is focused on the research of structure and function relationship in NMDARs and iGluRs in general.

Ionotropic glutamate receptors (iGluRs)

Based on distinct functional properties iGluRs are further discriminated into non-NMDA receptors, i.e. AMPA and kainate receptors, and NMDA receptors (Dingledine et al., 1999). Four AMPA receptor subunits exist, which are GluA1-4 and each subunit has two isoforms, i.e. flip or flop (Hollmann and Heinemann, 1994). For kainate receptors five subunits are known, i.e. GluK1-5 (Hollmann and Heinemann, 1994). Non-NMDA receptors are non-selective cationic channels. Thus, Na^+ and K^+ permeate through the ion channel pore, however, Ca^{2+} permeability depends on the subunit composition (Traynelis et al., 2010). AMPARs lacking the GluA2 subunit will be permeable for Ca^{2+}, but if a GluA2 subunit is incorporated it depends on post-transcriptional RNA editing at the so-called Q/R editing site, if the receptor is Ca^{2+} permeable or not (Traynelis et al., 2010). Non-NMDA receptors are mainly responsible for the fast depolarization of the post-synaptic membrane.

Subunits of the NMDA receptors are, GluN1 subunits with 8 isoforms, the GluN2A-D and GluN3A-B subunits (Monyer et al., 1994, Dingledine et al., 1999, Cull-Candy et al., 2001). NMDA receptors are obligate heteromeric complexes, the ‘conventional’ NMDA receptor is composed of two glycine-binding GluN1 subunits

and two glutamate-binding GluN2 subunits (Laube et al., 1998, Rosenmund et al., 1998, Dingledine et al., 1999, Furukawa et al., 2005). In comparison to AMPA and kainate receptors, the conventional NMDA receptors do not only conduct Na^+ and K^+ but are highly Ca^{2+} permeable (Mayer and Westbrook, 1987, Burnashev et al., 1995). Also, at resting potential conventional NMDA receptors are blocked by extracellular Mg^{2+}, which functions as a channel blocker (Dingledine et al., 1999). When the post-synaptic membrane is depolarized by non-NMDA receptors, Mg^{2+} ions are repelled from the NMDAR channel pore and NMDA receptors can be activated. Thus, conventional NMDA receptors become only active upon ligand-binding and membrane depolarization, therefore they are also referred to as coincidence detectors (Dingledine et al., 1999). The high Ca^{2+} permeability is important as Ca^{2+} triggers second messenger signal cascades inside the cell, which are required for learning and memory formation (Collingridge and Bliss, 1995, Yashiro and Philpot, 2008).

NMDA receptors composed of glycine binding GluN1 and GluN3 subunits are referred to as 'excitatory glycine receptors' and exhibit very small currents (Chatterton et al., 2002, Madry et al., 2007a, Awobuluyi et al., 2007). Although these receptors have not been identified *in vivo* yet, they pose a very interesting target for the study of structure and function relationship as receptor currents can be potentiated up to ~125-fold by the co-application of glycine, Zn^{2+} and a GluN1 antagonist (Madry et al., 2008, Madry et al., 2010).

NMDARs stand out in the iGluR family because of their obligate heteromeric assembly, ligand- and voltage-dependency, implication in neurological disorders and the high degree of receptor modulation (Dingledine et al., 1999, Madry et al., 2008, Traynelis et al., 2010). Thus, understanding structure and function relationship in NMDA receptors is a great and exciting challenge.

Modular composition of iGluRs

It is currently believed that iGluRs have evolved from bacterial ancestor proteins (Lampinen et al., 1998, Masuko et al., 1999, Chen et al., 1999, Wollmuth et al., 2004, Matsuda et al., 2005). This hypothesis was supported by the identification of a missing link, the glutamate-binding GluR0 subtype receptors, which show homologies to prokaryotic potassium channels and eukaryotic iGluRs. (Chen et al., 1999, Kuner et al., 2003). This evolutionary connection was further supported by the

identification of amino acid binding proteins, which show homologies to different domains in the modular composition of iGluRs.

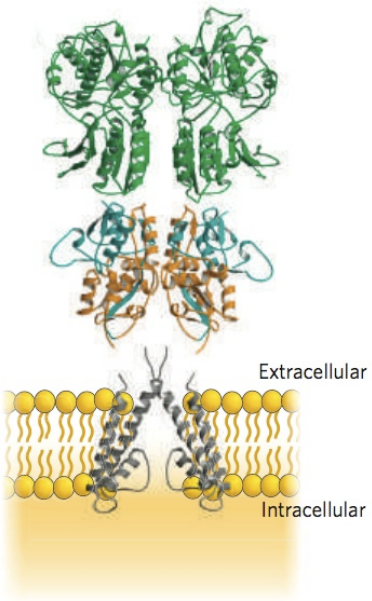

Fig. 2. Modular composition of iGluRs. Shown is a model of an iGluR dimer. Transmembrane region is grey, S1 and S2 subdomains of the LBD are colored blue and orange, respectively, NTDs are colored in green.

Mayer, 2006

The most distal part of an iGluR subunit from the membrane is the N-terminal domain (NTD). This domain shows sequence homology to the bacterial periplasmic Leucine-Isoleucine-Valine binding protein (LIVBP) and consists of ~400 amino acids (Masuko et al., 1999, Matsuda et al., 2005). The NTD has a bilobed structure, which means that the NTD is subdivided into the R1 and R2 domains. At the interface between these two subdomains a cavity is formed that is also a binding-site for allosteric modulators, e.g. Zn^2, which has been shown to inhibit GluN1/GluN2A receptor currents (Paoletti et al., 1997, Herin and Aizenman, 2004). The R1 and R2 subdomains are in constant movement *in vivo* opening and closing the binding-site periodically. This movement has been termed 'oscillation' and the frequencies of these oscillations are subunit specific and largely affect desensitization and channel open probability (P_0) of GluN1/GluN2 receptors (Yuan et al., 2009, Gielen et al., 2009). Structure and function studies with AMPA receptors have implicated that the NTDs determine the subunit specific assembly. In detail, GluA1 and GluA3 subunits as well as GluA2 and GluA4 dimerize readily whereas GluA1 and GluA2 or GluA2 and GluA3 subunits do not (Ayalon and Stern-Bach, 2001, Ayalon and Stern-Bach,

2005, Rossmann et al., 2011). However, if the NTDs are removed the subunits dimerize with no favored combination (Ayalon and Stern-Bach, 2001, Pasternack et al., 2002). Taken together, NTDs are implicated in the assembly of iGluRs and the modulation of iGluR function. However, little is known about the functional roles of the GluN3 NTDs.

The ligand-binding domain (LBD) lies between the NTD and the transmembrane domain (TMD). The LBD is homologous to the Lysine-Arginine-Ornithine binding protein (LAOBP) and is also bilobed and as such subdivided into the S1 and S2 subdomains (Lampinen et al., 1998, Matsuda et al., 2005). Similar to the NTDs, the ligand-binding site is located at the interface between the S1 and S2 subdomains (Furukawa et al., 2003). They form a clamshell-like structure and the subdomains close in a 'venus-flytrap' like fashion upon agonist recognition (Furukawa et al., 2003). This conformational change is transduced to the TMD and leads to the opening of the ion channel pore (Armstrong and Gouaux, 2000, Furukawa et al., 2003). It has been suggested that the degree of clamshell-closure is directly correlated to the extent of receptor activation (Armstrong and Gouaux, 2000, Furukawa et al., 2003). According to this hypothesis antagonists would prevent clamshell-closure, partial agonists, which induce submaximal activation would allow for partial clamshell-closure and only agonists would allow for full clamshell-closure. However, crystallization studies have shown that also partial agonists are capable of inducing full clamshell-closure (Inanobe et al., 2005). Thus, the exact molecular mechanism of partial agonism is unclear.

The TMD is homologous to the KcsA-type potassium channel, which has two transmembrane domains (TM1, TM3) and one re-entrant loop (M2)(Doyle et al., 1998, Wollmuth et al, 2004, Sobolevsky et al., 2009). The TMDs of iGluRs share the same organization but resemble the situation of an inverted KcsA channel and additionally a fourth membrane domain, the TM4, is present (Wollmuth et al., 2004, Sobolevsky et al., 2009). Crystallization studies have shown that the TM3 lines the ion channel pore but the M2 domain determines the ion selectivity (Doyle et al., 1998, Sobolevsky et al., 2009). The role of the TM4 is currently not well understood as this domain is absent in KcsA channels it doesn't seem to be required for proper channel function. A study by Horak et al. (2008) identified endoplasmatic reticulum (ER) retention signals in the TM3s of GluN1 and GluN2B and it was shown that the TM4 is required to mask those ER retention signals. If not, the subunits remain ER localized

and are subsequently degraded. However, if this also applies to GluN1/GluN3 receptors and the non-NMDA receptors is not known. Also it is not known if the TM4 is further involved in receptor function as studies found that mutations in the TM4 affect channel gating (Beck et al., 1999, Ren et al., 2003). Therefore, it was suggested that the TM4 might directly contribute to the ion channel pore (Beck et al., 1999, Ren et al., 2003).

The C-terminal domain (CTD) of NMDA and non-NMDA receptors is localized intracellular and may interact with intracellular scaffolding proteins that determine their accumulation at post-synaptic membranes (Bolton et al., 2000).

As aforementioned, iGluR subunits show homologies to prokaryotic amino acid binding proteins (NTD and LBD) and to prokaryotic ion channels (TMD). One focus of structure and function relationship studies is to understand the role of each domain for receptor function. But another very interesting focus is to gain insight into the role of interfaces between subdomains in one subunit e.g. R1-R2 for the NTD and S1-S2 for the LBD or between domains of two neighboring subunits, such as NTD-NTD, LBD-LBD or TMD-TMD. Therefore, structural data is necessary, either by crystallizing the respective proteins or by using bioinformatic protocols, such as homology modelling. However, homology modelling always requires crystal structures of homologous proteins as templates. Several crystal structures have emerged throughout the years, which gave important insights into the overall organization of iGluRs.

Overall organization of iGluR structure

Due to the modular structure of iGluR subunits, it was possible to express the NTDs and LBDs as soluble proteins and subsequently crystallize them (Armstrong et al., 1998, Armstrong and Gouaux, 2000, Furukawa et al., 2003, Furukawa et al., 2005, Yao and Mayer, 2006, Yao et al., 2008, Jin et al., 2003, Kumar et al., 2009, Karakas et al., 2009, Karakas et al., 2011). Some of these crystal structures did not only show one domain but dimeric assemblies such as the heteromeric GluN1-GluN2A LBD dimer (Armstrong and Gouaux, 2000, Furukawa et al., 2005, Karakas et al., 2011). According to this crystal structure the LBDs are arranged in a ‘back-to-back’ conformation (Fig. 3A) and the interface between the subunits is subdivided into three distinct interaction sites (sites I-III, Fig. 2B)(Furukawa et al., 2005). The first interaction site is formed by the GluN1 D-helix and the J-helix of GluN2A (Fig. 3B,C).

The second interaction site is located between sites I and III and here the ß-sheets ß10 and ß14 of each subunit are mediating the contact (Fig. 3D). Lastly, the third interaction site is analogous to site I, here the GluN1 J-helix is forming a contact with the GluN2 J-helix (Fig. 3E).

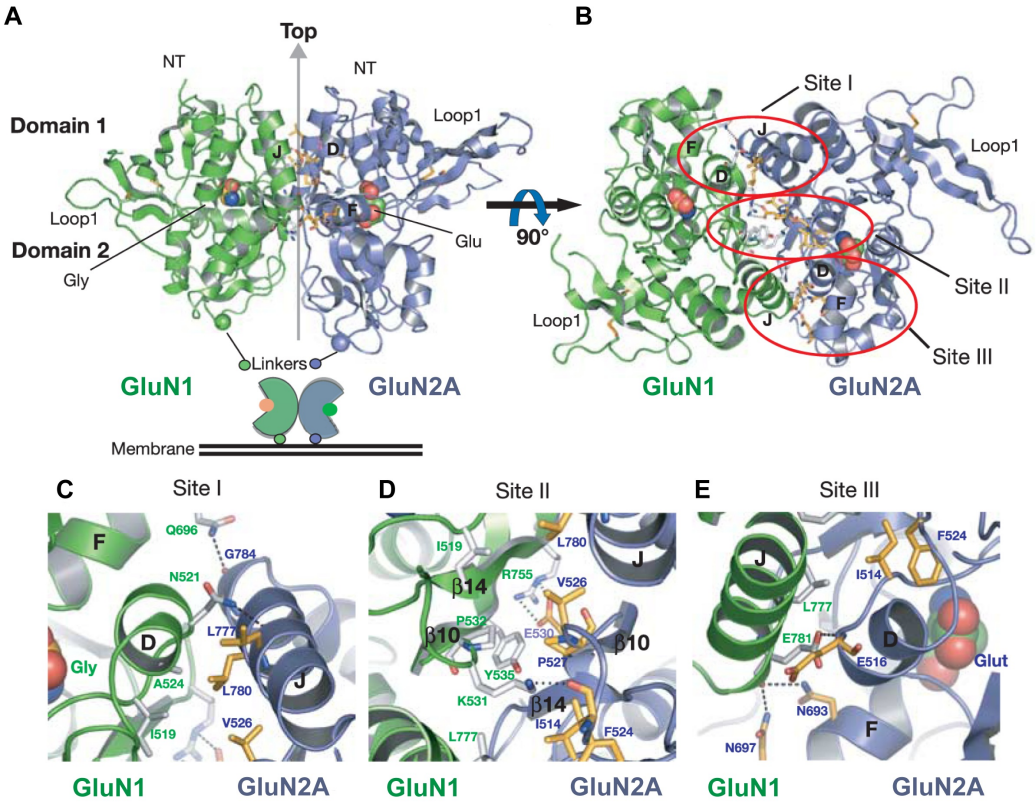

Fig. 3. Crystal structure of the GluN1-GluN2A-LBD (PDB ID: 2A5T, Furukawa et al., 2005). Shown are the LBDs of the GluN1 subunit (green) and the GluN2A subunit (blue). Residues implicated in intersubunit contacts are depicted as sticks. **(A)** Side view of the 'back-to-back' conformation. **(B)** Top view on the interface between the GluN1 and GluN2A subunits. The three distinct interaction sites are depicted in red ovals. **(C)** Close view of the interaction site I, D-helix of GluN1 and J-helix of GluN2A are forming this contact. **(D)** Close view of the interaction site II, ß-sheets 10 and 14 of each subunit are involved. **(E)** Close view of the interaction site III, J-helix of GluN1 and D-helix of GluN2A are forming this contact.

Adadpted from Furukawa et al., 2005

The strength of these interface interactions has been shown to critically determine the activation and desensitization properties of iGluRs (see 'Activation mechanism of iGluRs')(Stern-Bach et al., 1998, Armstrong et al., 2006, Traynelis et al., 2010).

Until recently the organization of the NTDs was suspected to be in a similar 'back-to-back' fashion as it was described for the LBD dimers (Paoletti et al., 2007, Gielen et al., 2009). However, in the most significant crystal structure for the past years, the tetrameric GluA2-type AMPA receptor structure (PDB ID: 3KG2), it was

shown that the NTDs are arranged in a side-by-side orientation (Fig. 4A,B)(Sobolevsky et al., 2009).

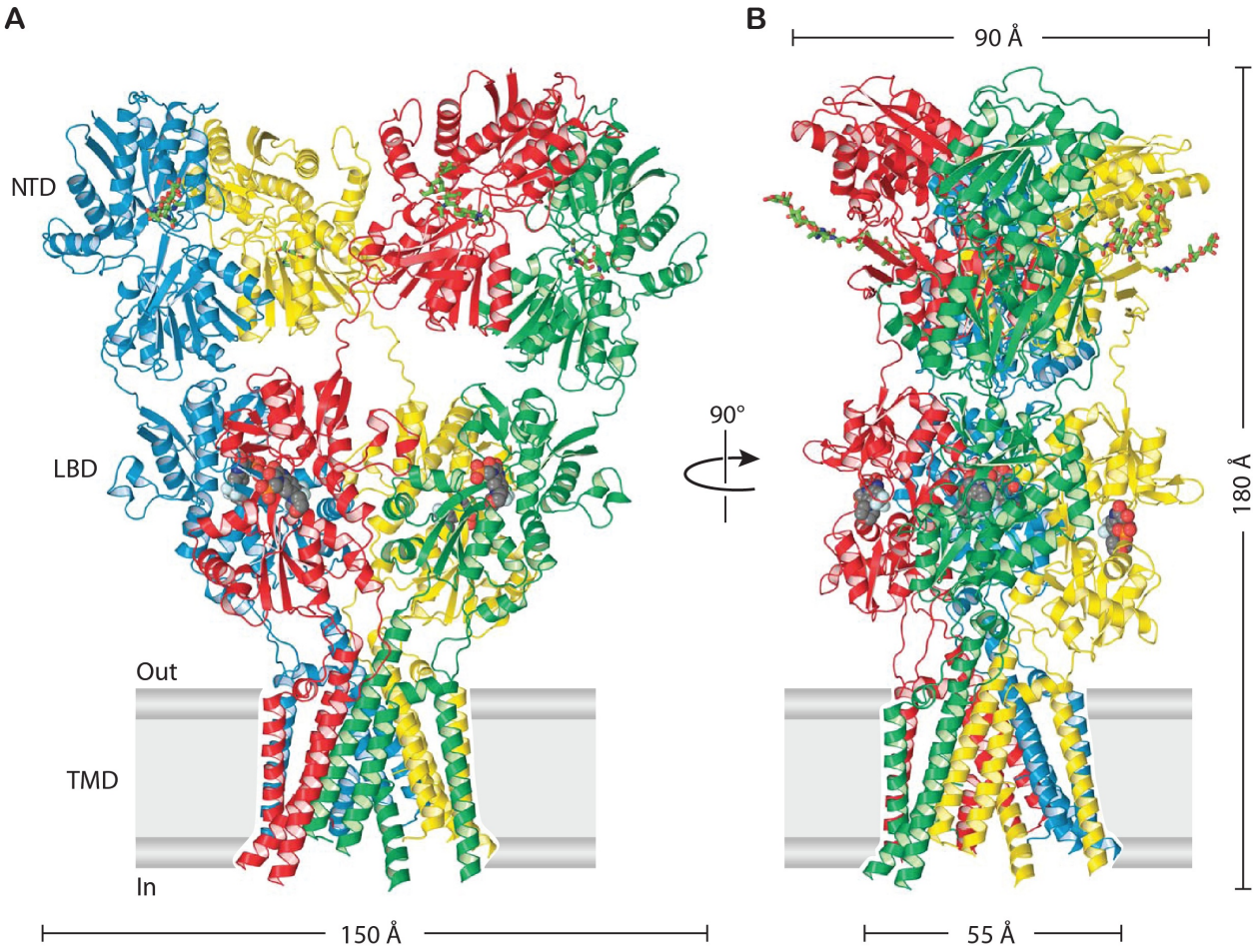

Fig. 4. Crystal structure of the tetrameric GluA2-type AMPA receptor (PDB ID: 3KG2, Sobolevsky et al., 2009). Colors indicate the tetrameric composition. **(A)** Side view on the homomeric GluA2-type AMPA receptor. **(B)** 90° degree rotated side view of the AMPA receptor structure.

Sobolevsky et al., 2009

According to this crystal structure, the NTDs can adopt two different orientations. First, the NTD of a subunit lines up with the subjacent LBD, which itself is lined up with the TMD (Fig. 5A) and Sobolevsky et al. (2009) suggest that in NMDARs GluN1 subunits adopt this conformation. Second, the NTD can adopt a conformation where it is not lined up with the respective LBD but orients itself to the diagonal subunit and it is thought that GluN2 NTDs adopt this conformation in NMDARs (Sobolevsky et al., 2009) and this idea is further supported by the introduction of cysteine residues and the formation of disulfide bridges and subsequent affinity purification in a study by Lee et al. (2011). According to these findings the GluN1-NTDs and GluN2-NTDs form local heterodimers but the GluN2-

NTDs additionally form a homodimeric contacts. The heterodimeric interface has been shown to govern the binding site for ifenprodil in GluN1/GluN2B receptors. Ifenprodil is a high affinity allosteric inhibitor of Glun1/GluN2B receptor function (Madry et al., 2007b). It was thought that ifenprodil binds in the binding pocket of the GluN2B-NTD (Madry et al., 2007b) but the crystal structure of the GluN1/GluN2B NTD with ifenprodil bound to the heterodimeric interface falsified this hypothesis (Karakas et al., 2011). Furthermore it was shown by Karakas et al. (2011) that ifenprodil binding to the interface reduces flexibility and thus increases the rigidity of the NTDs, which inhibits GluN1/GluN2B receptor function. However, we have no information about this interface in GluN1/GluN2A and GluN1/GluN3 receptors. As well, we do not know in which way the homodimeric contacts of the GluN2-NTDs are implicated in NMDAR function.

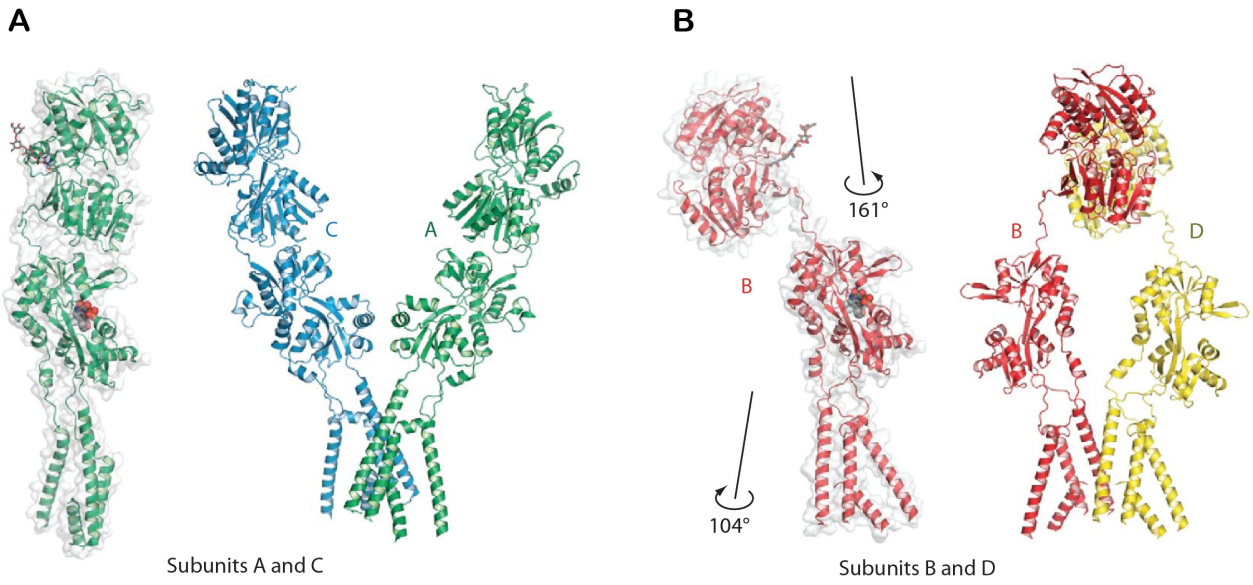

Fig. 5. Crystal structures of the single GluA2-subunits from the tetrameric GluA2-type AMPA receptor structure (PDB ID: 3KG2, Sobolevsky et al., 2009). Although this is a homomeric receptor crystal structure the subunits can adopt two different conformations. **(A)** Subunits A and C adopt the same conformation with the NTDs, LBDs and TMDs lined up. **(B)** The subunits B and D adopt a twisted conformation where the NTDs are rotated 161° and the TMDs are rotated by 104° with respect to the LBDs. The NTDs of subunits B and D are in close contact with each other.

Sobolevsky et al., 2009

The TMDs of iGluRs are homologous to prokaryotic potassium-conducting KcsA channels (Doyle et al., 1998, Sobolevsky et al., 2009). Despite the homology there

are also few differences. The first one is that the TMDs of iGluRs are inversely embedded into the membrane compared to the KcsA structure (Doyle et al., 1998, Sobolevsky et al., 2009). Second, iGluR TMDs possess a fourth membrane domain, the TM4, which is not present in the KcsA channel (Doyle et al., 1998). According to the AMPAR crystal structure, this TM4 domain is remotely located to the TMs of the same subunit, however, it is close to the TM1 and TM3 of the neighboring subunit (Fig. 6)(Sobolevsky et al., 2009). Based on this crystal structure it is possible to conduct structure and function relationship studies on the intersubunit interface that is formed by the TM4 of one subunit and the TM1 and TM3 of the neighboring subunit. It was suggested that the TM4 is an evolutionary addition to the iGluR TMDs but it is not known why this additional membrane domain was necessary.

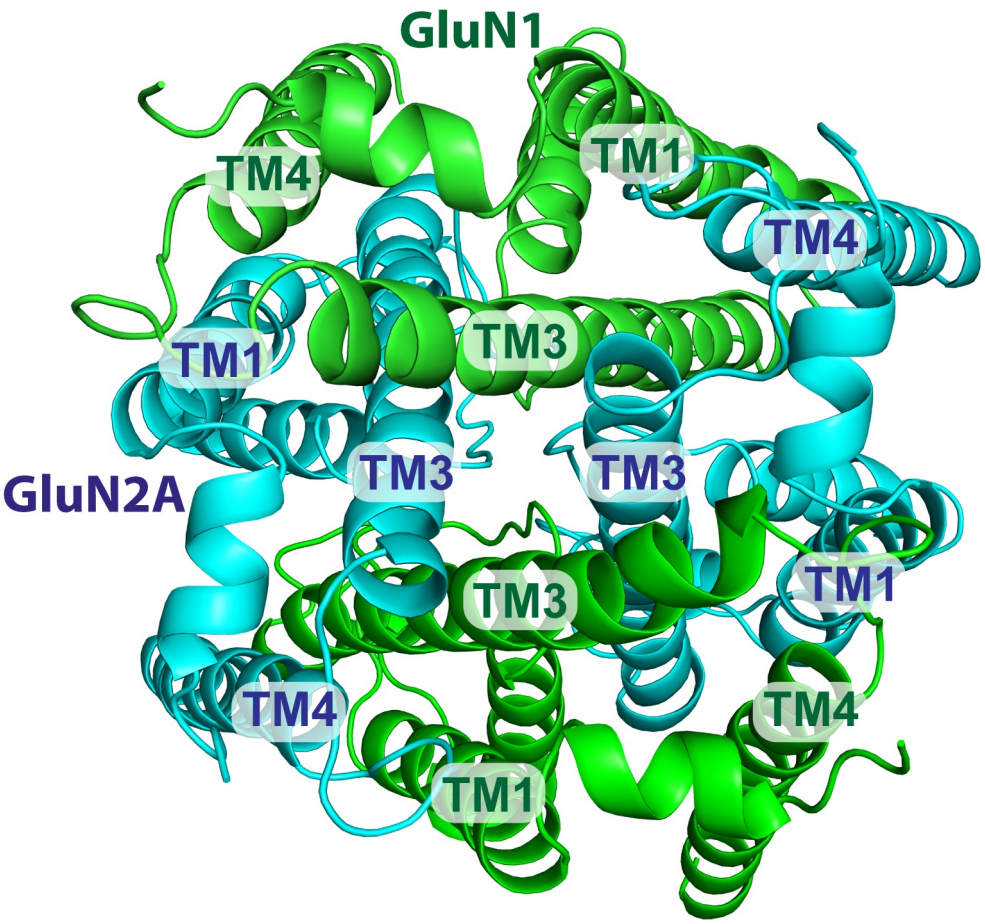

Fig. 6. Homology model of the GluN1-GluN2A TMDs. GluN1 subunits (green) and GluN2A subunits (cyan) are arranged highly symmetrical. The TM3 domains are lining the ion channel pore whereas the M2 domains are forming the selectivity filter (loop region). The TM4 domains of each subunit are engaged in intersubunit contacts with the neighboring subunits' TM1 and TM3 domain.

Activation mechanism of iGluRs

Functional and crystallization studies have focused on understanding the activation mechanism of iGluRs (Sun et al., 2002, Furukawa et al., 2003, Inanobe et al., 2005, Armstrong et al., 2006, Mayer, 2006). It was found that during receptor activation first the S2 subdomain approaches the S1 subdomain and thus the ligand-binding pocket is closed, this conformational rearrangement conveys enough strain to open the ion channel pore (Furukawa et al., 2003, Inanobe et al., 2005, Armstrong et al., 2006, Mayer, 2006). These initial LBD conformational changes also cause strain onto the LBD dimer interface and cause a rupture of the interface (Fig. 4), which in turn causes the ion channel to close (Mayer, 2006, Traynelis et al., 2010). In this situation the ligands are still bound to the LBDs but the ion channel is closed, this conformational state is termed the 'desensitized' state (Fig. 7A)(Sun et al., 2002, Armstrong et al., 2006, Mayer, 2006). This principle is thought to be valid for conventional NMDA receptors and non-NMDA receptors. But the activation mechanism depends not only LBD rearrangements, NTD truncations and NTD substitution experiments have shown that the NTDs play an important role in determining apparent agonist affinities, extent of desensitization, desensitization kinetics and channel open probability (P_0)(Madry et al., 2007b, Yuan et al., 2009, Gielen et al., 2009). In this respect 'oscillations' of the NTDs have been implicated, which are thought to be periodic movements that open and close the binding pocket of the respective NTDs. A high frequency of these oscillations leads to a reduced P_0 whereas lower frequencies increase the P_0 (Gielen et al., 2009). But it is still unclear how these oscillations are conveyed to the ion channel pore. In the aforementioned studies it was also found that the NTD-LBD linkers play an important role as for the NTD substitution experiments with GluN2 subunits it was necessary to not only substitute the NTD between subunits but also the linker region, in order to transfer GluN2 subunit specific properties from one GluN2 subunit to another GluN2 subunit (Yuan et al., 2009, Gielen et al., 2009).

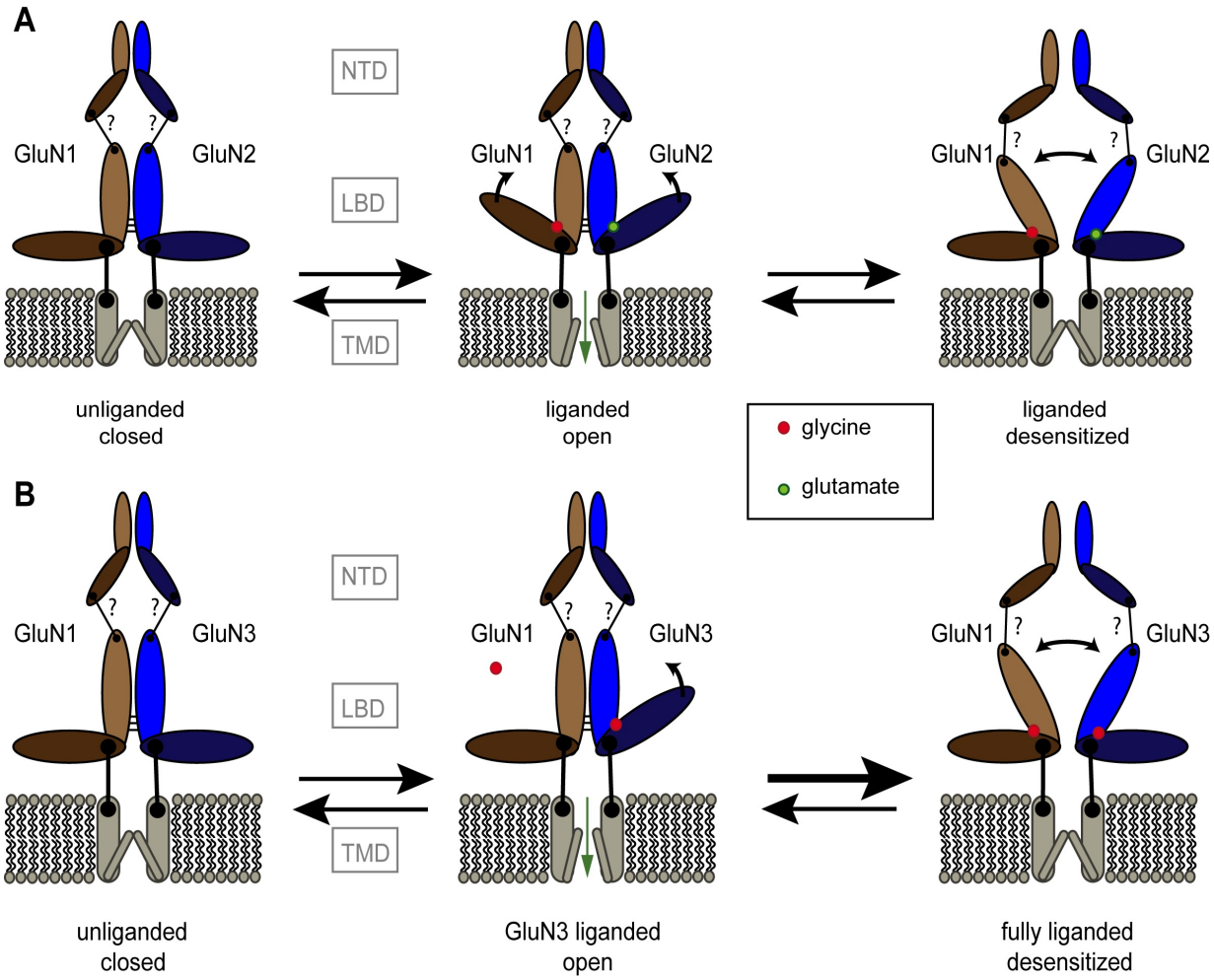

Fig. 7. Model for the activation mechanism in GluN1/GluN2A and GluN1/GluN3A receptors. Subdomains of the NTDs and LBDs are colored in different shades. Glycine molecules are depicted as red circles, glutamate is green. **(A)** GluN1/GluN2 receptors require ligand binding to GluN1 and GluN2 subunits to be activated. Upon agonist binding the S2 subdomains are rearranging to open the ion channel. This weakens the interface interactions, the receptor desensitizes depending on the strength of intersubunit interactions. **(B)** In GluN1/GluN3A receptors the GluN3A is the principal activating subunit. Agonist binding to the GluN3A subunit activates the receptor, whereas ligand binding to the GluN1 subunit is thought to induce receptor desensitization (Madry et al., 2007a).

Adapted from Madry et al., 2007a

The activation mechanism for GluN1/Glun3 receptors is thought to be different than the rest of the iGluRs (Madry et al., 2007a, Awobuluyi et al., 2007, Madry et al., 2008). In detail, ligand-binding to the GluN3 subunit alone induces sufficient conformational strain to induce channel opening, whereas ligand-binding to the GluN1 subunit immediately leads the receptor to desensitize (Madry et al., 2007a). This hypothesis is further supported by the ~25-fold potentiation of GluN1/GluN3A

receptor currents, if the GluN1 subunit is antagonized, e.g. by MDL-29951, or when the ligand-binding pocket is mutated (Madry et al., 2007a, Madry et al., 2008). Thus it is concluded that ligand-binding to the GluN1 and GluN3 subunits have distinct effects, ligand-binding to the GluN3 subunit activates the receptor and ligand-binding to the GluN1 subunit has an inhibitory effect. GluN1/GluN3 receptors exhibit very small currents upon glycine-application and it is thought that the underlying mechanism are the differential roles of the subunits for receptor activation. However, it is unclear why the GluN1 subunit is required for full activation in GluN1/GluN2 but in GluN1/GluN3 receptors it inhibits receptor function. Structure and function relationship studies should address the question in which way the NTDs or LBDs of GluN3 subunits are involved in the inhibitory role of the GluN1 subunit in GluN1/GluN3 receptors.

Aim of this work

As aforementioned, iGluRs have a modular structure and the NTDs, LBDs as well as the TMDs have prokaryotic homologs. Depending on the type of iGluR and its subunit composition the pharmacological and functional properties differ greatly. The aim of the work presented here was to investigate which functional properties, such as the activation mechanism, apparent agonist affinities, extent of desensitization and maximal inducible currents, of NMDARs are determined by intra- and intersubunit interfaces. For this purpose bioinformatics protocols, i.e. ligand docking studies, homology modelling and mutual information analysis (MI) were combined with electrophysiological as well as molecular biology methods, i.e. two-electrode voltage-clamp (TEVC) on *Xenopus laevis* oocytes and site-directed mutagenesis.

First, using molecular docking and homology modelling, the ligand-protein interactions were analyzed to disclose in which way the S1 and S2 subdomains interact with each other and what determines the efficacy of a ligand. Thus, we intended to gain insight into the molecular activation mechanism. Next, the role of the GluN1-GluN2 LBD heterodimer interface was analyzed using the MI analysis and by introducing amino acid mutations in the GluN1 subunit and characterizing these mutations using TEVC with regards to apparent agonist affinities, extent of desensitization an maximal inducible currents. These experiments were carried out on a reduced receptor model, i.e. NTD-lacking GluN1/GluN2 receptors. In comparison to GluN1/GluN2 receptors, GluN1/GluN3 receptors were found to have a very low efficacy. In order to understand which structural properties account for this difference, GluN1/GluN3 LBD heterodimer interface mutations and mutations in the GluN3A-NTDs were analyzed with respect to apparent agonist affinities, extent of desensitization and maximal inducible currents. For this, TEVC was combined with homology modelling. In addition to the analysis of NTD and LBD interactions, interactions in the TMDs were analyzed by MI analysis and by means of homology modelling and TEVC. Specifically, the question for the role of the TM4 domain in receptor function was addressed.

REFERENCES

Armstrong N, Sun Y, Chen GQ, Gouaux E. Structure of a glutamate-receptor ligand-binding core in complex with kainate. *Nature* 395: 913-917, 1998.

Armstrong N, Gouaux E. Mechanisms for activation and antagonism of an AMPA-sensitive glutamate receptor: crystal structures of the GluR2 ligand binding core. *Neuron* 28: 165-181, 2000.

Armstrong N, Jasti J, Beich-Frandsen M, Gouaux E. Measurement of conformational changes accompanying desensitization in an ionotropic glutamate receptor. *Cell* 127: 85-97, 2006.

Awobuluyi M, Yang J, Ye Y, Chatterton JE, Godzik A, Lipton SA, Zhang D. Subunit-specific roles of glycine-binding domains in activation of NR1/NR3 N-methyl-D-aspartate receptors. *Mol Pharmacol* 71: 112-122, 2007.

Ayalon G, Segev E, Elgavish S, Stern-Bach Y. Two regions in the N-terminal domain of ionotropic glutamate receptor 3 form the subunit oligomerization interfaces that control subtype-specific receptor assembly. *J Biol Chem* 280: 15053-15060, 2005.

Ayalon G, Stern-Bach Y. Functional assembly of AMPA and kainate receptors is mediated by several discrete protein-protein interactions. *Neuron* 31: 103-113, 2001.

Baulac S, Huberfeld G, Gourfinkel-An I, Mitropoulou G, Beranger A, Prud'homme JF, Baulac M, Brice A, Bruzzone R, LeGuern E. First genetic evidence of GABA(A) receptor dysfunction in epilepsy: a mutation in the gamma2-subunit gene. *Nat Genet* 28: 46-48, 2001.

Beck C, Wollmuth LP, Seeburg PH, Sakmann B, Kuner T. NMDAR channel segments forming the extracellular vestibule inferred from the accessibility of substituted cysteines. *Neuron* 22: 559-570, 1999.

Bolton MM, Blanpied TA, Ehlers MD. Localization and stabilization of ionotropic glutamate receptors at synapses. *Cell Mol Life Sci* 57: 1517-1525, 2000.

Burnashev N, Zhou Z, Neher E, Sakmann B. Fractional calcium currents through recombinant GluR channels of the NMDA, AMPA and kainate receptor subtypes. *J Physiol* 485: 403-418, 1995.

Chatterton JE, Awobuluyi M, Premkumar LS, Takahashi H, Talantova M, Shin Y, Cui J, Tu S, Sevarino KA, Nakanishi N, Tong G, Lipton SA, Zhang D. Excitatory glycine receptors containing the NR3 family of NMDA receptor subunits. *Nature* 415: 793-798, 2002.

Chen GQ, Cui C, Mayer ML, Gouaux E. Functional characterization of a potassium-selective prokaryotic glutamate receptor. *Nature* 402: 817-821, 1999.

Collingridge GL, Bliss TV. Memories of NMDA receptors and LTP. *Trends Neurosci* 18: 54-56, 1995.

Cull-Candy S, Brickley S, Farrant M. NMDA receptor subunits: diversity, development and disease. *Curr Opin Neurobiol* 11: 327-335, 2001.

De Fusco M, Becchetti A, Patrignani A, Annesi G, Gambardella A, Quattrone A, Ballabio A, Wanke E, Casari G. The nicotinic receptor beta 2 subunit is mutant in nocturnal frontal lobe epilepsy. *Nat Genet* 26: 275-276, 2000.

Dingledine R, Borges K, Bowie D, Traynelis SF. The glutamate receptor ion channels. *Pharmacol Rev* 51: 7-61, 1999.

Doyle DA, Morais Cabral J, Pfuetzner RA, Kuo A, Gulbis JM, Cohen SL, Chait BT, MacKinnon R. The structure of the potassium channel: molecular basis of K+ conduction and selectivity. *Science* 280: 69-77, 1998.

Endele S, Rosenberger G, Geider K, Popp B, Tamer C, Stefanova I, Milh M, Kortum F, Fritsch A, Pientka FK, Hellenbroich Y, Kalscheuer VM, Kohlhase J, Moog U, Rappold G, Rauch A, Ropers HH, von Spiczak S, Tonnies H, Villeneuve N, Villard L, Zabel B, Zenker M, Laube B, Reis A, Wieczorek D, Van Maldergem L, Kutsche K. Mutations in GRIN2A and GRIN2B encoding regulatory subunits of NMDA receptors cause variable neurodevelopmental phenotypes. *Nat Genet* 42: 1021-1026, 2010.

Engel AG, Hutchinson DO, Nakano S, Murphy L, Griggs RC, Gu Y, Hall ZW, Lindstrom J. Myasthenic syndromes attributed to mutations affecting the epsilon subunit of the acetylcholine receptor. *Ann N Y Acad Sci* 681: 496-508, 1993.

Furukawa H, Gouaux E. Mechanisms of activation, inhibition and specificity: crystal structures of the NMDA receptor NR1 ligand-binding core. *EMBO J* 22: 2873-2885, 2003.

Furukawa H, Singh SK, Mancusso R, Gouaux E. Subunit arrangement and function in NMDA receptors. *Nature* 438: 185-192, 2005.

Garcia PS, Kolesky SE, Jenkins A. General anesthetic actions on GABA(A) receptors. *Curr Neuropharmacol* 8: 2-9, 2010.

Gielen M, Retchless BS, Mony L, Johnson JW, Paoletti P. Mechanism of differential control of NMDA receptor activity by NR2 subunits. *Nature* 2009.

Herin GA, Aizenman E. Amino terminal domain regulation of NMDA receptor function. *Eur J Pharmacol* 500: 101-111, 2004.

Hollmann M, Heinemann S. Cloned glutamate receptors. *Annu Rev Neurosci* 17: 31-108, 1994.

Horak M, Chang K, Wenthold RJ. Masking of the endoplasmic reticulum retention signals during assembly of the NMDA receptor. *J Neurosci* 28: 3500-3509, 2008.

Inanobe A, Furukawa H, Gouaux E. Mechanism of partial agonist action at the NR1 subunit of NMDA receptors. *Neuron* 47: 71-84, 2005.

Jin R, Banke TG, Mayer ML, Traynelis SF, Gouaux E. Structural basis for partial agonist action at ionotropic glutamate receptors. *Nat Neurosci* 6: 803-810, 2003.

Kandel ER, Schwartz JH, Jessell TM. *Principles of neural science*. McGraw-Hill New York, 2000

Karakas E, Simorowski N, Furukawa H. Structure of the zinc-bound amino-terminal domain of the NMDA receptor NR2B subunit. *EMBO J* 2009.

Karakas E, Simorowski N, Furukawa H. Subunit arrangement and phenylethanolamine binding in GluN1/GluN2B NMDA receptors. *Nature* 475: 249-253, 2011.

Kumar J, Schuck P, Jin R, Mayer ML. The N-terminal domain of GluR6-subtype glutamate receptor ion channels. *Nat Struct Mol Biol* 16: 631-638, 2009.

Kuner T, Seeburg PH, Guy HR. A common architecture for K+ channels and ionotropic glutamate receptors? *Trends Neurosci* 26: 27-32, 2003.

Lampinen M, Pentikainen O, Johnson MS, Keinanen K. AMPA receptors and bacterial periplasmic amino acid-binding proteins share the ionic mechanism of ligand recognition. *EMBO J* 17: 4704-4711, 1998.

Laube B, Kuhse J, Betz H. Evidence for a tetrameric structure of recombinant NMDA receptors. *J Neurosci* 18: 2954-2961, 1998.

Lee CH, Gouaux E. Amino terminal domains of the NMDA receptor are organized as local heterodimers. *PLoS One* 6: e19180, 2011.

Madden DR. The structure and function of glutamate receptor ion channels. *Nat Rev Neurosci* 3: 91-101, 2002.

Madry C BH, Geiger JRP, Laube B. Supralinear potentiation of NR1/NR3A excitatory glycine receptors by Zn^{2+} and NR1 antagonist. *PNAS* 2008.

Madry C, Betz H, Geiger JR, Laube B. Potentiation of Glycine-Gated NR1/NR3A NMDA Receptors Relieves Ca-Dependent Outward Rectification. *Front Mol Neurosci* 3: 6, 2010.

Madry C, Mesic I, Bartholomaus I, Nicke A, Betz H, Laube B. Principal role of NR3 subunits in NR1/NR3 excitatory glycine receptor function. *Biochem Biophys Res Commun* 354: 102-108, 2007.

Madry C, Mesic I, Betz H, Laube B. The N-terminal domains of both NR1 and NR2 subunits determine allosteric Zn2+ inhibition and glycine affinity of N-methyl-D-aspartate receptors. *Mol Pharmacol* 72: 1535-1544, 2007.

Maksay G, Laube B, Betz H. Subunit-specific modulation of glycine receptors by neurosteroids. *Neuropharmacology* 41: 369-376, 2001.

Masuko T, Kashiwagi K, Kuno T, Nguyen ND, Pahk AJ, Fukuchi J, Igarashi K,

Williams K. A regulatory domain (R1-R2) in the amino terminus of the N-methyl-D-aspartate receptor: effects of spermine, protons, and ifenprodil, and structural similarity to bacterial leucine/isoleucine/valine binding protein. *Mol Pharmacol* 55: 957-969, 1999.

Matsuda S, Kamiya Y, Yuzaki M. Roles of the N-terminal domain on the function and quaternary structure of the ionotropic glutamate receptor. *J Biol Chem* 280: 20021-20029, 2005.

Mayer ML, Westbrook GL. Permeation and block of N-methyl-D-aspartic acid receptor channels by divalent cations in mouse cultured central neurones. *J Physiol* 394: 501-527, 1987.

Mayer ML. Glutamate receptors at atomic resolution. *Nature* 440: 456-462, 2006.

Monyer H, Burnashev N, Laurie DJ, Sakmann B, Seeburg PH. Developmental and regional expression in the rat brain and functional properties of four NMDA receptors. *Neuron* 12: 529-540, 1994.

Paoletti P, Ascher P, Neyton J. High-affinity zinc inhibition of NMDA NR1-NR2A receptors. *J Neurosci* 17: 5711-5725, 1997.

Paoletti P, Neyton J. NMDA receptor subunits: function and pharmacology. *Curr Opin Pharmacol* 7: 39-47, 2007.

Pasternack A, Coleman SK, Jouppila A, Mottershead DG, Lindfors M, Pasternack M, Keinanen K. Alpha-amino-3-hydroxy-5-methyl-4-isoxazolepropionic acid (AMPA) receptor channels lacking the N-terminal domain. *J Biol Chem* 277: 49662-49667, 2002.

Ren H, Honse Y, Karp BJ, Lipsky RH, Peoples RW. A site in the fourth membrane-associated domain of the N-methyl-D-aspartate receptor regulates desensitization and ion channel gating. *J Biol Chem* 278: 276-283, 2003.

Rosenmund C, Stern-Bach Y, Stevens CF. The tetrameric structure of a glutamate receptor channel. *Science* 280: 1596-1599, 1998.

Rossmann M, Sukumaran M, Penn AC, Veprintsev DB, Babu MM, Greger IH. Subunit-selective N-terminal domain associations organize the formation of AMPA receptor heteromers. *EMBO J* 30: 959-971, 2011.

Schorge S, Colquhoun D. Studies of NMDA receptor function and stoichiometry with truncated and tandem subunits. *J Neurosci* 23: 1151-1158, 2003.

Shiang R, Ryan SG, Zhu YZ, Hahn AF, O'Connell P, Wasmuth JJ. Mutations in the alpha 1 subunit of the inhibitory glycine receptor cause the dominant neurologic disorder, hyperekplexia. *Nat Genet* 5: 351-358, 1993.

Sobolevsky AI, Rosconi MP, Gouaux E. X-ray structure, symmetry and mechanism of an AMPA-subtype glutamate receptor. *Nature* 2009.

Steinlein OK, Mulley JC, Propping P, Wallace RH, Phillips HA, Sutherland GR, Scheffer IE, Berkovic SF. A missense mutation in the neuronal nicotinic acetylcholine receptor alpha 4 subunit is associated with autosomal dominant nocturnal frontal lobe epilepsy. *Nat Genet* 11: 201-203, 1995.

Sun Y, Olson R, Horning M, Armstrong N, Mayer M, Gouaux E. Mechanism of glutamate receptor desensitization. *Nature* 417: 245-253, 2002.

Thio LL, Shanmugam A, Isenberg K, Yamada K. Benzodiazepines block alpha2-containing inhibitory glycine receptors in embryonic mouse hippocampal neurons. *J Neurophysiol* 90: 89-99, 2003.

Thurmon TF. Evaluation of relatives for congenital heart defects. *J La State Med Soc* 148: 31-37, 1996.

Traynelis SF, Wollmuth LP, McBain CJ, Menniti FS, Vance KM, Ogden KK, Hansen KB, Yuan H, Myers SJ, Dingledine R. Glutamate receptor ion channels: structure, regulation, and function. *Pharmacol Rev* 62: 405-496, 2010.

Wallace RH, Marini C, Petrou S, Harkin LA, Bowser DN, Panchal RG, Williams DA, Sutherland GR, Mulley JC, Scheffer IE, Berkovic SF. Mutant GABA(A) receptor gamma2-subunit in childhood absence epilepsy and febrile seizures. *Nat Genet* 28: 49-52, 2001.

Wollmuth LP, Sobolevsky AI. Structure and gating of the glutamate receptor ion channel. *Trends Neurosci* 27: 321-328, 2004.

Yao Y, Harrison CB, Freddolino PL, Schulten K, Mayer ML. Molecular mechanism of ligand recognition by NR3 subtype glutamate receptors. *EMBO J* 27: 2158-2170, 2008.

Yao Y, Mayer ML. Characterization of a soluble ligand binding domain of the NMDA receptor regulatory subunit NR3A. *J Neurosci* 26: 4559-4566, 2006.

Yashiro K, Philpot BD. Regulation of NMDA receptor subunit expression and its implications for LTD, LTP, and metaplasticity. *Neuropharmacology* 55: 1081-1094, 2008.

Yuan H, Hansen KB, Vance KM, Ogden KK, Traynelis SF. Control of NMDA receptor function by the NR2 subunit amino-terminal domain. *J Neurosci* 29: 12045-12058, 2009.

CHAPTER 2
IN SILICO APPROACH TO DETERMINE THE MOLECULAR ACTION OF LIGAND BINDING TO NMDAR SUBUNITS

Ceyhun Tamer[1,2], Bodo Laube[1,2]
[1]Department of Neurochemistry, Max-Planck-Institute for Brain Research, Deutschordenstrasse 46, 60528 Frankfurt am Main, Germany
[2]Department of Molecular and Cellular Neurophysiology, TU-Darmstadt, Schnittspahnstrasse 3, 64287 Darmstadt, Germany

ABSTRACT

Ionotropic glutamate receptors (iGluRs) are ligand-gated ion channels that mediate the majority of excitatory neurotransmission in the mammalian central nervous system. A unique feature of the respective subunits is the clamshell like closure of the ligand-binding domains (LBD) upon agonist recognition. To date, a lot of effort went into analyzing whether the extent of clamshell closure of the LBD is correlated to the extent of receptor activation. In order to understand how conformational states induced by full and partial agonists modulate the activity of the receptor we conducted docking experiments with crystal structures and homology models. First, we used GluN1 LBD crystal structures to determine if agonists, partial agonists and antagonists energetically prefer distinct conformations, i.e. closed-cleft, partially closed-cleft or open-cleft, respectively. Indeed, we found that agonists have their lowest binding energy in the closed-cleft conformation whereas partial agonists and antagonists dock best into partially closed-cleft and open-cleft conformations, respectively. Subsequently, we constructed homology models for GluN2A and GluN3A LBDs using GluN1 LBD crystal structures with different extents of clamshell closure and used these models for docking experiments. We did not find a strong correlation between the action of the ligand and the extent of clamshell closure for agonists and partial agonists. This finding might indicate that GluN1 and GluN2A/GluN3A subunits do not use the same molecular mechanism to distinguish between agonists and partial agonists, notwithstanding the loss of accuracy between docking experiments with crystal structures and homology models. Also it is possible that the LBDs behave differently when expressed as isolated, soluble proteins as it is required for X-ray crystallography. Thus, it would not be possible to disclose

the molecular mechanism that defines the action of a ligand by analyzing crystal structures or homology models of iGluR subunits.

INTRODUCTION

Ionotropic glutamate receptors (iGluRs) are tetrameric complexes of homologous subunits, such as GluA1-4 for AMPA receptors, GluK1-4 for kainate receptors and GluN1, GluN2A-D as well as GluN3A-B for NMDA receptors. All of these subunits share a common modular structure composed of i) a bilobed, extracellular N-terminal domain (NTD), ii) a bilobed, extracellular ligand-binding domain (LBD), iii) a membrane-bound domain consisting of 3 transmembrane helices (TM1, TM3 and TM4) and one pore-forming re-entrant loop (M2) and lastly iv) an intracellular C-terminal domain (CTD)(overview in Madden, 2002). The bilobed LBD is formed by the two subdomains S1 and S2, the S1 subdomain consists of the ~150 AAs before the TM1 and the S2 consists of a ~150 amino acids (AAs) extracellular loop between TM3 and TM4. The LBD shows similarity to the bacterial, periplasmic Lysine-Arginine-Ornithine binding protein (LAOBP)(Lampinen et al., 1998). It is known that the two subdomains are arranged in a clamshell-like architecture and upon ligand binding the two subdomains approach each other, i.e. the binding pocket closes, in a clamshell like mechanism. It is suggested that this conformational movement is required for the opening of the ion channel pore (Armstrong and Mayer, 2000, Furukawa et al., 2003, Inanobe et al., 2005). In this respect, especially partial agonists are useful molecules with which to probe the relationship between agonist binding, conformational changes and ion channel activation. According to del Castillo and Katz (1957) a partial agonist is a ligand that produces a channel open probability (P_0) of less than 1 upon occupancy of all binding sites. Later, the Monod-Wyman-Changeux model (Monod et al., 1965) claimed that ligand-gated ion channels are in an equilibrium between two distinct states: closed/inactive and open. An agonist would then be a molecule that is maximally effective in shifting the equilibrium from closed/inactive to open. Li et al. (1997) extended this model by saying that partial agonists are less effective than full agonists in shifting the equilibrium to the open state. Although this hypothesis might appear logical, crystallization studies suggest that the LBDs are present in several distinct conformational states (Armstrong and Mayer, 2000)

GluA2 LBD crystallization studies with agonists, partial agonists and antagonists suggested that the degree to which the LBD clamshell closes is correlated to the extent of receptor activation. Accordingly, a full agonist would induce a complete closure of the LBD clamshell, whereas a partial agonist would stabilize a partially closed-cleft conformation and an antagonist would prevent the conformational change and stabilize an apo-state like conformation, the conformation before a ligand is bound. As NMDARs and non-NMDARs share the same modular composition it was expected that NMDAR subunits would behave like their AMPAR counterparts. But crystallization of the GluN1 LBD with partial agonists, such as D-cycloserine (DCS), 1-aminocyclopropane-1-carboxylic acid (ACPC) and 1-aminocyclobutane-1-carboxylic acid (ACBC), revealed that partial agonists can induce a full closure of the LBD similar to full agonists (i.e. glycine and D-serine)(Furukawa et al., 2003, Inanobe et al., 2005). However, agonist efficacies seem to be correlated to the size of the ligand as, compared to glycine, the larger ligand ACPC resulted in only 80% activation, ACBC with one carbon atom more induced 42% activation and cycloleucine with one more carbon atom did not elicit currents in concentrations up to 50mM. The respective crystal structures show that while the ACPC- and ACBC-bound structures (PDB IDs: 1Y1Z, 1Y20) show a fully closed clamshell, the cycloleucine-bound structure (PDB ID: 1Y1M) has a partially open-cleft. The size of a ligand is reasonably correlated to its function but for the small ligands, additional discrimination mechanisms might be present (Inanobe et al., 2005). In this respect Inanobe et al. (2005) reported that the glycine- and ACPC- or ACBC-bound structures differ in 8 residues, which are located in the so-called hinge region (GluN1 T749-S756). It has been observed that the L538 residue in the GluN1-LBD made a hydrogen-bonded interaction with F754 in the glycine-bound structure, whereas in the ACPC- and ACBC-bound structure the interaction was with F753. It was suggested that this switch from F754 to F753 might be responsible for the discrimination between agonists and partial agonists. It was also reported that W731 and V689 are sensitive to the size of the ligand and thus large ligands cannot induce a full closure of the LBD due to steric effects.

Based on the previous findings we hypothesized that the action of a ligand is mainly determined by its size. Although ligands such as ACPC and ACBC can induce a full closure of the GluN1 LBD (in the crystal structure), we believe that *in vivo* partial agonists would energetically prefer a partially closed- cleft conformation. Thus, we

docked 21 ligands (agonists, partial agonists and antagonists, Fig. 1) to the crystal structures of the glycine- (1PB7, closed-cleft conformation), cycloleucine- (1Y1M, partially closed-cleft conformation) and 5,7-dichlorokynurenic acid (DCKA)-bound LBD structures (1PBQ chain A and B, open-cleft conformations). For each ligand we compared how well it docks into each conformer. We expect that the conformer with the lowest energy for each ligand will be its favored state *in vivo*.

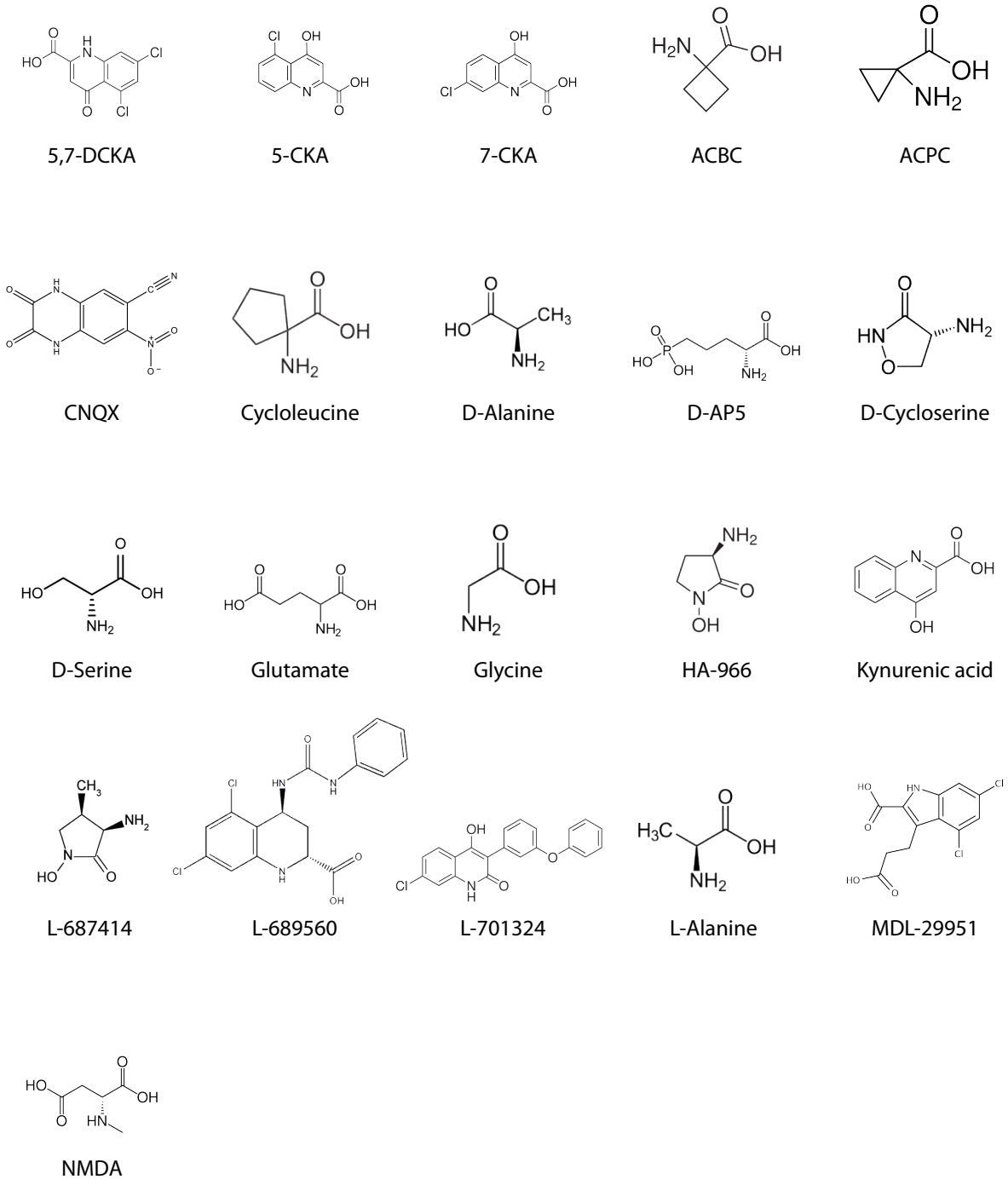

Fig. 1 Agonists, partial agonists and antagonists of NMDAR-subunits.

In order to assess the feasibility of docking experiments on homology models, we compared docking results from crystal structures and homology models. For this, homology models for the GluN1 LBD were computed based on GluA2 crystal structures: closed-cleft AMPA-bound structure, partially closed-cleft kainate-bound structure, open-cleft UBP277-bound structure and maximally open-cleft UBP282-bound structure (PDB IDs respectively: 1FTM, 1FTK, 3H03, 3H06). To further analyze whether GluN1, GluN2 and GluN3 LBDs share the same molecular mechanisms to discriminate between agonists and partial agonists, i.e. extent of clamshell closure, we constructed homology models for the GluN2A and GluN3A LBDs based on the different conformers of the GluN1 LBD. Using this approach we intended to overcome the problem that no crystal structures for partial agonist or antagonist bound GluN2 or GluN3 LBDs are available. By these means we simulated different degrees of clamshell closure, from the apparent apo-state to the fully closed state. These models were then used for docking experiments using the same 21 ligands that were used for the GluN1 LBDs (Fig. 1). An overview of the known actions of these ligands on the respective LBDs is summarized in Table 1.

	Activity on ligand-binding domain					
Compound	**GluN1**	**Reference**	**GluN2A**	**Reference**	**GluN3A**	**Reference**
5,7-DCKA	Antagonist	Leeson et al., 1991 Foster et al., 1992				
5-CKA	Antagonist	Leeson et al., 1991 Foster et al., 1992				
7-CKA	Antagonist	Leeson et al., 1991 Foster et al., 1992				
ACBC	part. Agonist	Inanobe et al., 2005				
ACPC	part. Agonist	Inanobe et al., 2005				
CNQX	Antagonist	Ramakers et al., 1991			Antagonist	Yao et al., 2006 Madry et al., 2007a
Cycloleucine	Antagonist	Inanobe et al., 2005				
D-Alanine	Agonist	McBain et al., 1989				
D-AP5			Antagonist	Collingridge et al., 1983		
D-Cycloserine	part. Agonist	Furukawa et al., 2003				
D-Serine	Agonist	Furukawa et al., 2003			Agonist	Chatterton et al., 2002
Glutamate			Agonist	Furukawa et al., 2005	n/a	Chatterton et al., 2002
Glycine	Agonist	Furukawa et al., 2003 Furukawa et al., 2005			Agonist	Madry et al., 2007a Yao et al., 2008
HA-966	part. Agonist	Priestley et al., 1995				
Kynurenic acid	Antagonist	Elmslie et al., 1985				
L-Alanine	part. Agonist	McBain et al., 1989				
L-687414	part. Agonist	Priestley et al., 1995				
L-689560	Antagonist	Ivanovic et al., 1998				
L-701324	Antagonist	Kulagowski et al., 1994 Konieczny et al., 1999				
MDL-29951	Antagonist	Ivanovic et al., 1998				
NMDA			Agonist	Erreger et al., 2007	n/a	Chatterton et al., 2002

Table 1. Ligands of NMDAR-subunits and their respective published activity.
n/a means that no activity was measurable.

Our approach is based on several assumptions, one of these assumptions is that the LBD crystal structures reflect the *in vivo* behavior of the LBDs. Also we assumed that all of the ligands bind in the same binding pocket, as indicated by previous crystal structures (Furukawa et al., 2003, Inanobe et al., 2005), and that the 5,7-DCKA-bound GluN1 structure (PDB ID: 1PBQ) reflects the apo-state of the LBD as suggested by Furukawa et al. (2003).

EXPERIMENTAL PROCEDURES

Molecular modeling of the NMDAR LBDs - Sequence alignment of the NMDA receptor subunits was taken from Sobolevsky et al. (2009). GluN1 LBD homology models are based on GluA2 crystal structures from: 1FTM (closed-cleft), 1FTK (partially closed-cleft), 3H03 (open-cleft) and 3H06 (maximally open-cleft). The GluN2A and GluN3A models are based on the GluN1 crystal structures of: 1Y1M

(partially closed-cleft), 1PBQ chain B (open-cleft), 1PBQ chain A (maximally open-cleft). We compared docking results from energy-minimized structures and non-minimized structures and we found that energy minimization led to an inaccessible binding pocket and therefore non-minimized structures were used in the docking experiments.
The models for the LBDs were generated using the Modeller program 9v7 (Fiser and Sali, 2003) and energy-minimized using Chimera build 2577 (Pettersen et al., 2004).

Docking experiments - The docking experiments with crystal structures and homology models were conducted using Autodock Vina (Trott et al., 2010). Autodock Vina has improved accuracy and speed compared to the commonly used Autodock 4. The scoring function in Autodock Vina assesses hydrophobic (i.e. van der Waals) interactions, hydrogen-bonded interactions as well as torsional penalties. Based on these parameters Autodock Vina calculates a gradient while seeking a local optimum. The final docked energy represents the binding energy of the ligand to the receptor. Thus, the binding energy largely depends on the ligand, consequently it is not advisable to compare binding energies between ligands. However, it is feasible to compare the binding energies of one ligand to different conformers. For each docking run the following residues were selected to have flexible side chains, their selection is based on direct involvement in binding modes observed in crystal structures (Furukawa et al., 2003, Inanobe et al., 2005, Furukawa et al., 2005, Yao et al., 2008):

- GluN1: F408, F484, T518, R523, S688, W731, D732
- GluN2A: H485, S511, T513, R518, S689, T690, D731
- GluN3A: Y605, S631, S633, R638, S801, D845

Note: Glycine and proline residues cannot have flexible side chains because glycine only has one hydrogen atom as its side chain and proline has no rotatable bonds.
A boundary box, also called the grid box, restricts the 3-dimensional docking space for the ligand. The grid box' size was adjusted to engulf the binding pocket and all the residues with flexible side chains. Autodock Vina then calculates grid maps for each atom type present in the protein and the ligand. Based on these grid maps the docking is being performed with the selected ligands (Fig. 1).

Pymol 1.3 (Schrödinger Inc., New York, NY, USA) was used for illustration.

RESULTS

Assessing the feasibility of docking experiments with crystal structures and homology models - According to the available crystal structures of the GluN1 LBD with glycine, cycloleucine and 5,7-DCKA (PDB IDs: 1PB7, 1Y1M, 1PBQ, respectively) the LBD can adopt conformations with differing clamshell-closure degrees. The S1 and S2 domains behave as relatively rigid bodies apart from the hinge region (Furukawa et al., 2003). In order to compare the 'openness' of the binding pocket we selected residues in each subdomain and measured the distance between their Cα-atoms. For GluN1 these are M501 (C-helix) with S688 (F-helix) and F458 (B-helix) with A714 (H-helix). The distances increase from 11.8/16.9 Å (closed-cleft) up to 14.6/19.9 Å (open-cleft)(Fig. 2A-D).

In a first set of experiments we tested whether Autodock Vina is able to predict the correct ligand bound conformations known from the crystal structures. For this, we used the following crystal structures and measured the root mean squared deviation (RMSD) in Angstrom (Å) from the crystallized position of the ligand:

- GluN1:	1PB7 (glycine)	0.624 Å
	1Y1M (cycloleucine)	0.034 Å
	1PBQ_B (5,7-DCKA)	0.045 Å
	1PBQ_A (5,7-DCKA)	0.056 Å
- GluN2A:	2A5S (glutamate)	1.395 Å
- GluN3A:	2RC7 (glycine)	0.578 Å
- GluA2:	1FTM (AMPA)	0.739 Å
	1FTK (kainate)	0 Å
	3H03 (UBP277)	0.793 Å
	3H06 (UBP282)	0.344 Å

Note: None of the docking results showed a greater RMSD than 1.395 Å, thus we conclude that the predicted binding modes by Autodock Vina are reliable.

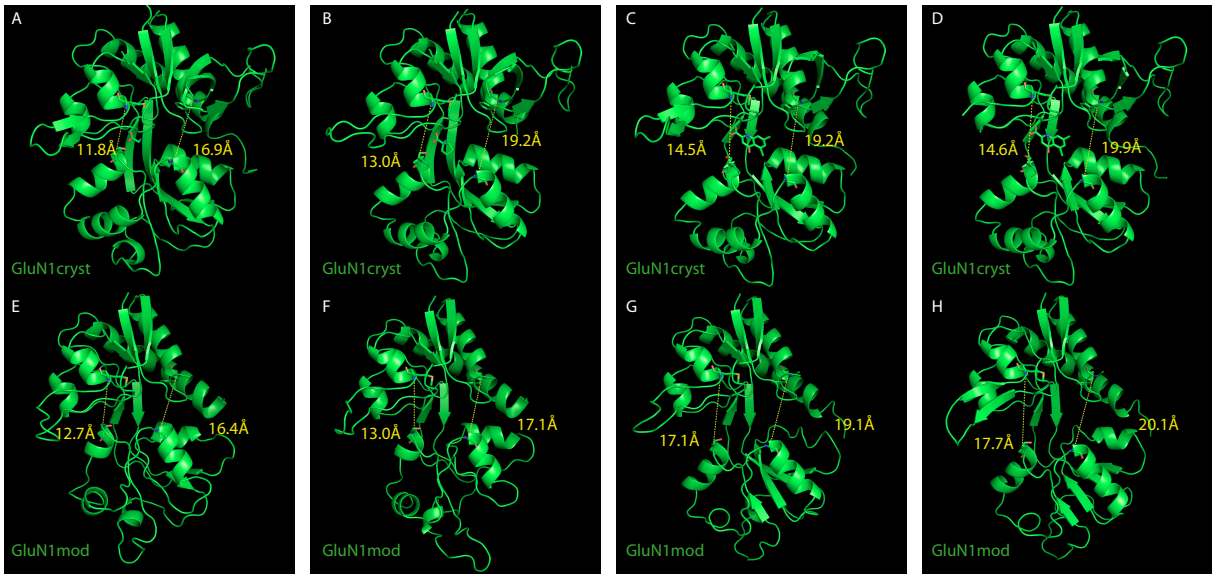

Fig. 2. Crystal structures and homology models of the GluN1 LBD. (A-D) GluN1 LBD crystal structures, PDB IDs 1PB7, 1Y1M, 1PBQ chain B and 1PBQ chain A, respectively, **(E-H)** GluN1 LBD homology models based on GluA2 LBD crystal structures, PDB IDs 1FTM, 1FTK, 3H03 and 3H06, respectively.
Yellow dotted lines indicate Cα-atom distances between residues M501 and S688 (left) and F458 and A714 (right).

In order to assess the feasibility of docking experiments with homology models we constructed models of the GluN1 LBD based on crystal structures of GluA2 LBDs. These were AMPA-bound (closed-cleft), kainate-bound (partially closed-cleft), UBP277-bound (open-cleft) and UBP282-bound structures (maximally open-cleft)(PDB IDs: 1FTM, 1FTK, 3H03 and 3H06, respectively). The GluA2 and GluN1 LBDs share a sequence identity of 30%. Again, measuring the distances between M501 and S688, as well as F458 and A714 of GluN1 shows an increase from 12.7/16.4 Å up to 17.7/20.1 Å (Fig. 2E-H). Comparing these distances to the GluA2 crystal structures that we used as templates we see deviations of not more than 1 Å. On the other hand, when we compare the distances from the GluN1 homology models to their respective crystal structures (PDB IDs: 1PB7, 1Y1M, 1PBQ chain B and 1PBQ chain A), we see deviations of up to ~3 Å. These deviations most probably arise because the different GluA2 conformers do not represent the exact degree of clamshell closure of the GluN1 LBD crystal structures.

Subsequently, we used the GluN1 LBD crystal structures and homology models for docking experiments. Each of the 21 ligands was docked into the four conformers of the crystal structures and the four conformers of the homology models and the binding energies were evaluated (Table 2). According to our hypothesis, each ligand will favor one conformer where the binding energy will be the lowest, this would be

reflected in the activity of the ligand *in vivo* (agonist, partial agonist, antagonist). In line with our hypothesis, large ligands docked best into the open-cleft conformers, i.e. 1PBQ chain B and 1PBQ chain A, whereas smaller ligands preferred the partially closed-cleft or closed-cleft conformations, i.e. 1Y1M and 1PB7, respectively. Looking at the docking energies with the GluN1 homology models we were surprised to see that 18 out of 21 ligands dock best into the partially closed-cleft conformation, i.e. N1_1FTK. This discrepancy with our hypothesis might be due to the fact that the GluA2 template structure possesses a larger binding pocket, as the respective agonist is glutamate, which is significantly larger than the GluN1 agonist glycine, i.e. the homology models might not recognize small changes in ligand size.

	GluN1 structures				GluN1 models			
Compound	**1PB7**	**1Y1M**	**1PBQ_B**	**1PBQ_A**	**N1_1FTM**	**N1_1FTK**	**N1_3H03**	**N1_3H06**
	binding energy [kcal/mol]				binding energy [kcal/mol]			
5,7-DCKA	-	-7.9	**-8.8**	-8.6	-	-8.7	-6.4	-6.0
5-CKA	-	-8.1	**-8.2**	-7.9	-	-8.4	-6.4	-6.3
7-CKA	-	-7.8	**-8.6**	-8.5	-	-8.2	-6.1	-6.0
ACBC	-	**-5.9**	-4.9	-4.4	-	-4.8	-3.7	-3.4
ACPC	-2.5	**-5.3**	-4.4	-4.3	-3.7	-4.6	-3.3	-3.3
CNQX	-	-8.0	**-8.5**	-8.3	-6.5	-7.8	-6.7	-6.2
Cycloleucine	-	**-6.6**	-5.2	-5.0	-4.0	-5.3	-4.1	-4.3
D-Alanine	-3.5	**-4.7**	-3.9	-3.8	-3.6	-4.1	-3	-3.2
D-AP5	-	**-5.7**	-5.2	-4.8	-5.2	-5.6	-7.2	-4.0
D-Cycloserine	-3.2	**-5.0**	-4.0	-4.0	-	-4.1	-2.8	-3.7
D-Serine	-3.9	**-4.8**	-4.2	-4.1	-3.4	-4.2	-2.6	-2.9
Glutamate	-	**-5.8**	-5.0	-5.0	-5.2	-5.6	-4.8	-3.9
Glycine	**-4.1**	-3.9	-3.5	-3.4	-3.4	-4.1	-2.7	-2.4
HA-966	-1.5	**-5.8**	-4.4	-4.4	-	-4.9	-3.5	-3.5
Kynurenic acid	-	-7.3	**-8.0**	-7.8	-6.8	-8.1	-6.2	-6.3
L-Alanine	-3.5	**-4.7**	-3.8	-3.9	-3.7	-4.0	-2.7	-3.2
L-687414	-	**-5.8**	-4.9	-4.7	-	-5.3	-4	-3.8
L-689560	-	-5.5	**-10.1**	-10.0	-	-	-8.9	-7.9
L-701324	-	-9.6	-10.3	**-10.9**	-	-	-9.7	-8.6
MDL-29951	-	-7.5	**-8.3**	-7.9	-4.4	-8.3	-6.5	-6.6
NMDA	-	**-5.4**	-4.7	-4.6	-	-5.7	-3.8	-3.3

Table 2. Docked energies of each ligand to GluN1 LBD crystal structures and homology models.
Lowest docked energies for each ligand are depicted in yellow.

Comparing the docking energies from GluN1 crystal structures and from homology models we found that out of 21 ligands, 13 ligands (~62%) are classified into the same group/activity (Table 2). The remaining 8 ligands (38%) differ in the conformer that results in the lowest binding energy. This indicates that our homology models lead to differing results in 8 of the 21 ligands compared to results obtained from crystal structures. Nevertheless, with 62% accuracy it should still be possible to estimate whether ligand size is the main determinant of ligand action or not. Next, we compared these docking results with the published functional activity of each ligand (Table 4). We consider a ligand as an agonist if the binding energy is lowest for the

closed-cleft conformation (Fig. 2A/E), a partial agonist if the energy is lowest for the partially closed-cleft conformation (Fig. 2B/F) and an antagonist if the energy is lowest for one of the two open-cleft conformations (Fig. 2C/D and G/H). According to this discrimination, the docking with the GluN1 crystal structures (Fig. 2A-D) leads to a ~90% correct prediction of the ligand activity whereas with the GluN1 homology models (Fig. 2E-H) we only get 50% correct predictions.

In summary, Autodock Vina correctly identifies ligand-binding modes verified with crystal structures. Furthermore, our hypothesis that the size of the ligand mainly determines its activity on the GluN1 LBD, by stabilizing different degrees of clamshell-closure, seems to be valid. Lastly, homology models that are used for docking experiments have a reduced, approx. 62%, accuracy compared to results obtained from crystal structures. Furthermore, the prediction of ligand activity based on our docking results with the GluN1 homology models is 50% accurate, i.e. in line with published functional activity.

Molecular mechanism of ligand activity at GluN2A and GluN3A LBDs - To date GluN2A and GluN3A LBDs have been crystallized only in the agonist bound closed-cleft conformation. Accordingly, we have no partial agonist or antagonist bound structure, which would help to disclose the conformational changes induced by agonist binding. In order to circumvent this problem we built homology models of the GluN2A and GluN3A LBDs using partial agonist and antagonist bound GluN1 LBD crystal structures (PDB IDs: 1Y1M, 1PBQ chain B and 1PBQ chain A)(Fig. 3B-D and 3F-H). Using this approach, we were able to generate different conformers with different degrees of clamshell-closure of the respective LBDs. In order to assess the degree of closure we measured the distances between the Cα-atoms of M462 and S655, as well as F425 and V679 of the GluN2A subunit. The homologous residues in the GluN3A subunit are L616 and S801, as well as Y579 and T825 (Fig. 3). Note that the distances closely resemble the distances measured in the GluN1 LBD (Fig. 2A-D).

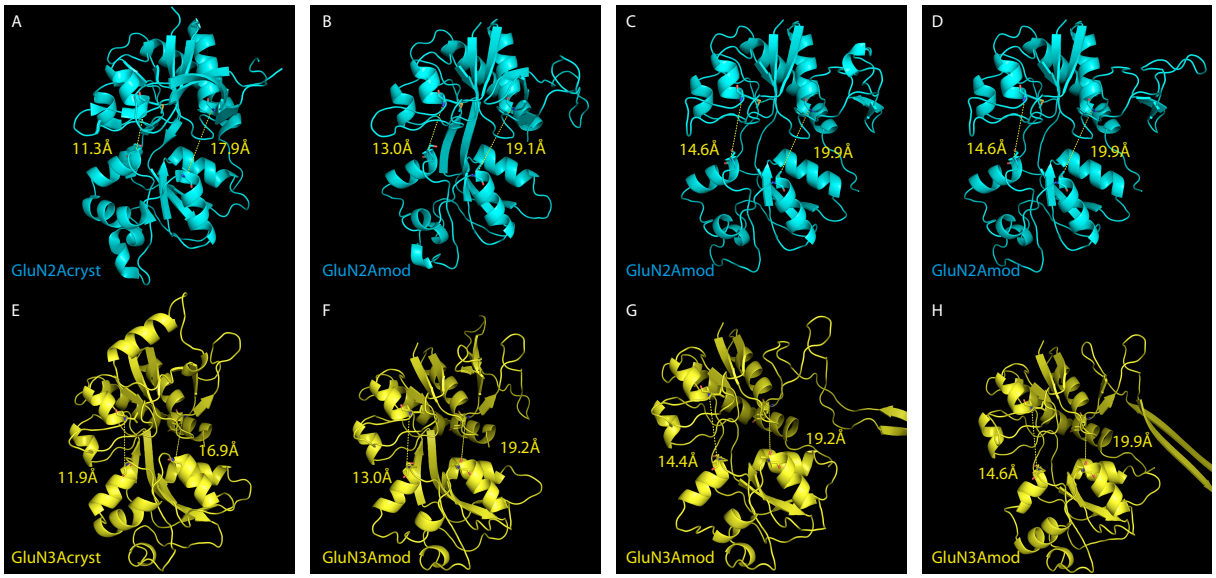

Fig. 3. Crystal structures and homology models of GluN2A and GluN3A LBDs. (A) GluN2A LBD crystal structure (PDB ID: 2A5S), **(B-D)** GluN2A LBD homology models based on GluN1 LBD crystal structures (PDB IDs: 1Y1M, 1PBQ chain B and 1PBQ chain A, respectively), **(E)** GluN3A LBD crystal structure (PDB ID: 2RC7), **(F-H)** GluN3A LBD homology models based on GluN1 LBD crystal structures (PDB IDs: 1Y1M, 1PBQ chain B and 1PBQ chain A, respectively).
Yellow dotted lines indicate Cα-atom distances between residues M462 (L616) and S655 (S801) (left) and F425 (Y579) and V679 (T825) of GluN2A (GluN3A) (right).

The fact that we have used GluN1 LBD crystal structures for modeling the GluN2A and GluN3A LBDs also means that we assume that these NMDAR LBDs perform the same conformational changes upon ligand binding. Whether this assumption holds true will only be uncovered when partial agonist- and antagonist-bound structures become available. Furthermore, based on our previous docking experiments with GluN1 homology models we can expect a 62% accuracy for docking to our homology models compared to results obtained from docking to crystal structures. Thus, we may not be able to correctly assign the conformation that is best stabilized by each ligand but a general tendency should become evident.

We docked the same 21 ligands which we used for the GluN1 LBD docking experiments and evaluated which conformer is favored by each ligand (Table 3).

	GluN2A models				GluN3A models			
Compound	**2A5S**	**N2A_1Y1M**	**N2A_1PBQ_B**	**N2A_1PBQ_A**	**2RC7**	**N3A_1Y1M**	**N3A_1PBQ_B**	**N3A_1PBQ_A**
	binding energy [kcal/mol]				binding energy [kcal/mol]			
5,7-DCKA	-	**-8.1**	-7.5	-7.5	-	**-8.0**	-7.3	-8.0
5-CKA	-4.7	**-7.9**	-6.9	-7.1	-	**-7.1**	-7.0	-7.0
7-CKA	-4.7	**-7.8**	-7.4	-7.3	-	-7.1	-7.0	**-7.3**
ACBC	**-5.6**	-5.0	-4.4	-4.8	-4.2	**-5.6**	-4.5	-4.2
ACPC	**-5.0**	-4.7	-3.4	-4.5	-4.5	**-4.8**	-3.6	-3.9
CNQX	-	-7.8	**-8.1**	-7.7	-	-7.3	**-8.6**	-8.4
Cycloleucine	**-6.0**	-5.4	-4.1	-5.2	-3.3	**-5.6**	-4.2	-4.6
D-Alanine	-3.8	**-4.5**	-3.6	-4.0	**-4.7**	-4.3	-2.5	-3.4
D-AP5	-5.2	**-5.4**	-4.5	-4.7	-	**-4.9**	-3.3	-4.1
D-Cycloserine	**-5.1**	-4.8	-4.2	-4.3	**-5.1**	-4.8	-3.4	-3.6
D-Serine	**-4.1**	-3.6	-4.0	-4.1	**-4.6**	-3.6	-3.4	-3.3
Glutamate	-5.3	**-5.6**	-4.9	-4.9	-	**-5.5**	-3.7	-4.0
Glycine	-	**-7.6**	-7.5	-7.4	-	**-7.8**	-7.0	-6.9
HA-966	**-4.7**	-4.5	-4.1	-4.1	**-4.7**	-3.9	-3.0	-3.7
Kynurenic acid	-5.3	-5.2	-5.5	**-5.6**	-	**-5.0**	-4.7	-4.7
L-Alanine	-4.1	-8.4	**-8.6**	-8.6	-	-7.4	-9.0	**-9.4**
L-687414	-7.0	-9.2	-9.2	**-9.8**	-	**-10.5**	-9.9	-9.9
L-689560	-4.5	-6.7	-6.8	**-7.0**	-	**-7.9**	-6.5	-7.6
L-701324	**-5.8**	-5.6	-5.8	-5.8	-4.2	-4.8	**-5.2**	-5.2
MDL-29951	**-6.7**	-5.6	-5.0	-5.0	**-5.4**	-5.4	-4.9	-4.9
NMDA	**-6.3**	-5.4	-4.9	-4.8	-4.6	**-5.3**	-5.0	-4.1

Table 3. Docked energies of each ligand to GluN2A and GluN3A LBD homology models.
Lowest docked energies for each ligand are depicted in yellow.

The homology models were built using the same templates, thus, one might expect that the results are very similar. Out of the 21 ligands that were docked only 10 ligands (48%) display the same docking results, i.e. have their lowest energies at the same conformers. This is a good indication that the results are not dominated by the template structure that has been used to build these models. It is noteworthy that large ligands such as MDL-29951 can also be docked into the closed-cleft conformation of GluN2A and GluN3A. But there is still a tendency that larger ligands dock best into the partially closed-cleft or open-cleft conformers (compare 5,7-DCKA, 5-CKA, 7-CKA, CNQX, D-AP5, Kynurenic acid and L-687414). Comparing the activity of each ligand, proposed by the docking results with the published activity, we find that for GluN2A only NMDA is correctly identified as an agonist (Table 4). L-Glutamate and D-AP5 have their lowest binding energy in the partially closed-cleft conformation rendering them falsely partial agonists in our model. The dockings correctly identified D-serine and CNQX as agonist and antagonist, respectively, of the GluN3A LBD (Table 4). Despite this, the agonist glycine docked best into the partially closed-cleft conformation.

Comparison of known and proposed activity of ligands on NMDAR LBDs

Compound	GluN1 cryst	GluN1 models	GluN2A models	GluN3A models
5,7-DCKA	Antagonist	part. Agonist	part. Agonist	part. Agonist
5-CKA	Antagonist	part. Agonist	part. Agonist	part. Agonist
7-CKA	Antagonist	part. Agonist	part. Agonist	Antagonist
ACBC	part. Agonist	part. Agonist	Agonist	part. Agonist
ACPC	part. Agonist	part. Agonist	Agonist	part. Agonist
CNQX	Antagonist	part. Agonist	Antagonist	Antagonist
Cycloleucine	part. Agonist	part. Agonist	Agonist	part. Agonist
D-Alanine	part. Agonist	part. Agonist	part. Agonist	Agonist
D-AP5	part. Agonist	Antagonist	part. Agonist	part. Agonist
D-Cycloserine	part. Agonist	part. Agonist	Agonist	Agonist
D-Serine	part. Agonist	part. Agonist	Agonist	Agonist
Glutamate	part. Agonist	part. Agonist	part. Agonist	part. Agonist
Glycine	Agonist	part. Agonist	part. Agonist	part. Agonist
HA-966	part. Agonist	part. Agonist	Agonist	Agonist
Kynurenic acid	Antagonist	part. Agonist	Antagonist	part. Agonist
L-Alanine	part. Agonist	part. Agonist	Antagonist	Antagonist
L-687414	part. Agonist	part. Agonist	Antagonist	part. Agonist
L-689560	Antagonist	Antagonist	Antagonist	part. Agonist
L-701324	Antagonist	Antagonist	Agonist	Antagonist
MDL-29951	Antagonist	part. Agonist	Agonist	Agonist
NMDA	part. Agonist	part. Agonist	Agonist	part. Agonist

Table 4. Comparison of docking results with proposed activities. Based on which LBD conformer each ligand docked to with the lowest energy we classified the ligands as agonist (docked best to closed-cleft conformation), partial agonist (docked best to partially closed-cleft conformation) or antagonist (docked best to open-cleft conformations). We used green color to highlight results that are in agreement with published results and red if they were not. No color means that no published results are available.

Out of 9 large ligands (5,7-DCKA, 5-CKA, 7-CKA, CNQX, D-AP5, Kynurenic acid, L-689560, L701324 and MDL-29951) 3 were found to dock best into the open-cleft conformation of GluN2A and GluN3A (N2A_1PBQ and N3A_1PBQ). For the partially closed-cleft conformations (N2A_1Y1M and N3A_1Y1M) 4 of the 9 large ligands for GluN2A and 5 ligands for GluN3A were found to have their lowest binding energy. The closed-cleft structure was preferred by 2 ligands for GluN2A and 1 ligand

for GluN3A, respectively. Taken together we found a general tendency that large ligands seem to stabilize conformations where the clamshell is at least partially open.

DISCUSSION

A unique feature of ionotropic glutamate receptors is the bilobed, clamshell-like structure of the LBDs and the clamshell closure upon ligand recognition. Crystal structures of various subunits of the different iGluR families have indicated that agonists and partial agonists induce the same degree of clamshell-closure. Here, we used an *in silico* approach to verify our hypothesis that partial agonists can induce full closure of the bilobed LBDs but the equilibrium is shifted towards a partially closed clamshell.

Our results show a tendency that more than other properties, the size of the ligand determines its activity (agonist, partial agonist or antagonist). However, using homology models for docking experiments reduces the significance and the accuracy of the results but this approach can give a rough estimate of a ligands action when no structural information is present.

GluN1, GluN2A and GluN3A LBDs might share similar ligand recognition mechanisms - According to our working hypothesis, i.e. ligand activity is determined by the degree of clamshell-closure and stabilization of this conformation, we were able to correctly identify the activity of a ligand with an accuracy of 83% using GluN1 LBD crystal structures. Using GluN1 LBD homology models this high degree of accuracy dropped to ~50%. For example with our docking approach, using GluN1 LBD crystal structures, we were able to correctly predict 8 out of 9 antagonists correctly, one wrongly identified as a partial agonist. In contrast, using the GluN1 LBD homology models, only 3 antagonists were correctly identified, the remaining 6 antagonists were classified as partial agonists. We obtained similar results from GluN2A and GluN3A docking experiments. For each subunit, 3 large ligands were identified as antagonists, 4 ligands for GluN2A and 5 ligands for GluN3A were classified as partial agonists, lastly 2 ligands for GluN2A and 1 ligand for GluN3A were classified as agonists. We take this as an indication that the mechanism of antagonism is similar or conserved between the NMDAR- as well as other iGluR-subunits. Despite these similarities the mechanism of partial agonism is more delicate. The GluN2 subunits are activated by glutamate and NMDA, molecules that

are larger in size than glycine, thus the binding pocket in the GluN2 subunits must be larger to accomodate the ligand. It is conceivable that partial agonists for the GluN2 subunits might be recognized by other mechanisms than their size.

Crystal structures and homology models are not ideal to analyze partial agonism - As aforementioned we cannot exclude the possibility that partial agonism relies on different molecular mechanisms in the different iGluR subunits. In order to find possible explanations other than the size of the ligand we closely investigated the crystal structures of GluA2 and GluN1 LBDs in agonist-bound and partial agonist-bound conformations. In a study by Furukawa et al. (2003) it was reported that a hydrogen-bonded interaction of L538 with F754 in the glycine-bound structure switches to F753 in the partial agonist-bound structures, which might be the cause for the low efficacy of partial agonists. However, the same has not been observed for AMPAR-subunits (Armstrong and Mayer, 2000). Thus, it is questionable if this interaction is the key to partial agonism. In our evaluations of the crystal structures we did not find possible explanations for the differences between agonism and partial agonism. This led us to rethink our assumptions. One of our assumptions was that the crystal structures resemble the *in vivo* behavior of the LBDs. But the LBDs are expressed as soluble proteins lacking other parts of the receptor. Thus, it might be the case that the molecular mechanism of partial agonism cannot be explained by analyzing the crystal structures of the isolated LBDs.

Using locked LBDs as a tool to identify partial agonists - Our data indicate that partial agonism might not be solely controlled by the (isolated) LBDs. While determining the action of a ligand is feasible in homodimeric receptors, such as GluA2-type AMPA receptors, it is more complicated in heterodimeric receptors such as NMDA-receptors. In order to use *in silico* approaches it is necessary to validate the models that are being used. Therefore, ligands must be unambiguously characterized and identified as partial agonists. Because of the complex structure of NMDA-receptors this is rather difficult. Previous studies have employed NMDAR subunits where the S1 and S2 subdomains are locked in the closed-cleft conformation using disulfide bridges by introducing cysteine mutations (Blanke and VanDongen, 2008, Kussius et al., 2010). It was found that locking the GluN1 LBD in its closed-cleft conformation leads to solely glutamate-gated GluN1/GluN2A

receptors. On the contrary, locking the GluN2A LBD leads to an overall agonist-independent increase in channel activity. This indicates that GluN1 and GluN2 subunits unequally participate in receptor activation with the GluN2 subunits being more important. We propose that such LBD locked subunits might prove useful tools to determine the activity of different ligands in detail. It is also advisable to combine docking experiments with molecular dynamics simulations. In detail, a LBD would be simulated for a fixed period and different conformations would then be used for docking experiments. This approach would provide many more conformers, thus a more complete understanding might be gained instead of using only 4 different conformers.

Conclusions - Using docking experiments with different crystal structures and homology models we put forward a model where the size of the ligand mainly determines its activity (agonist, partial agonist or antagonist) at iGluR LBDs. We did find good indications that this holds true for agonists and antagonists at GluN1, GluN2A and GluN3A LBDs. We have also good indications that partial agonists at the GluN1 LBD are not efficient at stabilizing the closed-cleft conformation. Docking experiments with homology models are not accurate enough to disclose whether GluN2A and GluN3A LBDs behave similar to the GluN1 LBD in this respect.

REFERENCES

Armstrong N, Gouaux E. Mechanisms for activation and antagonism of an AMPA-sensitive glutamate receptor: crystal structures of the GluR2 ligand binding core. *Neuron* 28: 165-181, 2000.

Blanke ML, VanDongen AM. Constitutive activation of the N-methyl-D-aspartate receptor via cleft-spanning disulfide bonds. *J Biol Chem* 283: 21519-21529, 2008.

Chatterton JE, Awobuluyi M, Premkumar LS, Takahashi H, Talantova M, Shin Y, Cui J, Tu S, Sevarino KA, Nakanishi N, Tong G, Lipton SA, Zhang D. Excitatory glycine receptors containing the NR3 family of NMDA receptor subunits. *Nature* 415: 793-798, 2002.

Collingridge GL, Lester RA. Excitatory amino acid receptors in the vertebrate central nervous system. *Pharmacol Rev* 41: 143-210, 1989.

Del Castillo J, Katz B. Interaction at end-plate receptors between different choline derivatives. *Proc R Soc Lond B Biol Sci* 146: 369-381, 1957.

DeLano WL. PyMOL. 2002.

Elmslie KS, Yoshikami D. Effects of kynurenate on root potentials evoked by synaptic activity and amino acids in the frog spinal cord. *Brain Res* 330: 265-272, 1985.

Erreger K, Geballe MT, Kristensen A, Chen PE, Hansen KB, Lee CJ, Yuan H, Le P, Lyuboslavsky PN, Micale N, Jorgensen L, Clausen RP, Wyllie DJ, Snyder JP, Traynelis SF. Subunit-specific agonist activity at NR2A-, NR2B-, NR2C-, and NR2D-containing N-methyl-D-aspartate glutamate receptors. *Mol Pharmacol* 72: 907-920, 2007.

Fiser A, Sali A. Modeller: generation and refinement of homology-based protein structure models. *Methods Enzymol* 374: 461-491, 2003.

Foster AC, Kemp JA, Leeson PD, Grimwood S, Donald AE, Marshall GR, Priestley T, Smith JD, Carling RW. Kynurenic acid analogues with improved affinity and selectivity for the glycine site on the N-methyl-D-aspartate receptor from rat brain. *Mol Pharmacol* 41: 914-922, 1992.

Furukawa H, Gouaux E. Mechanisms of activation, inhibition and specificity: crystal structures of the NMDA receptor NR1 ligand-binding core. *EMBO J* 22: 2873-2885, 2003.

Furukawa H, Singh SK, Mancusso R, Gouaux E. Subunit arrangement and function in NMDA receptors. *Nature* 438: 185-192, 2005.

Inanobe A, Furukawa H, Gouaux E. Mechanism of partial agonist action at the NR1 subunit of NMDA receptors. *Neuron* 47: 71-84, 2005.

Ivanovic A, Reilander H, Laube B, Kuhse J. Expression and initial characterization of a soluble glycine binding domain of the N-methyl-D-aspartate receptor NR1

subunit. *J Biol Chem* 273: 19933-19937, 1998.

Konieczny J, Ossowska K, Schulze G, Coper H, Wolfarth S. L-701,324, a selective antagonist at the glycine site of the NMDA receptor, counteracts haloperidol-induced muscle rigidity in rats. *Psychopharmacology (Berl)* 143: 235-243, 1999.

Kulagowski JJ, Baker R, Curtis NR, Leeson PD, Mawer IM, Moseley AM, Ridgill MP, Rowley M, Stansfield I, Foster AC, et a. 3'-(Arylmethyl)- and 3'-(aryloxy)-3-phenyl-4-hydroxyquinolin-2(1H)-ones: orally active antagonists of the glycine site on the NMDA receptor. *J Med Chem* 37: 1402-1405, 1994.

Kussius CL, Popescu GK. NMDA receptors with locked glutamate-binding clefts open with high efficacy. *J Neurosci* 30: 12474-12479, 2010.

Lampinen M, Pentikainen O, Johnson MS, Keinanen K. AMPA receptors and bacterial periplasmic amino acid-binding proteins share the ionic mechanism of ligand recognition. *EMBO J* 17: 4704-4711, 1998.

Leeson PD, Baker R, Carling RW, Curtis NR, Moore KW, Williams BJ, Foster AC, Donald AE, Kemp JA, Marshall GR. Kynurenic acid derivatives. Structure-activity relationships for excitatory amino acid antagonism and identification of potent and selective antagonists at the glycine site on the N-methyl-D-aspartate receptor. *J Med Chem* 34: 1243-1252, 1991.

Li J, Zagotta WN, Lester HA. Cyclic nucleotide-gated channels: structural basis of ligand efficacy and allosteric modulation. *Q Rev Biophys* 30: 177-193, 1997.

Madden DR. The structure and function of glutamate receptor ion channels. *Nat Rev Neurosci* 3: 91-101, 2002.

Madry C, Mesic I, Bartholomaus I, Nicke A, Betz H, Laube B. Principal role of NR3 subunits in NR1/NR3 excitatory glycine receptor function. *Biochem Biophys Res Commun* 354: 102-108, 2007.

McBain CJ, Kleckner NW, Wyrick S, Dingledine R. Structural requirements for activation of the glycine coagonist site of N-methyl-D-aspartate receptors expressed in Xenopus oocytes. *Mol Pharmacol* 36: 556-565, 1989.

Monod J, Wyman J, Changeux JP. ON THE NATURE OF ALLOSTERIC TRANSITIONS: A PLAUSIBLE MODEL. *J Mol Biol* 12: 88-118, 1965.

Pettersen EF, Goddard TD, Huang CC, Couch GS, Greenblatt DM, Meng EC, Ferrin TE. UCSF Chimera--a visualization system for exploratory research and analysis. *J Comput Chem* 25: 1605-1612, 2004.

Priestley T, Laughton P, Myers J, Le Bourdelles B, Kerby J, Whiting PJ. Pharmacological properties of recombinant human N-methyl-D-aspartate receptors comprising NR1a/NR2A and NR1a/NR2B subunit assemblies expressed in permanently transfected mouse fibroblast cells. *Mol Pharmacol* 48: 841-848, 1995.

Ramakers GM, Peeters BW, Vossen JM, Coenen AM. CNQX, a new non-NMDA receptor antagonist, reduces spike wave discharges in the WAG/Rij rat model of absence epilepsy. *Epilepsy Res* 9: 127-131, 1991.

Sobolevsky AI, Rosconi MP, Gouaux E. X-ray structure, symmetry and mechanism of an AMPA-subtype glutamate receptor. *Nature* 2009.

Trott O, Olson A. J. AutoDock Vina: improving the speed and accuracy of docking with a new scoring function, efficient optimization and multithreading, *Journal of Computational Chemistry 31 (2010) 455-461*

Yao Y, Mayer ML. Characterization of a soluble ligand binding domain of the NMDA receptor regulatory subunit NR3A. *J Neurosci* 26: 4559-4566, 2006.

FOOTNOTES

*This study was supported by the Max-Planck Gesellschaft, Deutsche Forschungsgemeinschaft (B.L., LA 1086/4-2), Gemeinnützige Hertie-Stiftung (B.L.) and Fonds der Chemischen Industrie (H.B.).

CHAPTER 3
ROLE OF HETERODIMER INTERFACE INTERACTIONS IN THE LIGAND-BINDING DOMAIN FOR NMDA RECEPTOR FUNCTION

Ceyhun Tamer[1,2], Heinrich Betz[1,+], Kay Hamacher[3] and Bodo Laube[1,2]
From [1]Department of Neurochemistry, Max-Planck-Institute for Brain Research, Deutschordenstrasse 46, 60528 Frankfurt am Main, Germany
[2]Department of Molecular and Cellular Neurophysiology, TU-Darmstadt, Schnittspahnstrasse 3, 64287 Darmstadt, Germany
[3]Department of Computational Biology and Simulation, TU-Darmstadt, Schnittspahnstrasse 9, 64287 Darmstadt, Germany
[+]Present address: Max-Planck-Institute for Medical Research, Jahnstrasse 29, 69120 Heidelberg, Germany

***N*-Methyl-D-Aspartic acid (NMDA) receptors belong to the family of ionotropic glutamate receptors (iGluRs) that mediate the majority of the excitatory neurotransmission in the mammalian central nervous system. Conventional NMDA receptors composed of two glycine-binding GluN1 and two glutamate-binding GluN2 subunits require simultaneous binding of both ligands within their ligand-binding domains (LBD) for channel opening. Based on structural and functional studies, a mechanistic model for the activation and desensitization of the NMDA receptor has emerged. Accordingly, agonist occupation of both, the GluN1 and GluN2 LBDs, which are arranged as hetero-dimers in a ´back-to-back´ fashion, leads to closures of the LBDs that generates sufficient conformational strains resulting in channel opening. Subsequent weakening of the heteromeric GluN1/GluN2-LBD dimer interface is assumed to lead to receptor desensitization which is influenced by the N-terminal domains (NTD) of the respective subunits. Thus, to investigate the impact of residues within the GluN1/GluN2 LBD heterodimer interface for NMDAR function we generated single-point mutations in the interface of the GluN1/GluN2 LBDs in NTD-deleted NMDA receptor subunits (GluN1$^{\Delta}$, GluN2$^{\Delta}$) and analyzed their functional properties by TEVC upon heterologous expression in *Xenopus* oocytes. Residues implicated in interface interactions were identified by the GluN1/GluN2A LBD crystal structure and mutual information and mutated to alanine. The mutations we introduced caused changes in apparent glycine and glutamate affinities and also desensitization properties as well as maximal inducible currents were affected. However, the effects were moderate and unspecific. Thus, it was not possible to infer specific roles for the interface interactions. Nevertheless, the GluN1-E781A mutation consistently led to a decrease in apparent glutamate affinity and I_{Max}**

in GluN1$^{\Delta}$/GluN2A$^{\Delta}$ and GluN1$^{\Delta}$/GluN2B$^{\Delta}$ receptors. This effect was rescued by the GluN1-NTD but not the NTD of GluN2A. Our data show that reduced stability of GluN1/GluN2 LBD interactions upon mutation of single interface residues can be compensated selectively by the GluN1 NTD implicating a prominent role of the GluN1 NTD on LBD interface stability.

Introduction

N-Methyl-D-aspartic acid (NMDA) receptors are heterotetrameric complexes that are involved in excitatory neurotransmission in the CNS (Johnson and Ascher, 1987, Laube et al., 1998). Together with the (RS)-2-amino-3-(3-hydroxy-5-methyl-4-isoxazolyl)propionic acid (AMPA) and kainate (KA) receptors they form three distinct subfamilies in the family of ionotropic glutamate receptors (iGluRs). The respective subunits of the iGluRs share a common modular composition of (i) a large extracellular N-terminal domain (NTD) which was implicated in oligomerization of subunits and modulation of receptor function, (ii) a bilobed extracellular ligand-binding domain (LBD), (iii) the channel forming membrane associated domain (TMD) consisting of three membrane spanning domains and one re-entry loop, and (iv) an intracellular C-terminal domain (CTD) involved in interactions with scaffolding and signal transduction proteins (reviewed in Madden, 2002). NMDA-receptors are unique within the family of iGluRs with respect to their pharmacological properties and their pivotal role during brain development and neurological disorders (Nakanishi et al., 1992, Collingridge et al., 1995, Dingledine et al., 1999, Endele et al., 2010). In the heterotetrameric complex two obligate GluN1-subunits are associated with two GluN2-subunits in the case of the conventional NMDA-receptor (Sucher et al., 1995, Laube et al., 1997, Nishi et al., 2001, Yao and Mayer, 2006). The GluN1- and GluN2-LBDs form heterodimers in a back-to-back conformation similar to AMPA- (GluA) and kainate-LBDs (GluK) (Armstrong and Gouaux 2000, Furukawa et al., 2005, Mayer et al., 2006). Although previous studies examined the role of LBD interface contacts it is still a matter of debate if and in which way these contacts determine functional properties such as ligand affinities, desensitization and maximal inducible currents (I_{Max}) (Swanson et al., 1997, Stern-Bach et al., 2000, Sun et al., 2002, Furukawa et al., 2005, Borschel et al., 2011).

Studies on AMPA- and kainate-receptors demonstrated that during receptor activation the ligand-binding domain closes in a clamshell-like fashion, i.e. the S2-

subdomain converges towards the S1-subdomain, which results in opening of the ion channel. This conformation however strains the LBD dimer interface and, depending on the stability of the LBD dimer interface interactions, these contacts are disrupted and the receptor adopts a desensitized state (see Fig. 1A). Thus it is thought that the strength of the dimer interface contacts is directly correlated to the desensitization properties and even a single mutation (e.g. L483Y in GluA2) is capable of rendering the receptor non-desensitizing (Stern-Bach et al., 1998, Sun et al., 2002, Mayer 2006, Armstrong et al., 2006, Chaudhry et al., 2009).

The crystallization of the heterodimeric GluN1-GluN2A LBD crystal structure allows further analysis with respect to structure-function relationship of NMDA-receptors (Furukawa et al., 2005). Three distinct interface contacts (sites I-III, see Fig. 1B) between the GluN1- and GluN2A-LBDs were identified and the GluN1 residues N521, K531, Q696, R755 and E781A were reported to make polar contacts with the GluN2A-LBD. Due to similarities with the GluA2 dimer interface it is concluded that the D- and J-Helices (sites I and III, see Fig 1B,C and E) determine receptor desensitization properties (e.g. GluN1-N521 and GluN1-E781)(Fig. 1). It was also reported that the site I residue GluN1-N521 is involved in the heterodimerization process, whereas site II contacts, especially GluN1-Y535, are thought to be involved in receptor deactivation. Site II is also known as a binding site for allosteric modulators in AMPA-receptors and thus it is hypothesized that the large GluN1-Y535 side chain is an inherent modulator of NMDA-receptor deactivation.

However, there is no study to date that characterizes the sites I-III extensively in NMDA-receptors. In spite of the homology between AMPA-, kainate- and NMDA-receptors there are also large differences with regard to the extent of receptor desensitization (i.e. NMDA-receptors desensitize much slower), the unique requirement in conventional NMDA-receptors for two agonists (i.e. glycine and glutamate), the Mg^{2+}-block at NMDARs at resting membrane potential and the obligate heteromeric stoichiometry. The heterodimerization of NMDA-receptor subunits poses an important step in the assembly process (Schuler et al., 2008). As NTD-lacking NMDA-receptors are able to form functional receptors (Madry et al., 2007b) we hypothesized that the heterodimeric LBD contacts might play an essential role in the assembly process. Thus, we reasoned that subtype-specific heterodimer association is organized by certain contacts in the LBDs.

In order to identify residues that are important for receptor function and assembly, we analyzed the GluN1-GluN2A LBD crystal structure by Furukawa et al. (2005). We also applied a bioinformatics approach called mutual information (MI). This approach can be used to identify residues in the NMDA-receptor heterodimer interface that are evolutionary interdependent (Weil et al., 2009). The MI analysis quantifies the amount of information about one specific position in the alignment inferred from knowing the amino acid at another specific position (MacKay, 2003). Such information about another position might be present because such two positions require mutating simultaneously in order to keep the receptor functional for example. Also such two positions might be interdependent because they are in close proximity, and thus interact with each other, in the tertiary structure despite the fact that MI calculation only uses 1-dimensional (i.e. sequence) information. Using the MI approach we identified residues in the D- and J-Helices that gave highly significant interdependency signals.

We chose to assess the effect of single amino acid substitutions in NTD-lacking receptors as it was reported that the NTDs of NMDA-receptors are able to determine receptor properties such as agonist affinities, open probability, deactivation and desensitization (Madry et al., 2007b, Gielen et al., 2009, Yuan et al., 2009). Working on such a reduced receptor model (i.e. NTD-lacking receptor) should allow for unambiguous interpretation of the effects caused by the mutations. Also we tested the effect of interface mutations with partially NTD-deleted receptors.

EXPERIMENTAL PROCEDURES

cDNA constructs, heterologous expression and electrophysiology - The cDNA constructs of GluN1-1a, GluN1$^{\Delta}$, GluN2A, GluN2A$^{\Delta}$ and GluN2B$^{\Delta}$ have been described previously (Madry et al., 2007b). Single point mutations were introduced via site-directed mutagenesis (QuikChange XL Site-Directed Mutagenesis Kit, Stratagene) and confirmed by DNA sequencing (Eurofins MWG Operon). All constructs were linearized and transcribed into cRNA (mCAP mRNA Capping Kit, Ambion) as described (Madry et al., 2010). For electrophysiological analysis, *Xenopus laevis* oocytes were injected with 40 ng of the respective wt or mutant GluN1 and GluN2 cRNAs at a ratio of 1:2. Oocytes were isolated enzymatically or manually and maintained as described previously (Laube et al., 1997). 2-4 days after

injection, two-electrode voltage-clamp (TEVC) recordings of whole-cell currents was performed according to (Laube et al., 1997).

Mutual Information analysis - Sequence alignment of the iGluR-receptor subunits was taken from (Sobolevsky et al., 2009) and supplemented with the sequences of GluA1-4, GluK1-4, GluN1, GluN2A-D and GluN3A-B from different species which gave a total of 257 sequences that were downloaded from NCBI. The alignments were computed using Geneious Software (v.4.8.3, Biomatters Ltd., Auckland, New Zealand) and then the alignment was optimized by hand and trimmed to the D- and J-Helices only. The data set consisting of all 257 sequences is referred to as 'iGluR alignment', whereas a second data set consisting of all the iGluR-subunits without the GluN2- and GluN3-subunits is referred to as 'iGluR w/o GluN2/3 alignment' (210 sequences) and should resemble the LBDs that are capable of forming homodimers. Last, a third data set consisting of only the GluN2/3-subunits was composed and is referred to as 'GluN2/3 alignment' (47 sequences), which should resemble the LBDs that strictly require heterodimerization. These different data sets have been used to identify residues that are especially important for the heterodimeric NMDA-receptors. In the MI analysis interdependencies between pairs of positions in a multiple sequence alignment are calculated. If it is possible to infer the amino acid at a certain position by knowing the amino acid at another position, these two positions will have a high MI value, thus they are interdependent. If it is not possible to infer the amino acid at another position, such a pair will have a low MI value and thus they are not interdependent. The MI is calculated according to the following equation:

$$MI(X;Y) = \sum_{x}\sum_{y} p(x,y)\log_2\left(\frac{p(x,y)}{p(x)p(y)}\right)$$

p(x) and *p(y)* represent the frequencies of each amino acid type at position *X* or *Y*, respectively. The probability to observe the combination of these two amino acids is given by *p(x,y)*. Apart from the 20 standard amino acids, *x* and *y* can have a gap "-" or "X" for non-standard amino acids as their values. The MI calculation results in a *N x N* matrix with *N* being the sequence length of the multiple sequence alignment. Thus the symmetrical MI matrix holds $\frac{N(N+1)}{2}$ values, one for each pair of positions in the alignment. The calculation was performed using the statistical software package R (v.2.10, R Development Core Team 2011) and the BioPhysConnectoR library

(Hoffgaard et al., 2010). Based on the sequence alignment the MI matrix was computed and standardized to a null model with 10,000 randomization steps (White et al., 2007, Weil et al., 2009). The null model consists of the same alignment but the amino acids in each column are shuffled vertically in their position as to remove the sequence correlation. In each randomization step a new null model MI matrix is computed. The expectation value from the null model m_{ij} is the average of the 10,000 *(i,j)* entries and together with the corresponding variances the Z-scores can be calculated. For this, the null model was subtracted from the MI matrix and the resulting matrix was divided by the standard deviation (square root of the variance). The entries in the resulting matrix represent Z-scores, which are normalized onto the standard deviation. Thus each Z-score has the standard deviation as its unit e.g. a value of 10 means that the Z-Score is 10 standard deviations away from the expectation value m_{ij}. Because of its symmetry the diagonal and the lower triangle of the Z-score matrix were set to 0. For subsequent data analyses Microsoft Excel (v.2011) and for visualization purposes PyMOL v.1.3 (Schrödinger Inc., New York, NY, USA) were used.

For statistical data analysis Graphpad Prism v.5.0a (GraphPad Software Inc., San Diego, CA, USA) has been used.

For all analyses, values are given as means ± SEM if not stated otherwise.

Statistical significance was tested with one-way ANOVA and the Dunnett Post-Hoc-Test. For all *p*-values applies (*) $p<0.01$, (**) $p<0.001$ if not stated otherwise.

RESULTS

Our aim was to identify crucial LBD interface interactions that determine functional properties such as apparent agonist affinities, extent of receptor desensitization and the maximal inducible currents. Also we would like to understand how obligatory heterodimerization of the NMDA-receptor subunits is accomplished on a molecular level.

Selection of amino acids for mutagenesis studies - First the GluN1-GluN2A LBD crystal structure by Furukawa et al. (2005)(Fig. 1A, 1B) was analyzed and we focused on the interaction site I which involves the D-Helix of the GluN1 and the J-Helix of the GluN2-subunits. In this site, the GluN1-N521 residue forms a polar interaction with the backbone carbonyl oxygen of L777 in GluN2A (L778 in GluN2B)

(Fig. 1C). This interaction has been implicated in desensitization and assembly of AMPA- and NMDA-receptors (Stern-Bach et al., 1998, Furukawa et al., 2005).

The site II interactions include a hydrogen-bond between K531 in the GluN1 with the backbone carbonyl oxygen of a phenylalanine residue (Fig. 1D) (F524 in GluN2A, F525 in GluN2B). Notably, this interaction is conserved between all AMPA- and NMDA-receptor subunits. The role of this interaction is presently unclear.

Another residue at site II is GluN1-Y535. Previously it was found that mutations of the GluN1-Y535 residue modulate deactivation (Furukawa et al., 2005) and it was concluded that the large side chain of the tyrosine residue mimics the action of allosteric modulators (e.g. Aniracetam) known to bind in the LBD dimer interface in AMPA-receptors (Jin et al., 2005).

In a similar vein to site I, the site III interaction involves the J-Helix of GluN1 and the D-Helix of GluN2. Here the GluN1-E781 residue in the GluN1 subunit makes a hydrogen-bonded interaction with the backbone nitrogen of E516 in the GluN2A (Fig. 1E) (E517 in GluN2B). Interestingly, this residue (GluN1-E781) is conserved in more than 97% of “iGluR w/o GluN2/3 alignment” subunits. The GluN2- and GluN3-subunits, however, have strictly aliphatic non-polar residues at this position.

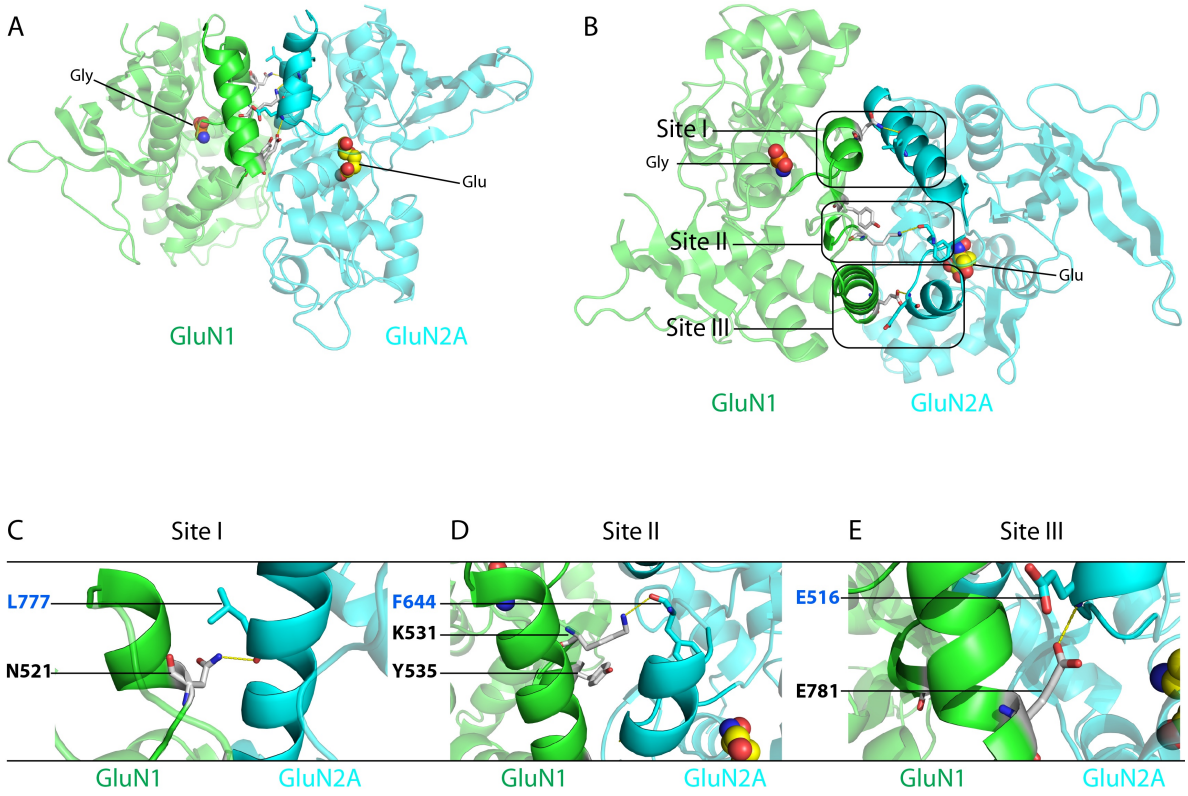

Fig. 1. GluN1-GluN2A LBD heterodimer interface interactions. (A) Side view of the GluN1-GluN2A heterodimer in the back-to-back conformation in complex with glycine and glutamate, respectively. The GluN1 subunit is colored in green whereas GluN2A is cyan. D- and J-helices of the respective subunits are highlighted for a better orientation. **(B)** Top view

of the GluN1-GluN2A heterodimer, the interface is classified into three distinct interaction sites (site I-III) depicted in the rectangles. This classification is according to Furukawa et al., 2005. **(C-E)** Magnification of the three interaction sites (I-III). Dashed lines indicate polar interactions. The residues participating in intersubunit contacts are shown as sticks and are colored in white (GluN1) and cyan (GluN2A).

Second MI analysis was applied to identify evolutionary interdependencies between residues in the D- and J-Helices (site I and III). First, we made a histogram of the Z-scores to get an idea how the values are distributed. The histogram indicates a bimodal distribution with the two centers of each distribution closely together (see Fig. 2A). This might be due to distinct signals, i.e. distributions, which are partially overlapping. Based on this observation we propose to discard the first culmination of Z-scores (Z-scores < 30) because supposedly these values may be distorted by a false random signal. We made the calculations for three data sets: iGluR alignment, iGluR alignment w/o GluN2/3 alignment and GluN2/3 alignment (see Experimental procedures). Out of the respective results we filtered correlations that were present in the iGluR alignment and the GluN2/3 alignment but not in the iGluR w/o GluN2/3 alignment. Thus, we intended to identify residues that are specifically important for the unique features of the heteromeric NMDA-receptors but not the iGluRs in general. The resulting correlations are shown in Fig. 2B for GluN1, GluN2A and GluN3A as examples as we focused on the analysis of NMDARs in this study. We did not observe motifs where every 3rdor 4th residue is correlated. Thus, we conclude that the residues that are correlated fulfill certain functions based on the nature of their interactions (e.g. polar interactions). In the following we will mainly concentrate on the GluN1-subunit as this subunit is incorporated into every NMDA-receptor and thus it is possible to analyze different subunit compositions (i.e. GluN1/GluN2A and GluN1/GluN2B). Interestingly the correlation that received the highest Z-score is between GluN1-N521 and GluN1-E781 (see Fig. 2C #1). These residues had been implicated in the dimerization and desensitization properties of AMPA- and NMDA-receptors (Stern-Bach et al., 1998, Furukawa et al., 2005). Both of these residues directly point and make hydrogen-bonds with the opposing subunit. For the correlations #2 and #8 (see Fig. 2C #2 and #8) a hydrophobic amino acid is correlated with a hydrophilic residue of which both point into the LBD dimer interface. These correlations might not be important for the GluN1-subunit but eventually for the GluN2- or GluN3-subunits. For example instead of the A524 residue in GluN1 the homologous position in the GluN3A-subunit is occupied by a hydrophilic serine (i.e.

S639). The remaining correlations #3-7 and #9-10 have either hydrophilic amino acids that do not point into the LBD dimer interface or they are pointing to the opposing subunit but are hydrophobic (see Fig. 2C #3-7 and #9-10). To test for a functional role we decided to introduce neutral alanine mutations at the positions GluN1-N521 and GluN1-E781. Also to assess the role of site II residues, we introduced alanine mutations at the positions GluN1-K531 and GluN1-Y535. (see Fig. 1D).

A

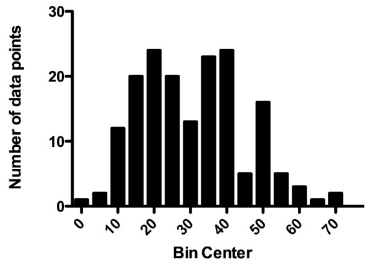

B

		GluN1		GluN2A		GluN3A	
	Z-score	Pos. 1	Pos. 2	Pos. 1	Pos. 2	Pos. 1	Pos. 2
1	36.44	E781	N521	G785	E516	S896	T636
2	34.90	E781	A524	G785	S519	S896	S639
3	26.39	K769	E522	K772	E517	T884	A637
4	23.62	E781	E522	G785	E517	S896	A637
5	20.56	S779	L777	F783	L780	Y894	S892
6	20.21	L774	K769	L777	K772	E889	T884
7	19.11	E781	Q525	G785	E520	S896	Q640
8	17.08	L777	N521	L780	E516	S892	T636
9	16.48	L777	E522	L780	E517	S892	A637
10	15.10	L777	N771	L780	Q774	S892	N886

C

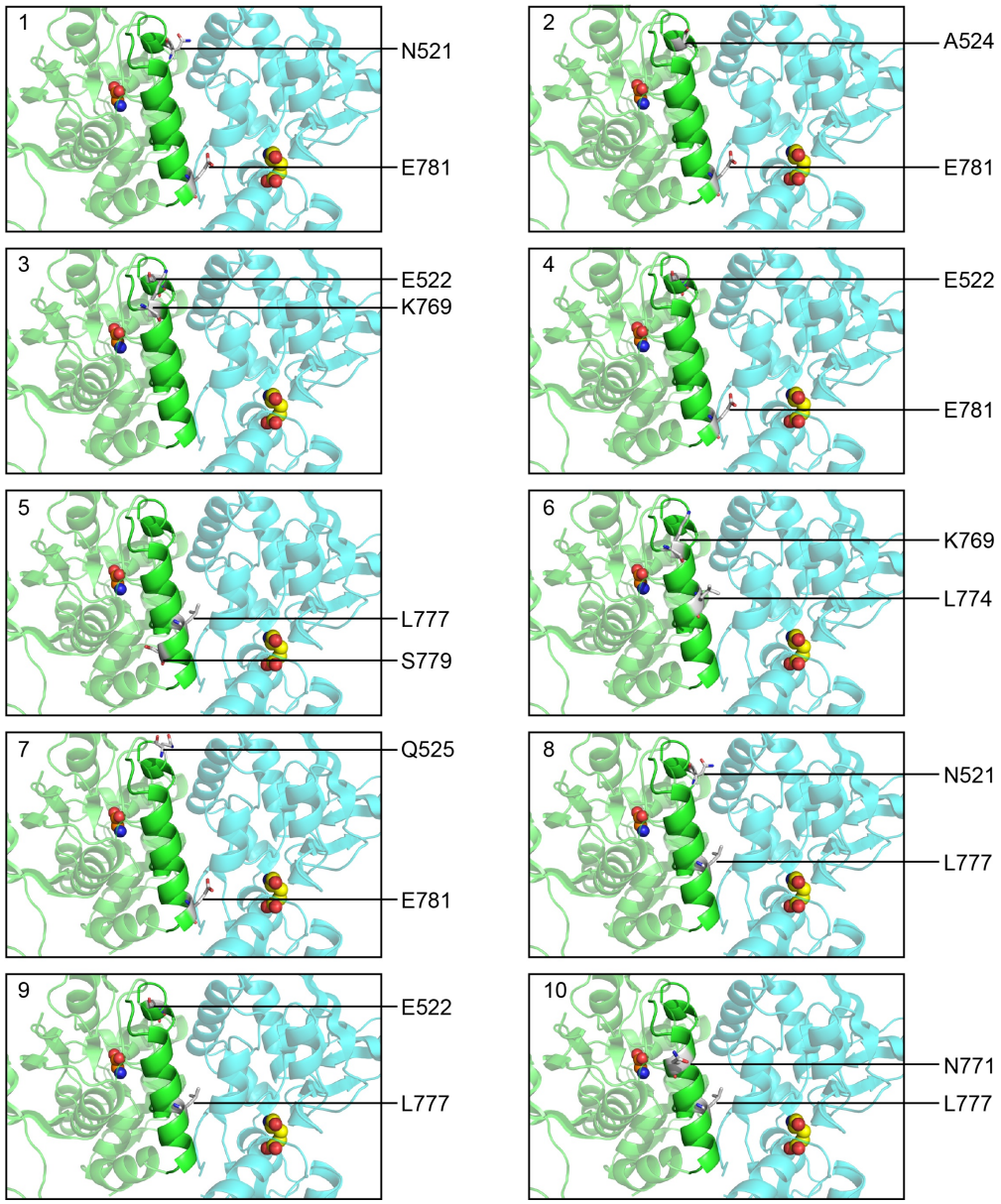

Fig. 2. Results of Mutual Information analysis. (A) Example of Z-score distribution for iGluR alignment. High values represent higher significance of the results. **(B)** Correlations that were found by MI analysis in the D- and J-Helices of GluN1-, GluN2A- and GluN3A-subunits. These results represent correlations that were found in the iGluR and GluN2-GluN3 LBD data set but not the homomeric iGluR LBD data set. **(C)** Visualization of the 10 most significant MI correlated residues (white sticks) in the GluN1 subunit (green) together with the GluN2A subunit (cyan).

We used the MI analysis as a tool to identify critical residues in the GluN1-GluN2A LBD crystal structure and we intend to identify molecular mechanisms that determine functional properties of the iGluR-subunits.

Electrophysiological characterization of GluN1 LBD mutations - We introduced mutations in the GluN1-LBD to disrupt the GluN1-GluN2 heterodimer interface. These mutations are GluN1-N521A, -K531A, -Y535A and –E781A. These mutants were expressed in the heterologous *Xenopus* oocyte system and characterized using TEVC. The GluN1 mutations were tested in NTD-lacking GluN1$^{\Delta}$/GluN2A$^{\Delta}$- and GluN1$^{\Delta}$/GluN2B$^{\Delta}$-receptors (Fig. 3A and 3B respectively). We assessed the effects of the mutations on apparent agonist affinities, extent of desensitization and maximal inducible currents (I_{Max})(Fig. 3).

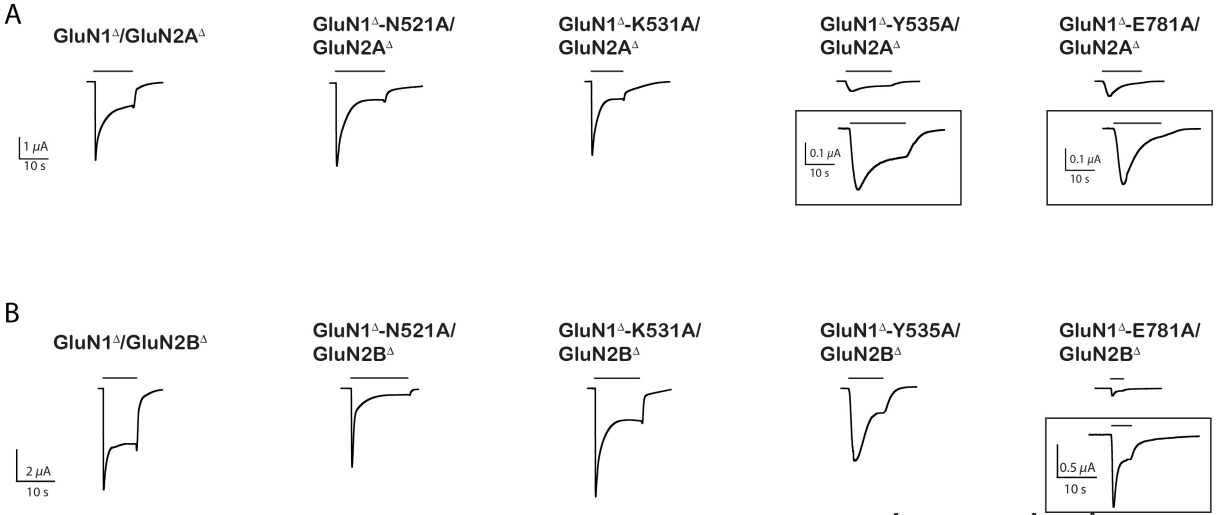

Fig. 3. Agonist-induced traces of N-terminal deleted GluN1$^{\Delta}$/GluN(2A$^{\Delta}$/2B$^{\Delta}$) NMDA receptors. (A and B) Here are shown agonist-induced traces of wt and mutant GluN1$^{\Delta}$/GluN2A$^{\Delta}$- and GluN1$^{\Delta}$/GluN2B$^{\Delta}$-receptors.

The analysis of glycine EC_{50} values shows that the GluN1-Y535A mutation decreases the apparent affinity in GluN1$^{\Delta}$/GluN2A$^{\Delta}$-receptors (wt 4.87±0.72μM, GluN1$^{\Delta}$-Y535A/GluN2A$^{\Delta}$ 16.29±1.73μM, p<0.001) whereas in GluN1$^{\Delta}$/GluN2B$^{\Delta}$-receptors it is the GluN1-E781A mutation that causes a decrease (wt 1.70±0.40μM, GluN1$^{\Delta}$-E781A/GluN2B$^{\Delta}$ 11.11±1.76μM, p<0.001)(Table 1 and Fig. 4A). A similar result was found for the glutamate EC_{50} values as the GluN1 mutant K531A caused a significant reduction in the apparent affinity when expressed with GluN2A$^{\Delta}$ (Table 1 and Fig. 4B). In combination with the GluN2B$^{\Delta}$ subunit this mutation had no effect. Instead the GluN1-N521A mutant reduced the glutamate EC_{50}. However, the GluN1-

Y535A and –E781A mutations decreased the glutamate EC_{50} significantly in both receptor combinations (Table 1 and Fig. 4B). Notably, the GluN1-Y535A and –E781A mutations each led to a reduction in EC_{50} in 4 of 5 cases. However the reduction was at best a highly significant but modest 14.5-fold (Glu EC_{50} $GluN1^{\Delta}/GluN2B^{\Delta}$ 0.62±0.05μM vs $GluN1^{\Delta}$-E781A/$GluN2B^{\Delta}$ 9.05±1.24μM, p<0.001).

Next we analyzed the extent of desensitization by comparing the agonist-induced peak currents and steady-state currents. The quotient of these two values gives an estimate of the extent of desensitization. According to our MI analysis we expected the GluN1-N521A and GluN1-E781A mutations to result in the strongest effects. Looking at the $GluN1^{\Delta}/GluN2A^{\Delta}$ receptor combination our hypotheses was validated; the extent of desensitization was increased from 48±9% to 78±3% (p<0.001) and 83±6% (p<0.001), respectively (Table 1 and Fig. 4C). However, we also observed an increase in the extent of desensitization with the GluN1-K531A mutation, which was 77±2%. In comparison with the $GluN1^{\Delta}/GluN2B^{\Delta}$ receptor combination we observed an increase in the extent of desensitization only with the GluN1-N521A mutation (wt 56±4%, $GluN1^{\Delta}$-N521A/$GluN2B^{\Delta}$ 87±1%, p<0.001)(Table 1 and Fig. 4C).

The last parameter we intended to determine is the I_{Max}. This parameter is very variable and largely depends on the variability of protein expression in *Xenopus* oocytes. Nonetheless, the $GluN1^{\Delta}$-K531A/$GluN2A^{\Delta}$ mutant receptor showed an increased I_{Max} (wt 4.00±0.44μA, $GluN1^{\Delta}$-K531A/GluN2A 7.97±1.15μA, p<0.001) whereas the GluN1-Y535A and –E781A mutations decreased the I_{Max} ($GluN1^{\Delta}$-Y535A/$GluN2A^{\Delta}$ 0.32±0.08μA, $GluN1^{\Delta}$-E781A/$GluN2A^{\Delta}$ 0.29±0.07μA, p<0.001)(Fig. 4D). In the $GluN1^{\Delta}/GluN2B^{\Delta}$ receptor combinations only the GluN1-E781A mutation led to a significant decrease in the I_{Max} (Fig. 4D).

Subunit Composition	EC_{50}		I_{Max}	I_{Max}/I_{SS}
	Gly	Glu		
	μM		μA	
GluN1$^{\Delta}$/ GluN2A$^{\Delta}$	4.87 ± 0.72	1.15 ± 0.15	4.00 ± 0.44	0.52 ± 0.09
GluN1$^{\Delta}$-N521A / GluN2A$^{\Delta}$	3.67 ± 0.61	4.39 ± 0.78	3.86 ± 0.81	0.78 ± 0.03**
GluN1$^{\Delta}$-K531A / GluN2A$^{\Delta}$	3.12 ± 1.66	6.04 ± 0.81**	7.97 ± 1.15**	0.77 ± 0.02*
GluN1$^{\Delta}$-Y535A / GluN2A$^{\Delta}$	16.29 ± 1.73**	5.15 ± 0.80**	0.32 ± 0.08**	0.49 ± 0.04
GluN1$^{\Delta}$-E781A / GluN2A$^{\Delta}$	5.60 ± 0.65	7.98 ± 1.43**	0.29 ± 0.07**	0.83 ± 0.06**
GluN1$^{\Delta}$/ GluN2B$^{\Delta}$	1.70 ± 0.40	0.62 ± 0.05	5.48 ± 0.48	0.56 ± 0.04
GluN1$^{\Delta}$-N521A / GluN2B$^{\Delta}$	4.52 ± 1.20	5.59 ± 1.02**	4.20 ± 0.49	0.87 ± 0.01**
GluN1$^{\Delta}$-K531A / GluN2B$^{\Delta}$	0.70 ± 0.10	1.90 ± 0.64	4.54 ± 1.27	0.69 ± 0.03
GluN1$^{\Delta}$-Y535A / GluN2B$^{\Delta}$	1.90 ± 0.54	4.58 ± 1.32*	4.04 ± 0.95	0.48 ± 0.09
GluN1$^{\Delta}$-E781A / GluN2B$^{\Delta}$	11.11 ± 1.76**	9.05 ± 1.24**	0.54 ± 0.13**	0.66 ± 0.06

* $P < 0.01$
** $P < 0.001$
n = 4-18

Table 1. Pharmacology of NTD-lacking wt and mutated GluN1$^{\Delta}$/GluN2A$^{\Delta}$ and GluN1$^{\Delta}$/GluN2B$^{\Delta}$ NMDA-receptors. Glycine and glutamate EC_{50} values as well as I_{Max} values were determined in the presence of 100 µM glycine or glutamate.

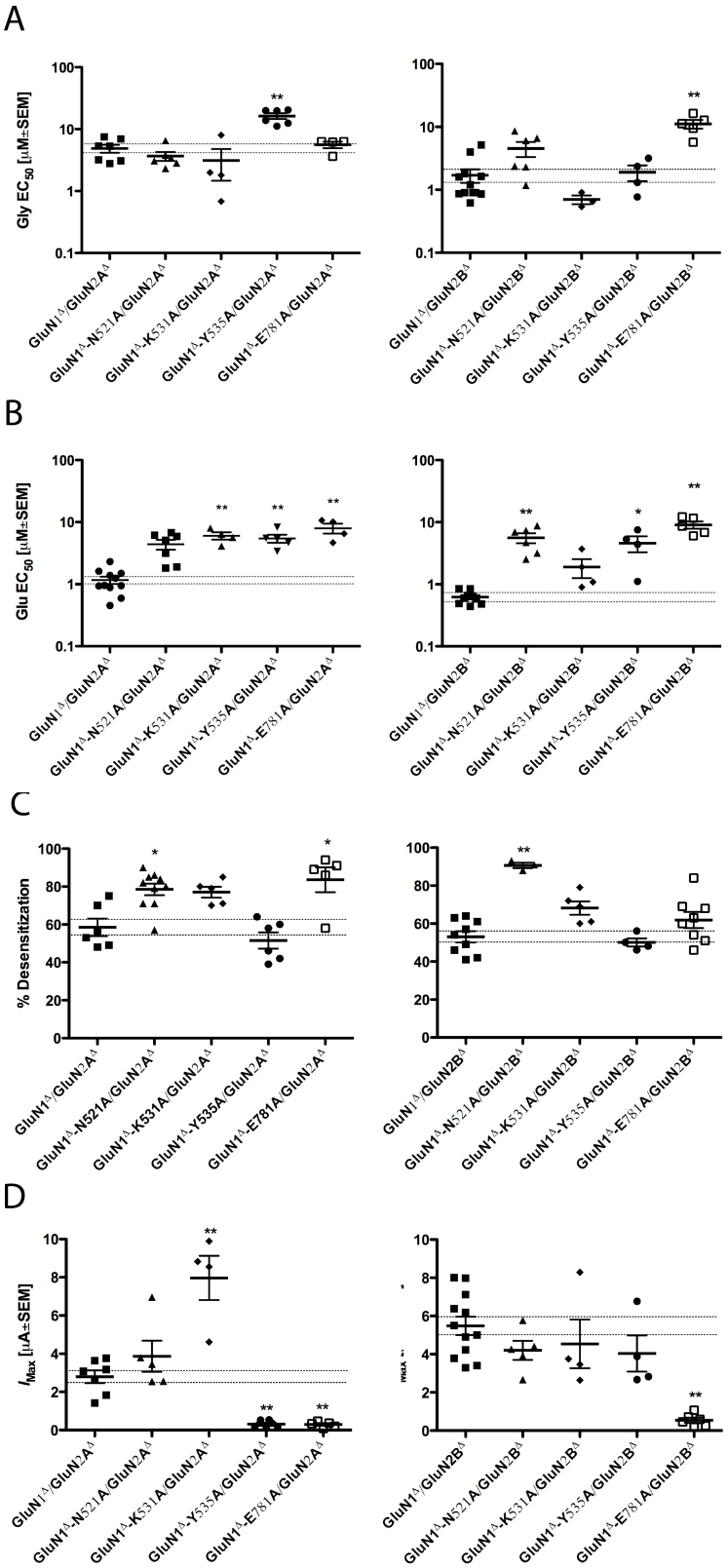

Fig. 4. Functional properties of wt and mutated GluN1$^{\Delta}$/GluN2(A$^{\Delta}$/B$^{\Delta}$) receptors. (A) Scatter plot with mean and SEM of the apparent glycine affinity for GluN1$^{\Delta}$/GluN2A$^{\Delta}$- (left) and GluN1$^{\Delta}$/GluN2B$^{\Delta}$-receptors (right). **(B)** Scatter plot with mean and SEM of the apparent glutamate affinity for GluN1$^{\Delta}$/GluN2A$^{\Delta}$- (left) and GluN1$^{\Delta}$/GluN2B$^{\Delta}$-receptors (right). **(C)** Scatter plot with mean and SEM of the I_{Max}/I_{SS} ratio (in percent) as a measure for the desensitization of GluN1$^{\Delta}$/GluN2A$^{\Delta}$- (left) and GluN1$^{\Delta}$/GluN2B$^{\Delta}$-receptors (right). **(D)** Scatter plot with mean and SEM of the maximal inducible current (I_{Max}) for GluN1$^{\Delta}$/GluN2A$^{\Delta}$- (left) and GluN1$^{\Delta}$/GluN2B$^{\Delta}$-receptors (right). (*) $p < 0.01$, (**) $p < 0.001$

In summary, the mutations in the LBD dimer interface appear to affect not only one parameter but always a combination of different parameters. It is therefore not possible to relate one effect to a specific interaction. Nevertheless, the GluN1-E781A mutation consistently led to a decrease in apparent glutamate affinity and I_{Max} in GluN1$^{\Delta}$/GluN2A$^{\Delta}$ and GluN1$^{\Delta}$/GluN2B$^{\Delta}$ receptors.

The GluN1-NTD compensates the reduced I_{Max} caused by the GluN1-E781A mutation in NTD-lacking GluN1/GluN2-receptors - In a last set of experiments we addressed the question if either the GluN1- or GluN2-NTDs are able to compensate the reduced I_{Max} of receptors carrying the GluN1-E781A mutation. Therefore we injected NTD-lacking subunits together with their full-length counterparts. Namely these receptor combinations were GluN1/GluN2A$^{\Delta}$, GluN1/GluN2B$^{\Delta}$ and GluN1$^{\Delta}$/GluN2A, GluN1$^{\Delta}$/GluN2B as well as the respective GluN1-E781A mutant receptor combinations. We determined the I_{Max} in these receptors (Fig. 5A) and it became evident that the GluN1-NTD recovers wt-like I_{Max} whereas the GluN2A-NTD does not (Fig. 5A and 5C). Obviously the GluN1-NTD has a pivotal role that is connected to the GluN1-E781 LBD dimer interface interaction. We asked ourselves which role this might be and hypothesized, relying on a study by Farina et al. (2011), that the GluN1-NTD homodimerization might be responsible for the recovery effect. Farina et al. identified the homodimer interface of the GluN1-NTDs and described two mutations that disturb/promote the homodimerization. The GluN1-Y109C mutation leads to a stabilization of the NTD homodimer interface leading to a reduction of surface expressed receptors. Vice versa, the GluN1-T110A mutation disturbs the NTD homodimerization leading to an increase in cell surface receptors. But it is also concluded that the GluN1-NTDs are required for efficient cell-surface expression. To analyze if the homodimerization feature of the GluN1-NTDs is related to the I_{Max} reduction caused by the GluN1-E781A mutation we introduced the Y109C and T110A mutations in the full-length GluN1-E781A subunits. Then we expressed these double mutants with GluN2A-subunits and determined the apparent agonist affinities as well as the I_{Max}. The double mutant receptors showed wt-like agonist-induced currents and we didn't find significant changes in the parameters analyzed (Fig. 5B-C).

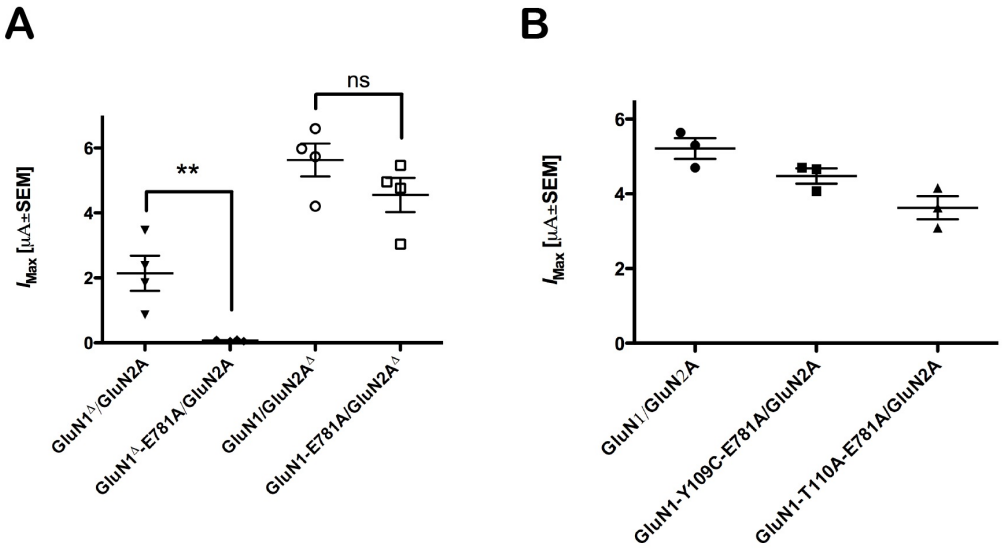

Fig. 5. Functional properties of partially NTD-deleted GluN1/GluN2A-receptors and double mutant GluN1/GluN2A-receptors. (A) Scatter plot with mean and SEM of the I_{Max} for wt and mutant GluN1$^{\Delta}$/GluN2A-receptors as well as wt and mutant GluN1/GluN2A$^{\Delta}$-receptors. **(B)** Scatter plot with mean and SEM of the I_{Max} for wt and double mutated GluN1/GluN2A-receptors.
(*) $p < 0.01$, (**) $p < 0.001$

Subunit Composition	EC_{50}		Gly I_{Max}
	Gly	Glu	
	μM		μA
GluN1$^{\Delta}$ / GluN2A	0.80 ± 0.38	1.76 ± 0.13	2.14 ± 0.54
GluN1$^{\Delta}$-E781A / GluN2A	1.26 ± 0.31	2.55 ± 0.68	0.07 ± 0.01
GluN1 / GluN2A$^{\Delta}$	2.30 ± 0.53	1.89 ± 0.35	5.63 ± 0.50
GluN1-E781A / GluN2A$^{\Delta}$	2.80 ± 0.71	2.91 ± 0.43	4.55 ± 0.52
GluN1 / GluN2A	0.97 ± 0.40	1.3 ± 0.32	5.47 ± 0.17
GluN1-Y109C-E781A / GluN2A	0.86 ± 0.18	1.60 ± 0.35	4.47 ± 0.20
GluN1-T110A-E781A / GluN2A	1.04 ± 0.03	2.23 ± 0.21	3.62 ± 0.30

* $P < 0.01$
** $P < 0.001$
n = 3-7

Table 2. Pharmacology of partially NTD-deleted wt and mutant GluN1/GluN2A- as well as double mutant GluN1/GluN2A-receptors. Glycine and glutamate EC_{50} values as well as I_{Max} values were determined in the presence of 100 μM glycine or glutamate.

This leads to the conclusion that the GluN1-NTD homodimerization does not interfere with the GluN1-E781A mutation. Thus the molecular mechanism of the GluN1-NTD induced recovery effect is yet to be determined.

DISCUSSION

In our studies we applied mutual information analysis and measured current responses to agonists to characterize the functional role of the ligand-binding domain heterodimer interface in NMDA-receptors. In our experiments we found mutations in the heterodimer interface that decrease the apparent agonist affinities but also increase the extent of desensitization and two out of four mutations led to a significant decrease in the I_{Max}.

The mutations we introduced resulted in pleiotropic effects on receptor function. Therefore we cannot ascribe single, specific roles to each of the three interaction sites. This observation suggests that the LBD dimer interface unspecifically participates in the conformational changes that occur during receptor activation. Hence, numerous interface residues might have an indirect effect on receptor function. Nonetheless, specific roles have been suggested for the homologous position to GluN1-N521 in AMPA- and kainate-receptors based on experimental data (Stern-Bach et al., 1998, Sun et al., 2002, Mayer, 2006, Armstrong et al., 2006, Chaudhry et al., 2009). Interestingly, glutamate-gated currents in AMPARs/KARs were not only non-desensitizing but also smaller than wt (Stern-Bach et al., 1998), consistent with the suggestion that the site I interaction of GluN1-N521 facilitates the heterodimerization which was shown by analytical ultracentrifugation of isolated GluN1 and GluN2A LBDs (Furukawa et al., 2005). We do not exclude the possibility that site I - and possibly site II - interactions contribute to the formation of heterodimers in NMDARs, however, our data indicate that the site III interaction of GluN1-E781 has a much more profound effect as it significantly reduces the I_{Max}. Whether this reduction is due to disturbed function, trafficking or assembly is yet to be determined. Remarkably, the homologous residue in GluN2A-B subunits is a glycine and in GluN3A-B a serine, meaning that this interaction is not symmetrical and the GluN1 subunit presumably contributes to a larger extent to the heterodimerization than the GluN2- or GluN3-subunits. Interestingly, our multiple sequence alignment shows that although the GluN1-E781 residue is not conserved among the NMDAR-subunits, it is very well conserved in the AMPAR- and KAR-

subunits. This also means that in an intact non-NMDA LBD dimer this interaction is symmetrical and from an evolutionary perspective the GluN2 and GluN3 subunits presumably have lost the negative charge at this position. It seems that the GluN2 and GluN3 subunits could homodimerize if a glutamate was introduced at the homologous position. It would be interesting to conduct affinity purification experiments with GluN2- and GluN3-subunits carrying asparagine and glutamate residues at the homologous positions to GluN1-N521 and GluN1-E781. Also relying on these observations and the GluN1-GluN2A LBD crystal structure as well as our MI analysis we suggest to introduce double mutations (based on the MI analysis see Fig. 2B), especially GluN1-N521A-E781A to see if their effects are additive with respect to receptor function according to our hypothesis.

As stated earlier we conducted our experiments on a reduced receptor model (NTD-lacking NMDA-receptors). By this means we were able to observe effects caused by the LBD dimer interface mutations that are else concealed by the NTDs. The GluN1-E781A mutation led to a significant decrease in I_{Max} in combination with NTD-lacking GluN2A or GluN2B receptors. The GluN1-NTD but not the GluN2-NTD is capable of compensating this effect (Fig. 6A). To date it has been reported that the NTDs are critically involved in the oligomerization of the iGluRs (Kuusinen et al., 1999, Leuschner and Hoch, 1999, Ayalon and Stern-Bach, 2001, Meddows et al., 2001, Greger et al., 2007). It was also reported that the GluN1-subunit homodimerizes in the ER, presumably through its NTD, but whether this observation is important for proper receptor assembly is still under debate (Schuler et al., 2008, Farina et al., 2011, Lee et al., 2011). Despite this, NTD-lacking receptors have been successfully expressed in other as well as our experiments indicating that the NTDs of iGluRs are not obligatory to form functional receptors (Pasternack et al., 2002, Armstrong et al., 2006, Madry et al., 2007b, Madry et al., 2008)(Fig. 6B). Thus an overarching functional role of the GluN1-NTD is currently unknown. Our finding, that the GluN1-NTD compensates a mutation based decrease in I_{Max} is to our knowledge the first time of a functional role of the GluN1-NTD. In order to understand the molecular mechanism of the GluN1-NTD-induced recovery we would suggest analyzing double mutations of the LBD dimer interface in full-length GluN1-subunits. Also it might be interesting to analyze the interface between the GluN1-NTD and the subjacent –LBD. Certain interactions in this interface might lead to a stabilization of

the LBD dimer contacts. However, as no full-length crystal structure is available, one has to rely on homology modeling based on the full-length GluA2 tetrameric structure (Sobolevsky et al., 2009).

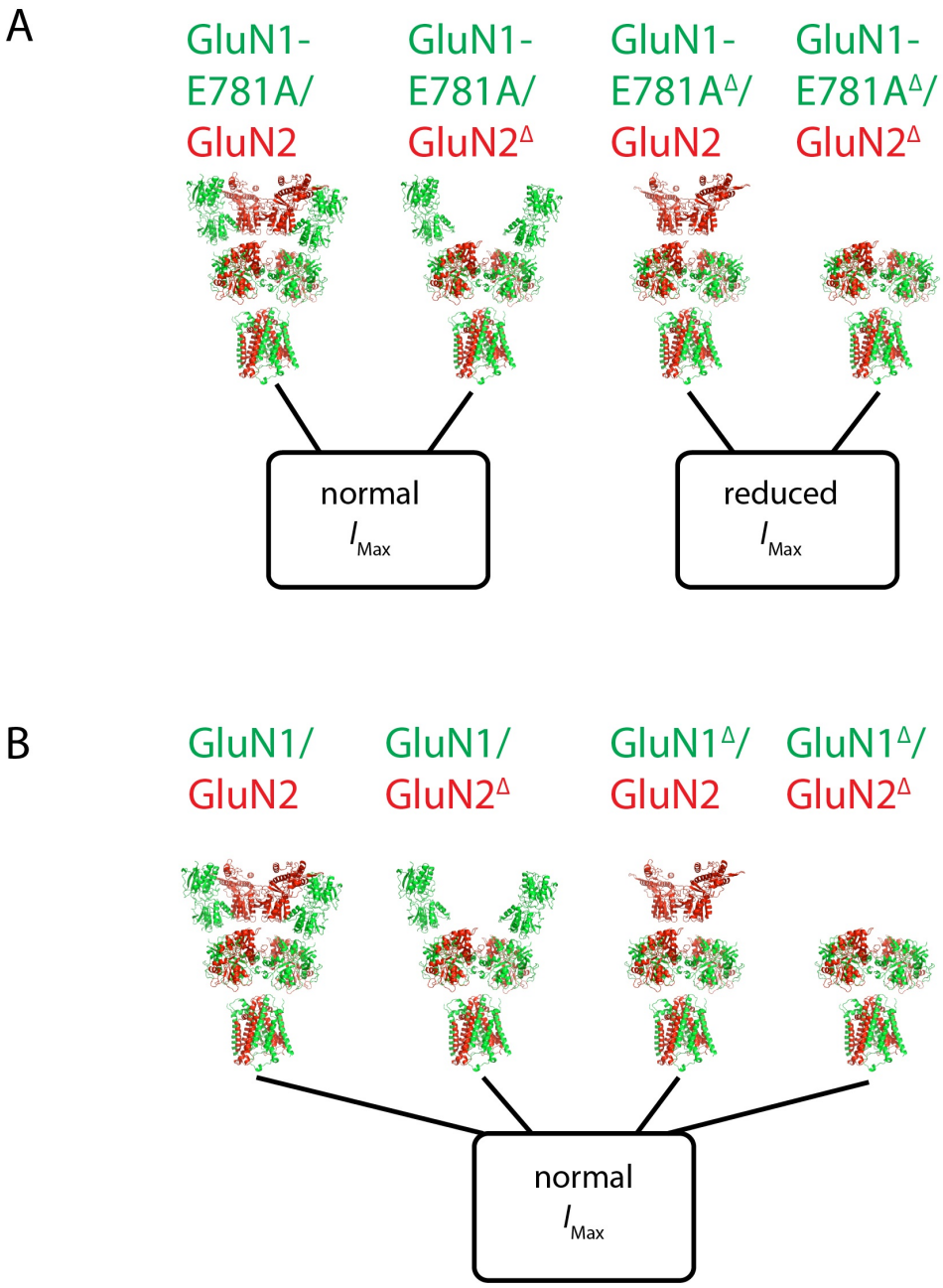

Fig. 6. Schematic representation of the influence of NTD-deletion and LBD mutation on the maximal inducible current. (A) Shown is a model of the tetrameric GluN1/GluN2A receptor in green and red, respectively. The partial or full deletion of the NTDs does not have a substantial effect on the I_{Max}. **(B)** Introducing a mutation (GluN1-E781A) in the heterodimer interface leads to a significant reduction in the I_{Max} of GluN1-NTD lacking receptors. Receptors where the GluN1-NTD is present are able to compensate the detrimental effect of the mutation.

Our aim was to gain insight into the heterodimer interface of the LBDs in NMDA-receptors. It is conceivable that interfaces between protomers require strong

interactions for the oligomers to remain stable. In spite of this, the interface interactions also need to allow for conformational changes that are necessary for the respective biological activity. Thus, such interfaces are likely to have conserved interactions that promote the oligomerization and secure the normal function of the oligomer. However, we reasoned that the LBD heterodimer interface might also contribute to the unique features of the NMDARs (Nakanishi et al., 1992, Dingledine et al., 1999). Our results show that although the GluN2A- and GluN2B-LBDs share a high sequence identity of ~82% the mutations analyzed in this study had partly differing effects on the respective receptor function. We reckon that the interface interactions are connected to other parts of the receptor which we cannot point at because of our poor understanding of the conformational changes involved. For instance, the GluN2A LBD was only crystallized in the agonist-bound conformation, to date we have no information about the respective apo-state. Nevertheless, the mutual information bioinformatics approach highlighted residues of functional significance and thus has the potential to identify the residues that account for the differences observed between the GluN2A- and GluN2B-receptor combinations.

Conclusions - In conclusion, the data presented here show that the LBD interface interactions of NMDAR-subunits are involved in receptor function in a non-specific way and various other molecular bases must underlie the unique NMDA-receptor functions. Also we identified a specific functional implication of the GluN1-NTD on receptor function as its presence, but not the GluN2-NTD, recovers the reduction in I_{Max} observed with the GluN1-E781A mutation.

We also used the mutual information approach to identify residues that are evolutionary correlated and we are convinced that this approach will help to understand the receptor function on a molecular level.

REFERENCES

Ayalon G, Stern-Bach Y. Functional assembly of AMPA and kainate receptors is mediated by several discrete protein-protein interactions. *Neuron* 31: 103-113, 2001.

Borschel WF, Murthy SE, Kasperek EM, Popescu GK. NMDA receptor activation requires remodelling of intersubunit contacts within ligand-binding heterodimers. *Nat Commun* 2: 498, 2011.

Chaudhry C, Weston MC, Schuck P, Rosenmund C, Mayer ML. Stability of ligand-binding domain dimer assembly controls kainate receptor desensitization. *EMBO J* 28: 1518-1530, 2009.

Collingridge GL, Bliss TV. Memories of NMDA receptors and LTP. *Trends Neurosci* 18: 54-56, 1995.

MacKay DJC. *Information Theory, Inference, and Learning Algorithms*. Cambridge University Press, 2003

Dingledine R, Borges K, Bowie D, Traynelis SF. The glutamate receptor ion channels. *Pharmacol Rev* 51: 7-61, 1999.

Endele S, Rosenberger G, Geider K, Popp B, Tamer C, Stefanova I, Milh M, Kortum F, Fritsch A, Pientka FK, Hellenbroich Y, Kalscheuer VM, Kohlhase J, Moog U, Rappold G, Rauch A, Ropers HH, von Spiczak S, Tonnies H, Villeneuve N, Villard L, Zabel B, Zenker M, Laube B, Reis A, Wieczorek D, Van Maldergem L, Kutsche K. Mutations in GRIN2A and GRIN2B encoding regulatory subunits of NMDA receptors cause variable neurodevelopmental phenotypes. *Nat Genet* 42: 1021-1026, 2010.

Furukawa H, Singh SK, Mancusso R, Gouaux E. Subunit arrangement and function in NMDA receptors. *Nature* 438: 185-192, 2005.

Gielen M, Retchless BS, Mony L, Johnson JW, Paoletti P. Mechanism of differential control of NMDA receptor activity by NR2 subunits. *Nature* 2009.

Greger IH, Esteban JA. AMPA receptor biogenesis and trafficking. *Curr Opin Neurobiol* 17: 289-297, 2007.

Hoffgaard F, Weil P, Hamacher K. BioPhysConnectoR: Connecting sequence information and biophysical models. *BMC Bioinformatics* 11: 199, 2010.

Jin R, Clark S, Weeks AM, Dudman JT, Gouaux E, Partin KM. Mechanism of positive allosteric modulators acting on AMPA receptors. *J Neurosci* 25: 9027-9036, 2005.

Kuusinen A, Abele R, Madden DR, Keinanen K. Oligomerization and ligand-binding properties of the ectodomain of the alpha-amino-3-hydroxy-5-methyl-4-isoxazole propionic acid receptor subunit GluRD. *J Biol Chem* 274: 28937-28943, 1999.

Laube B, Hirai H, Sturgess M, Betz H, Kuhse J. Molecular determinants of agonist

discrimination by NMDA receptor subunits: analysis of the glutamate binding site on the NR2B subunit. *Neuron* 18: 493-503, 1997.

Lee CH, Gouaux E. Amino terminal domains of the NMDA receptor are organized as local heterodimers. *PLoS One* 6: e19180, 2011.

Madden DR. The structure and function of glutamate receptor ion channels. *Nat Rev Neurosci* 3: 91-101, 2002.

Madry C BH, Geiger JRP, Laube B. Supralinear potentiation of NR1/NR3A excitatory glycine receptors by Zn^{2+} and NR1 antagonist. *PNAS* 2008.

Madry C, Betz H, Geiger JR, Laube B. Potentiation of Glycine-Gated NR1/NR3A NMDA Receptors Relieves Ca-Dependent Outward Rectification. *Front Mol Neurosci* 3: 6, 2010.

Madry C, Mesic I, Betz H, Laube B. The N-terminal domains of both NR1 and NR2 subunits determine allosteric Zn2+ inhibition and glycine affinity of N-methyl-D-aspartate receptors. *Mol Pharmacol* 72: 1535-1544, 2007.

Meddows E, Le Bourdelles B, Grimwood S, Wafford K, Sandhu S, Whiting P, McIlhinney RA. Identification of molecular determinants that are important in the assembly of N-methyl-D-aspartate receptors. *J Biol Chem* 276: 18795-18803, 2001.

Nakanishi S. Molecular diversity of glutamate receptors and implications for brain function. *Science* 258: 597-603, 1992.

Nishi M, Hinds H, Lu HP, Kawata M, Hayashi Y. Motoneuron-specific expression of NR3B, a novel NMDA-type glutamate receptor subunit that works in a dominant-negative manner. *J Neurosci* 21: RC185, 2001.

Pasternack A, Coleman SK, Jouppila A, Mottershead DG, Lindfors M, Pasternack M, Keinanen K. Alpha-amino-3-hydroxy-5-methyl-4-isoxazolepropionic acid (AMPA) receptor channels lacking the N-terminal domain. *J Biol Chem* 277: 49662-49667, 2002.

R Development Core Team (2011). R: A language and environment for statistical computing. R Foundation for Statistical Computing, Vienna, Austria. ISBN 3-900051-07-0, URL http://www.R-project.org

Schuler T, Mesic I, Madry C, Bartholomaus I, Laube B. Formation of NR1/NR2 and NR1/NR3 heterodimers constitutes the initial step in N-methyl-D-aspartate receptor assembly. *J Biol Chem* 283: 37-46, 2008.

Sobolevsky AI, Rosconi MP, Gouaux E. X-ray structure, symmetry and mechanism of an AMPA-subtype glutamate receptor. *Nature* 2009.

Stern-Bach Y, Russo S, Neuman M, Rosenmund C. A point mutation in the glutamate binding site blocks desensitization of AMPA receptors. *Neuron* 21: 907-918, 1998.

Sucher NJ, Akbarian S, Chi CL, Leclerc CL, Awobuluyi M, Deitcher DL, Wu MK, Yuan JP, Jones EG, Lipton SA. Developmental and regional expression pattern of a novel NMDA receptor-like subunit (NMDAR-L) in the rodent brain. *J Neurosci* 15: 6509-6520, 1995.

Sun Y, Olson R, Horning M, Armstrong N, Mayer M, Gouaux E. Mechanism of glutamate receptor desensitization. *Nature* 417: 245-253, 2002.

White RA, Szurmant H, Hoch JA, Hwa T. Features of protein-protein interactions in two-component signaling deduced from genomic libraries. *Methods Enzymol* 422: 75-101, 2007.

Weil P, Hoffgaard F, Hamacher K. Estimating sufficient statistics in co-evolutionary analysis by mutual information. *Comput Biol Chem* 33: 440-444, 2009.

Yuan H, Hansen KB, Vance KM, Ogden KK, Traynelis SF. Control of NMDA receptor function by the NR2 subunit amino-terminal domain. *J Neurosci* 29: 12045-12058, 2009.

FOOTNOTES

*This study was supported by the Max-Planck Gesellschaft, Deutsche Forschungsgemeinschaft (B.L., LA 1086/4-2), Gemeinnützige Hertie-Stiftung (B.L.) and Fonds der Chemischen Industrie (H.B.).

CHAPTER 4
GENERATION OF A HIGH EFFICACY GLUN1/GLUN3A NMDA RECEPTOR

Ceyhun Tamer[1,2], Ivana Mesic[1,2,*], Heinrich Betz[1,+] and Bodo Laube[1,2]
[1]Department of Neurochemistry, Max-Planck-Institute for Brain Research, Deutschordenstrasse 46, 60528 Frankfurt am Main, Germany
[2]Department of Molecular and Cellular Neurophysiology, TU-Darmstadt, Schnittspahnstrasse 3, 64287 Darmstadt, Germany
[+]Present address: Max-Planck-Institute for Medical Research, Jahnstrasse 29, 69120 Heidelberg, Germany
*Present address: Department of Psychiatry and Behavioral Sciences, Northwestern University Feinberg School of Medicine, 303 East Chicago Ave, Ward 9-217, Chicago, IL 60611, USA

ABSTRACT

***N*-methyl-D-aspartate (NMDA) receptors composed of glycine binding GluN1 and GluN3A subunits are referred to as excitatory glycine receptors. The binding of glycine to the GluN1/GluN3A receptor induces channel opening but with a very low efficacy. Preventing glycine binding to the GluN1 subunit results in a strong potentiation of the glycine-induced currents. Thus, it is thought that glycine binding to the GluN3A subunit induces channel opening whereas glycine binding to the GluN1 subunit forces the receptor into desensitization and thus channel closure. In another study, it was shown that polar residues in the interface of GluN1/GluN2A receptors prevent channel opening by raising the activation energy that is needed to induce conformational changes that are required for channel opening. Here we mutated polar residues in the GluN1 LBD interface to alanine to increase the low efficacy of GluN1/GluN3A receptors. Failing that, we tested N-terminal domain (NTD)-lacking NMDAR subunits and also used homology modeling to analyze NTD interactions and interactions in the linker connecting the NTD to the LBD (NTD–LBD linker). Our results demonstrate that the GluN3A-NTD is responsible for the low efficacy of GluN1/GluN3A receptors and mutations in the homophilic GluN3A-NTD interface as well as in the GluN3A-NTD-LBD linker region specifically increase glycine-gated currents without altering apparent glycine affinity. Thus, we generated a highly efficient GluN1/GluN3A receptor and uncovered the GluN3A-NTD to resemble the role of an autoinhibitory domain (AID), which is the first time that such a domain is described for a ligand-gated ion channel.**

INTRODUCTION

The *N*-methyl-D-aspartate (NMDA) subtype of ionotropic glutamate receptors (iGluRs) is a tetrameric protein composed of homologous GluN1 and GluN2 or GluN3 subunits, which require the binding of glycine and/or glutamate for efficient channel gating (Kuryatov et al., 1994, Sucher et al., 1995, Laube et al., 1997, Dingledine et al., 1999, Chatterton et al., 2002, Madry et al., 2007a, Awobuluyi et al., 2007, Smothers and Woodward, 2007). All iGluR subunits share a modular structure composed of: an extracellular N-terminal domain (NTD), a ligand-binding domain (LBD), a transmembrane domain (TMD) and an intracellular C-terminal domain (CTD) (reviewed in Madden, 2002). Crystallization studies revealed that the LBD dimers of iGluRs are organized in a 'back-to-back' fashion (Armstrong et al., 2000, Furukawa et al., 2005, Armstrong et al., 2006). Agonist binding to the respective subunits leads to a venus-flytrap like closure of the S1 and S2 subdomains of the LBD which results in ion channel opening (Armstrong et al., 2000, Furukawa et al., 2003, Inanobe et al., 2005, Ahmed et al., 2009). Functional and crystallization experiments show that during this process the stability of three distinct interaction sites (I-III) of the iGluR LBD dimer interface have an impact on the degree of receptor desensitization (Stern-Bach et al., 1998, Sun et al., 2002, Furukawa et al., 2005, Armstrong et al., 2006, Mayer, 2006). According to these findings, strong LBD dimer interface interactions would stabilize the activated conformation and prevent the receptor from desensitizing. Vice versa, weak interactions would result in brief channel opening and a rapid transition to the desensitized state and thus closure of the channel. Based on the current view of iGluR function, it is assumed that the low efficacy of GluN1/GluN3A receptors depends on weak LBD dimer interface interactions which cause the receptor to desensitize quickly after activation (Madry et al., 2007a, Awobuluyi et al., 2007). Furthermore, it was found that the GluN1 antagonist MDL-29951 as well as GluN1 ligand binding site mutations increase glycine-induced currents (Madry et al., 2007a). Thus, it is concluded that glycine binding to the GluN3A subunit is sufficient for channel opening whereas glycine binding to the GluN1 subunit presumably causes receptor desensitization. In a recent study by Borschel et al. cysteine mutations were introduced in the GluN1-GluN2A LBD dimer interface and single channel experiments were performed (Borschel et al., 2011). Upon modeling of the kinetic properties it became evident that it is not the desensitization that causes reduced receptor efficacy but a reduced activation.

Apparently, activation of the receptor requires rearrangements of the LBD dimer interface, which in turn means that this interface must be flexible. It is concluded that polar residues in the LBD dimer interface reduce flexibility and in consequence activation requires more energy. These results stand in stark contrast to previous views on receptor function because they suggest that removal of polar interactions in the GluN1-GluN3A LBD dimer interface might increase the efficacy of these receptors. Therefore we decided to substitute polar residues in the GluN1 LBD that make contacts with the GluN3A LBD, namely GluN1-N521A, -K531A, -Y535A and –E781A. The location of these residues in the LBD was described in Chapter 3 and in Furukawa et al. (2005).

However, we do not exclude the possibility that in addiction to the LBDs, the NTDs might play an essential role in determining GluN1/GluN3A receptor efficacy. NTDs have been implicated in receptor oligomerization, trafficking and also modulation of receptor function (Fayyazuddin et al., 2000, Papadakis et al., 2004, Qiu et al., 2005, Hu et al., 2005, Madry et al., 2007a, Yuan et al., 2009, Gielen et al., 2009, Hansen et al., 2010, Farina et al., 2011). With regard to receptor function, especially GluN2 NTDs have been shown to determine the channel open probability (P_0) (Yuan et al., 2009, Gielen et al., 2009). Studies that sought to alter subunit-specific receptor function by substituting NTDs between the different GluN2 subunits showed that conferral of specific function required the substitution of the NTD-LBD linker, in addition to the NTD (Yuan et al., 2009, Gielen et al., 2009). Therefore, we decided to also include the NTDs and the NTD-LBD linker in our analyses. In that respect we built a homology model for the full-length GluN1/GluN3A receptor based on the crystal structures of the full-length, homomeric GluA2-subtype AMPA-receptor by Sobolevsky et al. (2009), the GluN1-Glun2A LBD heterodimer by Furukawa et al. (2005) and the GluN2B NTD by Karakas et al. (2009). Subsequently we characterized partially NTD-lacking GluN1/GluN3A receptors as well as amino acid substitutions in the GluN3A-NTD and –NTD-LBD linker functionally by measuring whole-cell currents from *Xenopus* oocytes and biochemically using affinity purification and SDS-PAGE.

We show that the GluN3A-NTD is the structural determinant of the low efficacy of GluN1/GluN3A receptors and furthermore we describe mutations in the homophilic GluN3-NTD interface and especially the GluN3A-NTD-LBD linker that largely increase glycine-induced currents. By means of homology modeling and site-directed

mutagenesis we were able to generate a highly efficient 'excitatory' GluN1/GluN3A Glycine-receptor.

EXPERIMENTAL PROCEDURES

DNA constructs, oocyte expression and electrophysiology - The GluN1-1a, GluN1$^{\Delta}$, GluN3A and GluN3A$^{\Delta}$ expression constructs have been described previously (Madry et al., 2007a, Madry et al., 2008). Amino acid substitutions were generated via site-directed mutagenesis (QuikChange XL Site-Directed Mutagenesis Kit, Stratagene) and confirmed by DNA sequencing (Eurofins MWG Operon). All constructs were linearized and transcribed into cRNA (mCAP mRNA Capping Kit, Ambion) as described (Madry et al., 2010). For electrophysiological analysis, *Xenopus laevis* oocytes were injected with 40 ng of the respective wt or NTD-deleted GluN1 and GluN3 cRNAs at a ratio of 1:3. Oocytes were isolated manually or enzymatically and maintained as described previously (Laube et al., 1997). 3-4 days after injection, two-electrode voltage-clamp recording (TEVC) of whole-cell currents was performed according to (Laube et al., 1997). For the functional characterization of wt and mutated receptor complexes we determined apparent glycine and Zn^{2+} affinities, as well as maximal inducible currents by glycine and Zn^{2+} as well as GluN1 antagonist (MDL-29951) mediated potentiation of GluN1/GluN3A receptors as described in Madry et al. (2007a).

Metabolic [^{35}S]methionine labeling, purification and SDS-PAGE of NMDA receptor complexes - After cRNA injection, oocytes were labeled overnight by incubation in [^{35}S]methionine (>40 TBq/mM, Amersham Biosciences) at ~100 MBq/ml (0.2 MBq per oocyte) and thereafter chased for additional two days as described (10). Receptor complexes were purified from dodecylmaltoside extracts of the labeled oocytes via a His_6-tag added to the GluN1 and GluN1$^{\Delta NTD}$ C-terminus by Ni^{2+}-NTA agarose (Qiagen) chromatography as described previously (Madry et al., 2007b). [^{35}S]-Methionine-labeled protein samples were solubilized in SDS sample buffer containing 20 mM dithiothreitol and electrophoresed in parallel with molecular mass markers (SeeBlue® Plus2 Pre-Stained Standard, Invitrogen) on 8% tricine-SDS-polyacrylamide gels. Gels were blotted, fixed, dried, and exposed to BioMax MR films (Kodak, Stuttgart, Germany) at –80 °C.

Surface labeling with Cy5-NHS-ester - Three days after the injection of cRNAs, the injected and non-injected control oocytes were surface-labeled with 65 µM of Cy5-NHS-ester dye (Amersham Biosciences) and solubilized for affinity purification as described above. Gels containing Cy5-labeled protein samples were scanned with a gel imager (*Typhoon 9400*, Amersham Biosciences) as described (Madry et al., 2007a).

Glycosylation assay - To discriminate between mature and immature receptor complexes, 10 µl of the affinity-purified receptor were incubated in reducing sample buffer (20 mM DTT, 1% (w/v) SDS) containing 1% (w/v) octylglucoside with 5 U endoglycosidase H (Endo H) or peptide: N-Glycosidase F (PNGase F; NEB, Frankfurt, Germany) at 37°C for 1 h. Afterwards protein samples were analyzed by SDS-PAGE as described above.

Molecular modeling of the tetrameric GluN1/GluN3A receptor structure - Sequence alignment of the NMDA receptor subunits was taken from Sobolevsky et al. (2009) and supplemented with the sequences of the GluN2B-D and GluN3B subunits. The homology model of the GluN1/GluN3A receptor is based on the crystal structures of the GluN3A LBD (Yaol et al., 2008, PDB ID: 2RC7), GluN2B NTD (Karakas et al., 2009, PDB ID: 3JPW), GluN1-GluN2A-LBD-dimer (Furukawa et al., 2005, PDB ID: 2A5T) and the GluA2 receptor (Sobolevsky et al., 2009, PDB ID: 3KG2). The models for the protomers were generated using the Modeller program 9v7 (Fiser and Sali, 2003) and energy minimized using Chimera build 2577 (Pettersen et al., 2004). Arranging the protomers according to the GluA2 tetrameric structure was accomplished using lsqman 9.7.9 (Kleywegt, 1996). Protein fold prediction for the GluN3A-NTD-LBD linker was conducted using Scratch Protein Prediction Server (University of California, Scratch Protein Prediction Server; http://solpro.proteomics.ics.uci.edu/) and Wurst Server (University of Hamburg; http://neuropa.zbh.uni-hamburg.de/wurst/index.php). Molecular dynamics simulations were computed using Gromacs 4.0.5 (Hess et al., 2008). Pymol 1.3 (Schrödinger Inc., New York, NY, USA) was used for illustration.
For statistical data analysis Graphpad Prism v.5.0a (GraphPad Software Inc., San Diego, CA, USA) has been used.

For all analyses, values are given as means ± SEM. Statistical significance was determined at $p<0.01$ (*) and $p<0.001$ (**) levels using Student's *T*-test or one-way ANOVA and the Dunnett Post-Hoc-Test.

RESULTS

Analysis of putative GluN1-GluN3A LBD interface interactions - We used the crystal structures of the GluN1-GluN2A LBD dimer and the GluN3A LBD in order to make a model for the GluN1-GluN3A LBD heterodimer (Fig. 1A, 1B). Using this model we analyzed the three interaction sites that were described by Furukawa et al (Fig. 1B) (Furukawa et al., 2005). Our aim was to identify polar LBD interface interactions that might account for the low efficacy of GluN1/GluN3A receptors.

The interaction site I involves the D-Helix of the GluN1 and the J-Helix of the GluN2A/3A subunit. Residue N521 in GluN1 forms a polar interaction with the GluN3A-E889 residue (Fig. 1C). This interaction site has been previously implicated in desensitization and assembly of AMPA- and NMDA-receptors (Stern-Bach et al., 1998, Furukawa et al., 2005). We chose to mutate the GluN1-N521 residue to an alanine in order to remove this polar interaction.

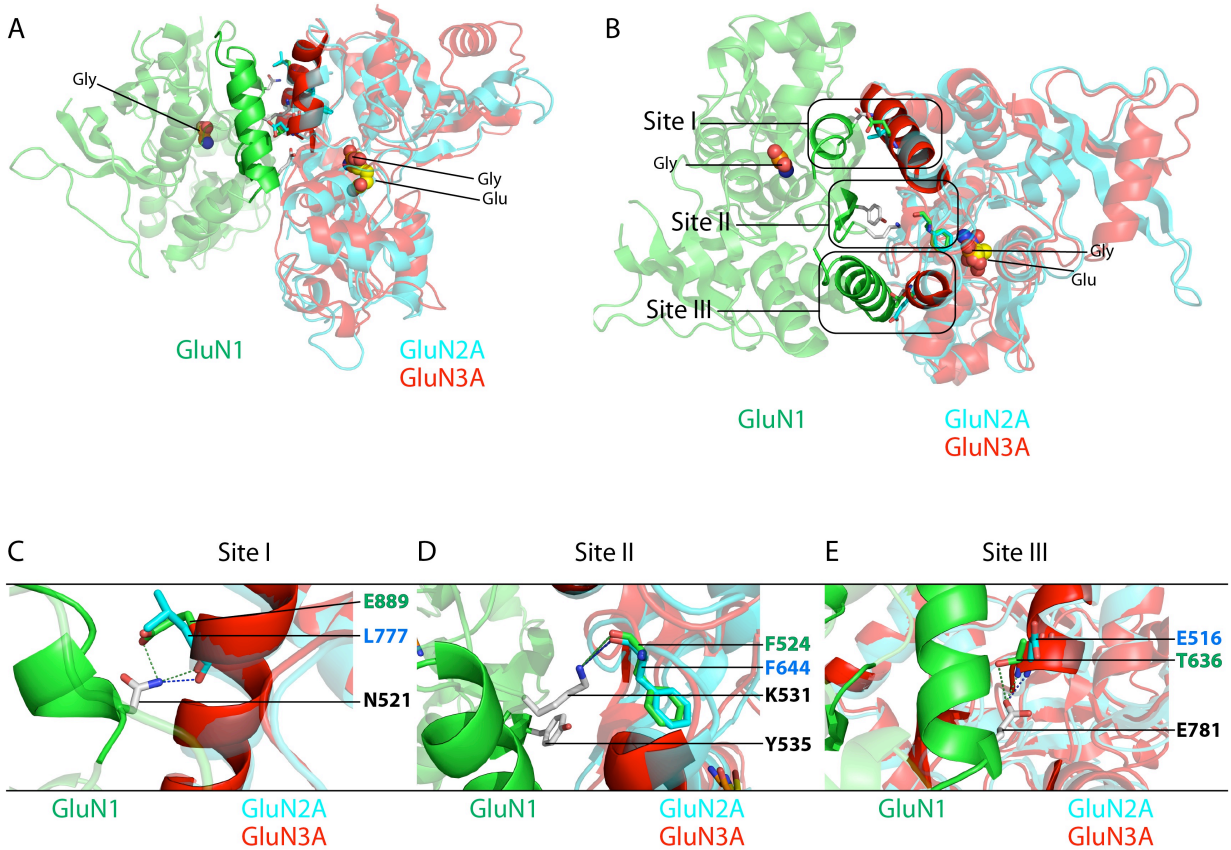

Fig. 1. Modeling of GluN1-GluN3A LBD heterodimer interface interactions. (A) Side view of the GluN1-GluN(2A/3A) LBD heterodimer in the back-to-back conformation in complex with glycine and glutamate, respectively. The GluN1 subunit is colored in green

whereas GluN2A is cyan and GluN3A is red. D- and J-Helices of the GluN1 and GluN3A subunits are highlighted for better orientation. **(B)** Top view of the GluN1-GluN(2A/3A) LBD heterodimer, the interface is separated into three distinct interaction sites (site I-III) depicted in the rectangles. This separation is according to Furukawa et al., 2005. **(C-E)** Magnification of the three interaction sites (I-III). Dashed lines indicate polar interactions. The residues participating in intersubunit contacts are shown as sticks and are colored in white (GluN1), cyan (GluN2A) and green (GluN3A).

The site II interactions include a conserved hydrogen-bonded interaction of K531 in the GluN1 with the backbone carbonyl oxygen of the phenylalanine residue F644 in GluN3A (Fig. 1D). Notably, multiple sequence alignment shows that this interaction is conserved between all AMPA- and NMDA-receptor subunits. In our previous study with GluN1/GluN2 heteromers the GluN1-K531A mutation led to a significant increase in agonist-induced currents. Therefore, we decided to incorporate this mutation in GluN1/GluN3A receptors. In a study by Furukawa et al. (2005), the GluN1-Y535 residue at site II was found to modulate deactivation properties of GluN1/GluN2A receptors, therefore we also analyzed a mutation at this position, namely GluN1-Y535A in the context of NTD-lacking GluN1$^{\Delta}$/GluN2$^{\Delta}$ receptors. In combination with GluN2A$^{\Delta}$ we saw a decrease in receptor currents whereas in combination with the GluN2B$^{\Delta}$ subunit no significant change in the I_{Max} was found (see Chapter II). Therefore, we were interested if this mutation might have an effect on macroscopic currents from GluN1/GluN3A receptors.

Next we analyzed the site III interactions that involve the J-Helix of GluN1 and the D-Helix of GluN2A/3A. As depicted in Fig. 1E the E781 residue in the GluN1 subunit makes a hydrogen-bonded interaction with the backbone nitrogen of E516 in the GluN2A or T636 in GluN3A. Additionally E781 in GluN1 is able to interact with the side chains of GluN2A-E516 or GluN3A-T636 (Fig. 1E). As stated in Chapter II this residue GluN1-E781 is conserved in the majority of all iGluR subunits except for the GluN2 and GluN3 subunits.

Our analysis of the heterodimer contacts in the LBD interface does not show huge differences between the GluN1-GluN2A and GluN1-GluN3A LBD heterodimer interface. Despite this, according to Borschel et al. (2011) removal of polar residues from the LBD dimer interface should increase the efficacy of GluN1/GluN3A receptors presumably by lowering the activation energy that is needed for channel opening. Therefore, we introduced amino acid mutations in the full-length GluN1 LBD at the three respective interaction sites (site I N521A; site II K531A and Y535A; site III E781A) and characterized them by using TEVC.

Functional characterization of GluN1-GluN3A LBD interface mutations - We conducted TEVC experiments on *Xenopus* oocytes (Fig. 2A) that were injected with cRNA and maintained for 3-4 days. From the currents measured we analyzed apparent glycine and Zn^{2+} affinities, GluN1 antagonist (MDL) mediated potentiation, and I_{Max} where possible (Fig. 2B, 3A-C). The GluN1-Y535A and –E781A mutations resulted in very small agonist-induced currents and thus measuring apparent affinities was not possible. It is known that glycine binds to the GluN1 and the GluN3A subunit but previously it was also found that Zn^{2+} is able to activate GluN1/GluN3A receptors to a similar extent as glycine, yet the binding site for Zn^{2+} has not been identified (Madry et al., 2008). However, we decided to include Zn^{2+}-activated currents in our analyses.

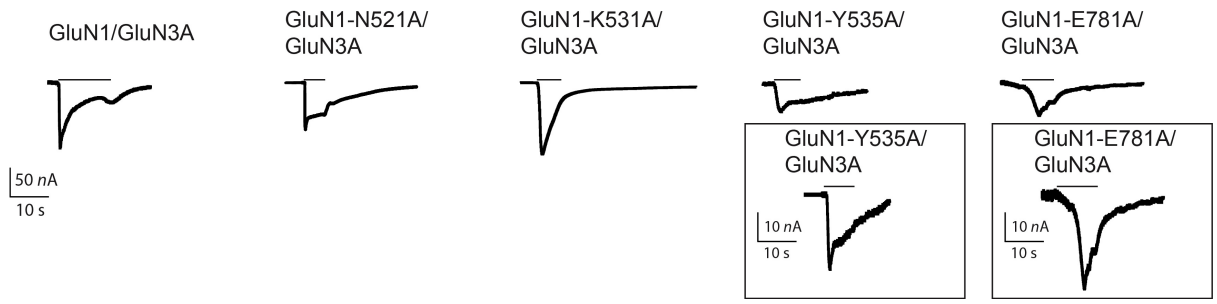

Fig. 2. Agonist-induced traces of wt and mutant GluN1/GluN3A NMDA receptors. (A) Agonist-induced responses of wt and mutant GluN1/GluN3A receptors to glycine. The currents for the receptors carrying the GluN1-Y535A and –E781A mutation were much smaller than the wt and are therefore magnified below, respectively. The bars indicate application of 1mM glycine

The site II GluN1-K531A mutation significantly decreased glycine and Zn^{2+} EC_{50} values (Fig. 2B, 3A). Compared to the wt glycine EC_{50} (4.46±0.58 μM) the EC_{50} for the GluN1-K531A/GluN3A receptor is ~5-fold reduced (24.02±4.03 μM, p<0.001). The same mutation decreased the Zn^{2+} EC_{50} by 3.7-fold, suggesting an increase in apparent affinity (wt: 371±21 μM vs. 100±11 μM, p<0.001). The fact that both apparent affinities are affected indicates a crucial role of this residue in the activation process of the receptor. In contrast, the site I GluN1-N521A residue only had an effect on the apparent Zn^{2+} affinity (Fig. 2B, 3A)(wt EC_{50}: 371±21 μM vs. 77±8.4 μM, p<0.001). It is noteworthy that the mutations caused a reduction in the apparent glycine affinity but an increase in the apparent Zn^{2+} affinity. This contradiction most probably lies in the molecular mechanism of the activation or the location of the putative binding site for Zn^{2+}.

Subunit Composition	EC_{50}		MDL potentiation	Gly I_{Max}	Zn^{2+} I_{Max}
	Gly	Zn^{2+}			
	μM		x-fold	*nA*	*nA*
GluN1 / GluN3A	4.46 ± 0.58	371 ± 21	18.3 ± 1.9	134 ± 17	724 ± 91
GluN1-N521A / GluN3A	2.61 ± 0.63	77 ± 8.4**	20.2 ± 2.2	51 ± 15**	133 ± 31**
GluN1-K531A / GluN3A	24.02 ± 4.03**	100 ± 11**	19.6 ± 1.3	103 ± 16	112 ± 38**
GluN1-Y535A / GluN3A	n.d.	n.d.	30.0 ± 5.8	16 ± 5.2**	n.d.
GluN1-E781A / GluN3A	n.d.	n.d.	8.7 ± 1.4	24 ± 5.8**	n.d.

* $P < 0.01$
** $P < 0.001$
n = 4-16

Table 1. Pharmacological and functional properties of wt and mutant GluN1/GluN3A receptors.
Values represent mean±SEM, n.d. – not detectable

Interestingly, none of the GluN1 mutants had a significant effect on the MDL-mediated potentiation (Fig. 2B, 3B left). This finding contradicts our current view of the molecular mechanism of the potentiation. We believe that MDL binding to the GluN1 subunit contributes to the stability of the LBD heterodimer interface (Madry et al., 2007a). In that respect we expected a significant reduction in MDL-mediated potentiation with one of the GluN1 mutants. In this respect the exact mechanism of the potentiation is apparently not well understood.

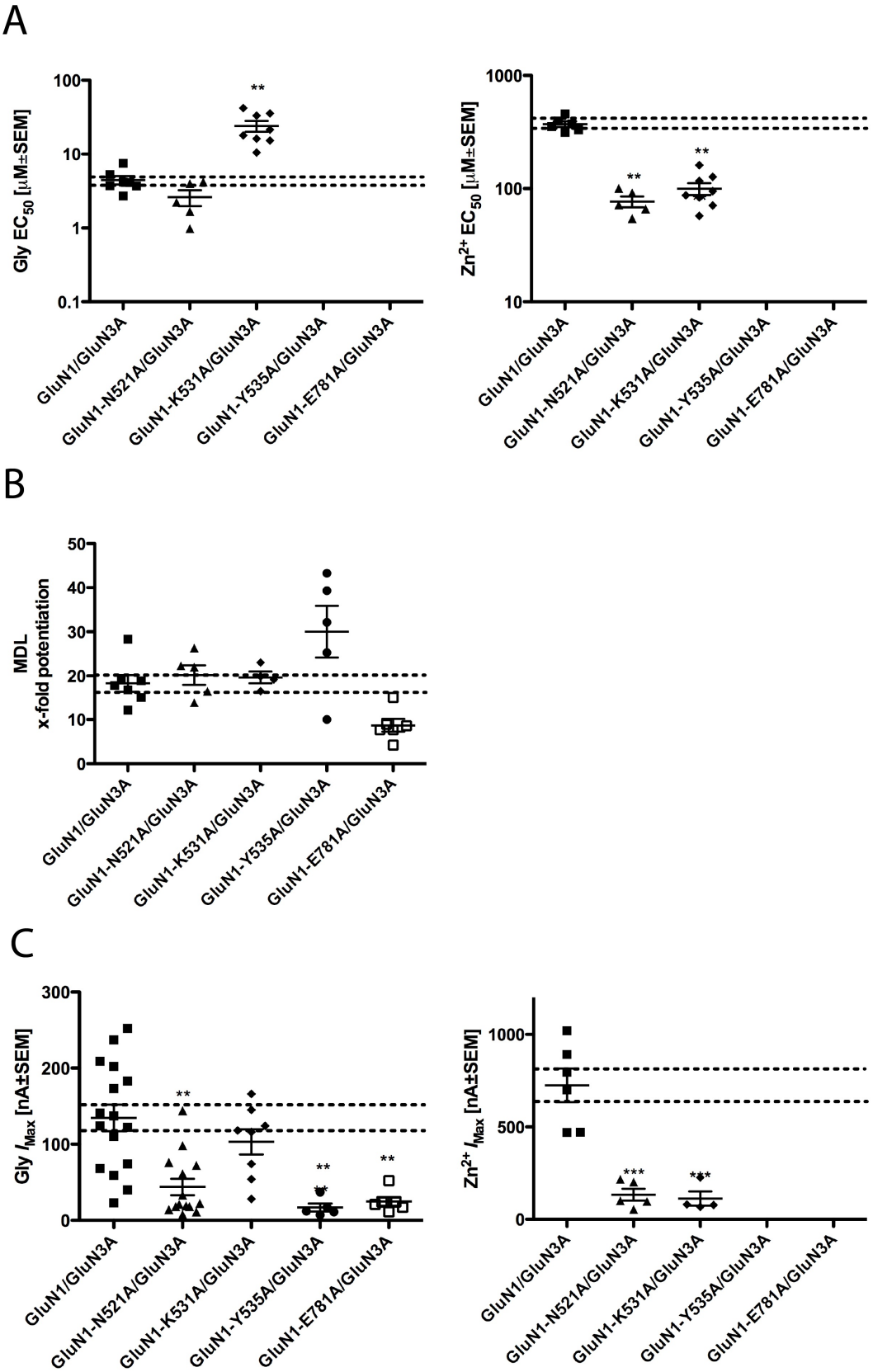

Fig. 3. Functional properties of wt and mutated GluN1/GluN3A receptors. (A) Scatter plot with mean and SEM of the apparent glycine affinity (left) and Zn^{2+} (right). **(B)** Scatter plot with mean and SEM of the GluN1 antagonist (MDL) mediated potentiation of glycine-induced currents. **(C)** Scatter plot with mean and SEM of the maximal inducible current (I_{Max}) for glycine (left) and Zn^{2+} (right).
(*) $p<0.01$, (**) $p<0.001$

Next we analyzed maximal-inducible currents by glycine and by Zn^{2+} (Fig. 3C). Except for the GluN1-K531A mutation, all other mutations (GluN1-N521A, -Y535A and –E781A) lowered the I_{Max} of glycine-induced currents significantly (Fig. 3C left)(wt: 134±17 nA, GluN1-N521A/GluN3A: 51±15 nA, GluN1-Y535A/GluN3A: 16±5.2 nA, GluN1-E781A/GluN3A: 24±5.8 nA, p<0.001). Consistent with the results from glycine-induced currents the GluN1-N521A mutation decreased the Zn^{2+} I_{Max} significantly (Fig. 3C)(wt: 724±91 nA vs. 133±31 nA, p<0.001). The GluN1-K531A mutation did not have a significant effect on maximal glycine-induced currents but it significantly decreased the I_{Max} in combination with Zn^{2+} (Fig. 3C right)(wt: 724±91 nA vs. 112±38 nA). We were surprised to see that the GluN1-Y535A and -E781A mutations completely abolished Zn^{2+}-activated currents (Fig. 3C right). Two possible explanations for this are that the Zn^{2+} binding site lies in the LBD dimer interface and is affected by the two mutations or the conformational changes upon Zn^{2+}-activation largely rely on the interactions of GluN1-Y535A and -E78A.

In conclusion, the site I mutation GluN1-N521A affected many parameters of receptor function, either these functions share a common structural basis that converges at GluN1-N521 or the GluN1-N521A mutation generally disrupts receptor function. The GluN1-K531A mutation affected mainly Zn^{2+}-activation, therefore this residue is quite specifically involved in the pharmacology of Zn^{2+} at GluN1/GluN3A receptors. The exact binding site and molecular mechanism of Zn^{2+}-activation is unknown, however, site II in the LBD heterodimer interface seems to play an important role in this respect. Surprisingly, we observed that GluN1-Y535A and -E781A largely interfere with the receptor function in GluN1/GluN3A receptors. This was not expected and also not seen with GluN1/GluN2 receptors (data not shown). Our aim was to increase the efficacy of GluN1/GluN3A receptors, but apparently mutations in the LBD heterodimer interface reduce the efficacy of this receptor type.

Analysis of partially NTD-deleted GluN1/GluN3A receptors reveal a prominent role for the GluN3A-NTDs in receptor efficacy (Note, the following experiments were conducted by Dr. Ivana Mesic) - Next, we expressed NTD-deleted subunits together with their full-length counterparts and analyzed the glycine-induced GluN1/GluN3A receptor currents. The I_{Max} of GluN1/GluN3A$^{\Delta}$ receptors were significantly higher (0.9±0.21 μA)(Table 1) compared to GluN1$^{\Delta}$/GluN3A (0.15±0.03 μA; p<0.01)(Table1) and wt GluN1/GluN3A receptors (0.15±0.02 μA, p<0.001) (Table

1). Thus, we found that the GluN3A-NTD seems to be critically involved in determining the low efficacy of GluN1/GluN3A receptors. Subsequently we also assessed the MDL-mediated potentiation and here we observed that GluN1$^{\Delta}$/GluN3A receptors are still strongly potentiated by MDL (~19-fold, Table 1), whereas in GluN1/GluN3A$^{\Delta}$ receptors the MDL-potentiation is almost abolished (~2-fold, Table 1). In summary, our data show that the GluN3A-NTDs markedly determine the efficacy of GluN1/GluN3A receptors, whereas the GluN1-NTDs are only marginally involved.

Modeling of the full-length GluN1/GluN3A receptor and analysis of NTD interactions - The previous experiments show that the GluN3A-NTD is the structural feature that determines the low efficacy of GluN1/GluN3A receptors. Therefore we aimed to identify residues in the GluN3A-NTD that are involved in the control of the receptor efficacy. Residues that are important for receptor function are commonly conserved among the distinct subunits but for the unique properties of the GluN3A subunit we expect this subunit to have distinct residues at homologous positions compared to their GluN2 counterparts. Due to the low sequence identity of the NTDs among the iGluR family members, it is not possible to identify residues involved in unique functions by amino acid sequence alignment alone.

Previously it was suggested that the NTDs of the GluN2 subunits are arranged as local homodimers by Sobolevsky et al. (2009) and thus we assume that the overall arrangement of the NTDs does not differ in the NMDAR family. Thus, we assume that the GluN3 NTDs are also arranged as local homodimers (Fig. 4A, blue subunits box #1). We built a homology model for the full-length GluN1/GluN3A receptor based on the full-length, homomeric GluA2-subtype AMPAR crystal structure by Sobolevsky et al. (2009). But we also used the GluN1-GluN2A LBD dimer crystal structure (Furukawa et al., 2005) and the GluN2B-NTD crystal structure (Karakas et al., 2009) as templates (see Experimental Procedures). Analyzing the homodimeric GluN3A-NTD interface we identified a (homophilic) interface consisting of the two α7-helices, one from each GluN3A NTD, interacting with the opposing loop between ß13 and ß14 of the other GluN3A NTD (Fig. 4A, box #1 and Fig. 4B).

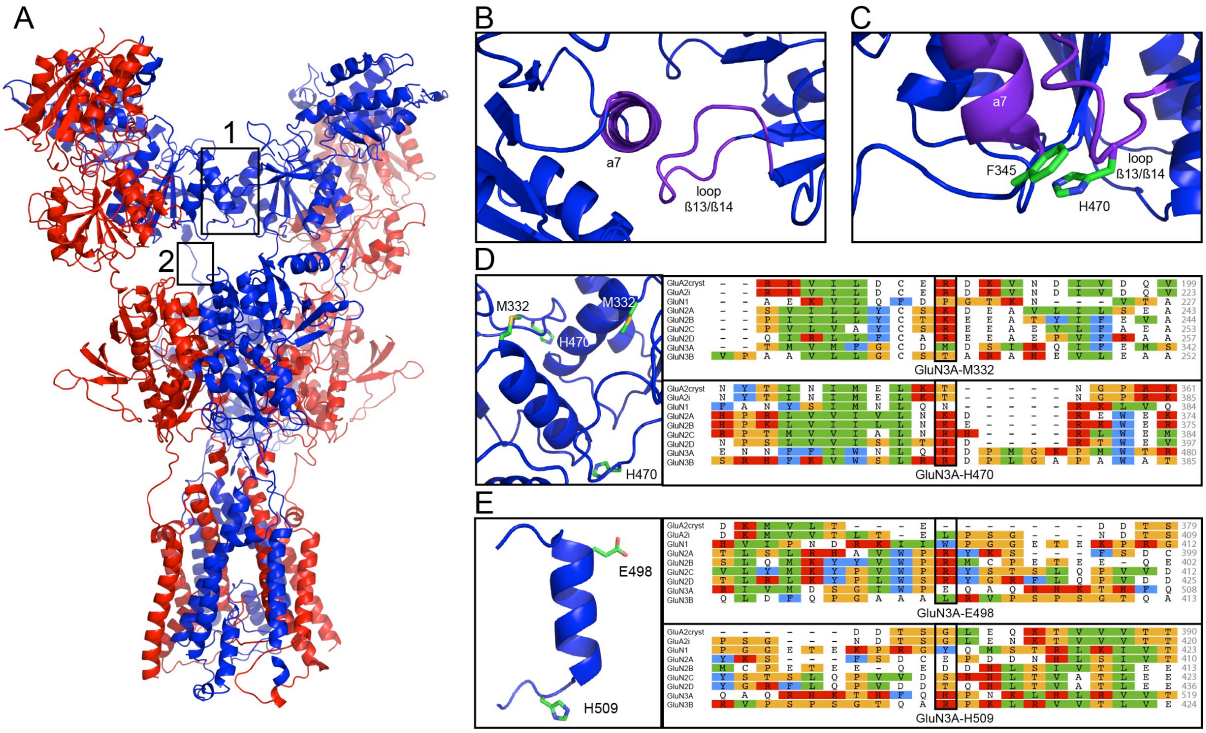

Fig. 4. GluN1/GluN3A model and partial amino acid sequence alignment of NMDA receptor subunits. (A) Model of the GluN1/GluN3A tetrameric complex (GluN1 red, GluN3A blue), box #1 depicts the homophilic GluN3A-NTD interface, the box #2 depicts the GluN3A NTD-LBD linker. **(B)** The homophilic interface consists of the α7-helix (purple) of one subunit interacting with the loop ß13/ß14 (purple) of the other GluN3A subunit. **(C)** Potential stacking interaction between GluN3A-H470 with -F345 in the NTD-interface. **(D)** Overview of the GluN3A-NTD interface and the amino acid substitutions together with the respective partial sequence alignments on the right. **(E)** Model of the secondary structure of a part of the GluN3A NTD-LBD linker with the amino acids that were mutated together with their respective partial sequence alignments to the right.
Model color code: GluN1 red, GluN3A blue (purple), the alignment is Clustal color coded.

The GluN3A-M332 residue is, according to the sequence alignment and homology model, part of the α7-helix. The homologous residues in the GluA2 and GluN2A-D subunits carry positive charges, which is an indication for a pivotal role of a positive charge at this position. The methionine residue at this position is interesting because of its nonpolar and neutral character. The mutation to the neutral but sterically shorter alanine should answer the question whether it is a steric effect of the methionine at this position that might be important for the unique features of the GluN3A NTD (Fig. 4D, upper alignment).

To further characterize the GluN3A NTD-NTD homophilic interface we generated the GluN3A-H470A mutation in the loop region between ß13 and ß14, which is, according to our model, the second region that forms the NTD-NTD interface by interacting with the respective α7-helix of the other GluN3A NTD. The GluN2A-D and GluN3B subunits carry positive charges at this position (Fig. 4D, lower alignment).

For GluN1/GluN3A we suggest that GluN3A-H470 is stacking with GluN3A-F345 and thereby stabilizing the interface (Fig. 4C). Therefore, we suggest that residues at this position either stabilize the loop itself or engage in interactions with the α7-helix.
In addition to the GluN3A NTD-NTD homophilic interface we selected mutations in the linker region between the GluN3A NTD and LBD (Fig. 4A, box #2). We focused on the negatively charged residue GluN3A-E498, as the GluN2A-D subunits possess residues with positive charges at this position (Fig. 4E, upper alignment). The homologous residues in GluN2 subunits play an active part in determining receptor kinetics, as it was shown by Gielen et al. (2009) and Yuan et al. (2009). We suggest, relying on the homology model, that these effects are exerted by their interaction with residues in the ß14 strand (e.g. R480 for GluN3A) of the NTD. Therefore, we decided to substitute the glutamate with a neutral alanine (GluN3A-E498A).

The next mutation we selected was GluN3A-H509D because; compared to the negatively charged residues in the GluN2A-B subunits, the GluN3A subunit has a histidine with an aromatic side chain (Fig. 4E, lower alignment). Although our model does not reveal a possible interfacial interaction with this residue, we chose to imitate the negative charge by mutating the histidine into aspartate.

In order to further assess this point and gain insight in the structure of the GluN3A-NTD-LBD linker region, we used protein folding prediction servers. This approach consistently showed an α-helix as well as a loop region in the GluN3A-NTD-LBD linker (Fig. 4E). To test the stability of the α-helix we constructed the GluN3A-NTD-LBD linker using the Chimera Software package and subsequently conducted MD simulations for 1 ns using Gromacs. During the simulation period the predicted α-helix remained stable. Taking together these indications, we put forward a model of the NTD-LBD linker that holds at least one α-helix. This α-helix is supposedly capable of making specific interactions, presumably with ß14 of the NTD, and this interaction largely determines kinetic properties of the NMDA receptors in general. In the case of GluN1/GluN3A receptors these interactions might account for the low efficacy of glycine-mediated receptor currents.

Functional and biochemical assessment of GluN3A-NTD mutations on receptor efficacy (Note, the following experiments were conducted by Dr. Ivana Mesic) - According to our results from the analysis of the GluN1/GluN3A homology model, we introduced the following single amino acid substitutions: GluN3A-M332A

and -H470A within the putative GluN3A-NTD homophilic interface, as well as GluN3A-E498A and -H509D in the GluN3A-NTD-LBD linker region (GluN3A 493-512). Expression of the GluN3A-M332A and GluN3A-H470A subunits with the wt GluN1 subunit resulted in glycine-gated currents that were up to 3- and 4-fold larger than the wt GluN1/GluN3A receptor (p<0.01 and p<0.001, respectively; Fig. 5A and Table 1). Analysing the GluN3A-NTD-LBD linker mutants GluN3A-E498A and GluN3A-H509D we obtained significantly higher glycine-mediated currents than those recorded from wt receptors (11- and 3-fold, respectively; p<0.001; Fig. 5A and Table 1). Interestingly, the GluN1/GluN3A-E498A receptors exhibited similar maximal inducible currents as we found for GluN1/GluN3A$^{\Delta}$ receptors (Table 1).

To exclude that the mutations cause an altered receptor expression or surface insertion, we affinity-purified wt and mutated GluN1/GluN3AHis receptors from [^{35}S]methionine and Cy5-labeled oocytes. SDS-PAGE from the wt and the mutated GluN1/GluN3A receptor proteins revealed no differences, either in the amount of total protein levels or in the cell-surface expression (Fig. 5B and 5C, respectively). We also analyzed whether the apparent glycine affinities of the GluN3A-mutated receptors differed from those seen with the wt GluN1/GluN3A receptor but no significant changes in the apparent glycine-affinity were detected (Table 1). Subsequently we assessed the MDL-mediated potentiation of the glycine-gated currents in the mutant GluN1/GluN3A receptors. With GluN1/GluN3A-H470A receptors we observed a reduced (8-fold) MDL-potentiation compared to the wt (>20-fold, p<0.01) (Fig. 5E and Table 1). The GluN3A-NTD-LBD linker mutant GluN3A-E498A resulted in a drastic decrease in MDL-potentiation compared to the wt (GluN1/GluN3A-E498A: 3-fold, p<0.001) (Fig. 5E and Table 1). Thus, mutations within the putative homophilic GluN3A-NTD interface and the GluN3A-NTD-LBD linker selectively increase the efficacy of GluN1/GluN3A receptors without affecting the apparent glycine-affinity or cell-surface expression.

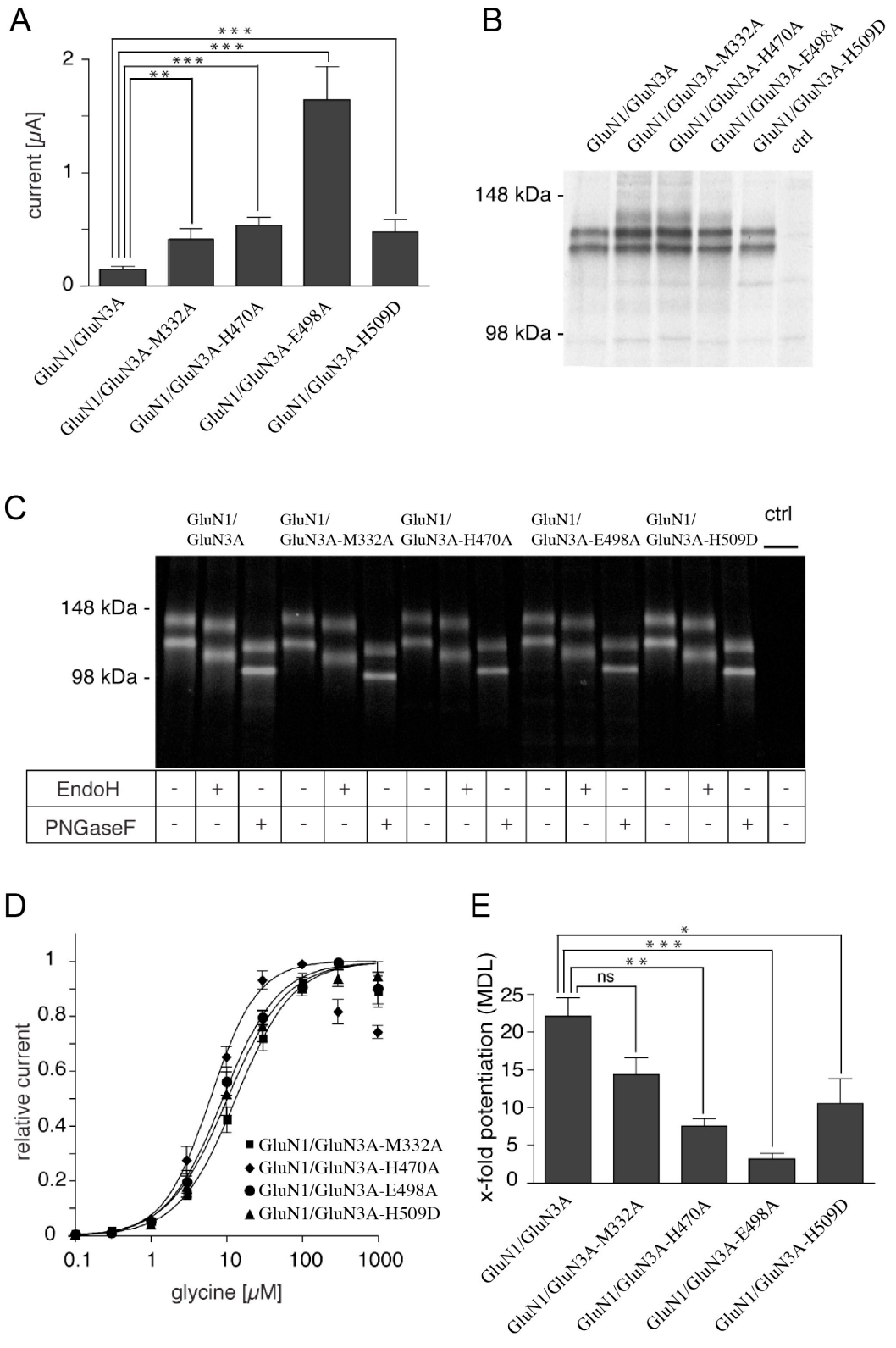

Fig. 5. Effects of GluN3A-NTD interface and GluN3A-NTD-LBD linker mutations on the functional and biochemical properties of GluN1/GluN3A receptors. (A) Mutant GluN1/GluN3A-M332A, GluN1/GluN3A-H470A, GluN1/GluN3A-E498A and GluN1/GluN3A-H509D receptors exhibit increased receptor currents upon application of 1 mM glycine compared to the wt GluN1/GluN3A receptor. **(B)** Radiogram of the SDS-PAGE of metabolically labeled and affinity-purified GluN1/GluN3A wt as well as mutant GluN1/GluN3A-M332A, GluN1/GluN3A-H470A, GluN1/GluN3A-E498A and GluN1/GluN3A-H509D receptor complexes expressed in *Xenopus* oocytes. The control (ctrl) indicates

proteins from non-injected oocytes. **(C)** Comparison of the intensities of affinity-purified Cy5 surface-labeled wt GluN1/GluN3A (lanes 1-3) as well as GluN1/GluN3A-M332A (lanes 4-6), GluN1/GluN3A-H470A (lanes 7-9), GluN1/GluN3A-E498A (lanes 10-12) and GluN1/GluN3A-H509D receptors (lanes 13-15) by SDS-PAGE revealed comparable surface-expression levels. Treatment with EndoH and PNGaseF is shown below the respective lanes indicating surface location of wt- and mutant GluN1/GluN3A receptors. The control (ctrl) denotes proteins from non-injected oocytes. **(D)** Glycine-dose response curves of GluN1/GluN3A-M332A (■), GluN1/GluN3A-H470A (◆), GluN1/GluN3-E498A (●) and GluN/GluN3A-H509D receptors (▲). **(E)** Quantitative analysis of the extent of MDL-potentiation of glycine-mediated currents from wt, as well as GluN3A-NTD interface and GluN3A-NTD-LBD linker mutant receptors. Note the highly significant decrease of MDL-potentiation in GluN1/GluN3A-H470A and GluN1/GluN3A-E498A receptors ($p < 0.001$).
(*) $p<0.05$, (**) $p<0.01$, (***) $p<0.001$
These experiments were conducted by Dr. Ivana Mesic.

Subunit Composition	Gly I_{Max} μA	Gly EC_{50} μM	MDL potentiation x-fold
GluN1/GluN3A	0.15 ± 0.02	6.5 ± 1.2	22 ± 2.6
$GluN1^{\Delta}$/GluN3A	0.15 ± 0.03	19 ± 3.2	18.8 ± 4.0
GluN1/$GluN3A^{\Delta}$	0.9 ± 0.21**	23 ± 0.95	1.9 ± 0.5**
$GluN1^{\Delta}$/$GluN3A^{\Delta}$	1.9 ± 0.23**	33 ± 2.4	2.0 ± 0.2**
GluN1/GluN3A-M332A	0.41 ± 0.1*	13.6 ± 2.4	14.4 ± 2.2
GluN1/GluN3A-H470A	0.54 ± 0.07**	6.5 ± 0.9	7.5 ± 1.0*
GluN1/GluN3A-E498A	1.64 ± 0.29**	9.4 ± 1.8	3.2 ± 0.8**
GluN1/GluN3A-H509D	0.48 ± 0.11**	11.1 ± 2.7	10.5 ± 3.3

* $P < 0.01$
** $P < 0.001$
n = 3-16

Table 2. Pharmacology from wt, mutated and NTD-deleted GluN1/GluN3A NMDA receptors after expression in *Xenopus laevis* oocytes.
Values represent means ± SEM
These experiments were conducted by Dr. Ivana Mesic.

Therefore, we suggest that GluN3A-H470 (GluN3A NTD-interface) and especially GluN3A-E498A (GluN3A-NTD-LBD linker) contribute to the low efficacy of GluN1/GluN3A receptors.

DISCUSSION

The glycine-gated GluN1/GluN3 receptors are unique among the NMDAR family because of their low-efficacy. To date it was known that the GluN1 ligand-binding site antagonist MDL-29951 and mutations within the GluN1 ligand-binding site increase glycine-induced currents (Madry et al., 2007a). However, the exact molecular mechanism of this apparent relief from auto-inhibition remained elusive. In the

present study, we generated a high-efficacy GluN1/GluN3A receptor by building and analyzing a homology model and introducing amino acid substitutions in the homophilic GluN3A-NTD interface and in the GluN3A-NTD-LBD linker region connecting the GluN3A-NTD to the subjacent GluN3A-LBD.

Our results establish a dominant negative role of the GluN3-NTDs for receptor function and thus we conclude that the GluN3-NTD resembles an auto-inhibitory domain of GluN1/GluN3 receptors.

The GluN3-NTD accounts for the low efficacy of GluN1/GluN3 receptors - Despite numerous studies on the role of the LBD dimer interface in the function of iGluRs it is not very clear if results from non-NMDARs also apply to NMDARs. For non-NMDARs it is commonly accepted that the stability of LBD dimer interactions largely determine the degree of receptor desensitization (Stern-Bach et al., 1998, Sun et al., 2002, Armstrong et al., 2006). Because of the close homology between non-NMDARs and NMDARs it was believed that the same mechanism for receptor desensitization applies to NMDARs (Furukawa et al., 2005). However, Borschel et al., (2011) reported from single-channel studies that it is not the degree of desensitization but the activation that is altered by LBD heterodimer mutations in NMDARs. Specifically, for receptor activation the LBD heterodimer interface undergoes conformational changes that are facilitated by non-polar residues, as polar residues raise the energy barrier that is needed for activation. Based on this precedent we analyzed amino acid substitutions in the GluN1-GluN3A LBD heterodimer at three distinct interaction sites (I-III) and aimed to increase the efficacy of GluN1/GluN3A receptors. Our findings indicate that the LBD heterodimer contacts are involved in general in receptor function, as we also found for $GluN1^{\Delta}/GluN2^{\Delta}$ receptors (see Chapter 2). None of the LBD heterodimer mutations enhanced responses to glycine, and in fact these mutations significantly decreased I_{Max} values for activation by glycine and Zn^{2+}. The GluN1-Y535A and -E781A mutations did not respond to Zn^{2+} and thus we reasoned that Zn^{2+} either binds or acts via the LBD heterodimer interface. Furthermore, our homology model-based analysis and mutation studies revealed the GluN3A-NTDs as the auto-inhibitory domain that dictates the low-efficacy. This finding, although surprising, is in accordance with results that underline the role of the GluN2-NTDs in NMDA-receptor function. Precisely, previous studies suggest that the GluN2-NTDs determine the apparent

glycine-affinity, deactivation time course, channel open probability and desensitization kinetics of GluN1/GluN2 receptors (Madry et al., 2007b, Yuan et al., 2009, Gielen et al., 2009). It was suggested that the bilobed GluN2-NTDs oscillate between distinct conformational states and these conformational changes are thought to be responsible for the aforementioned modulatory actions (Paoletti et al., 2007, Madry et al., 2007b, Yuan et al., 2009, Gielen et al., 2009). Furthermore, it was concluded that the frequency with which the GluN2-NTDs oscillate account for the differences between the distinct GluN2 subunits (i.e. GluN2A-D). In a similar vein, it is conceivable that the GluN3A-NTD oscillates between conformers and thus causing the low-efficacy of GluN1/GluN3A receptors. Our results demonstrate a pivotal role of the GluN3A-NTD-NTD interface and the GluN3A-NTD-LBD linker, which might be based on their involvement in GluN3A-NTD oscillations.

Importance of the NTD-LBD linker region and the putative NTD-NTD interface in determining NMDAR efficacy - As aforementioned, it is well known that the GluN2-NTDs modulate the kinetic properties of conventional NMDARs (Madry et al., 2007b, Yuan et al., 2009, Gielen et al., 2009). When substituting the NTDs between GluN2A-D subunits in order to transfer their specific properties, i.e. desensitization kinetics and P_0, it was necessary to also replace the linker regions in order to achieve the full effect (Yuan et al., 2009, Gielen et al., 2009). However, the exact mechanism that couples the modulatory action of the GluN2-NTDs and the NTD-LBD linker to the channel is yet unknown.

Similar to the findings with GluN2 NTD-LBD linkers (Yuan et al., 2009, Gielen et al., 2009), we observed that the GluN3A NTD-LBD linker participates in determining channel properties of GluN1/GluN3A receptors, since amino acid substitutions in this region largely enhanced the receptor efficacy. Despite the recent crystallization of the tetrameric $GluA2_{cryst}$ complex (Sobolevsky et al., 2009), we still lack information about the structure and conformation of the NTD-LBD linker of any of the iGluR members (Sobolevsky et al., 2009). In this crystal structure one of the four NTD-LBD linkers has a α-helical structure whereas the remaining three linkers are unwound. Thus, also in our GluN1/GluN3A homology model the NTD-LBD linkers are unwound. However, the presence of one α-helix in one of the NTD-LBD linkers in the $GluA2_{cryst}$ complex (Sobolevsky et al., 2009) provoked us to analyze this linker in more detail. Based on the aforementioned crystal structure and our secondary structure

prediction, as well as, molecular dynamics simulation we suggest that the NTD-LBD linker adopts a α-helical secondary structure and we further suggest that this structure is essential for NTD-mediated modulation of the receptor properties.

Besides the GluN3A NTD-LBD linker we have shown that mutations within the putative homophilic GluN3A NTD-interface also enhance GluN1/GluN3A receptor efficacy. The importance of this substructure in determining receptor efficacy becomes apparent when examining the heterotrimeric GluN1/GluN3A/GluN3B receptors. In contrast to the low-efficacy GluN1/GluN3A and GluN1/GluN3B receptors, these heterotrimeric receptors, that lack a homophilic GluN3-NTD interface, display large glycine-gated currents (Smothers and Woodward, 2007). According to our homology model of the GluN1/GluN3A receptor the GluN3 NTD-interface consists of two symmetrical contacts. Namely, the α7-helix of one GluN3-NTD interacts with the loop region between ß13 and ß14 of the opposing GluN3-NTD and vice versa. Our sequence analysis of the GluN3A and GluN3B NTD-interface shows a pair wise identity of 6.7% within the α7-helix and 41.7% in the loop ß13/ß14. The low identity in the α7-helix is due to a putatively shorter α7-helix in the GluN3B NTD. In our experiments disruption of the NTD-NTD-interface in GluN1/GluN3A receptors increased the receptor efficacy. Hence, we suggest that this asymmetric NTD-NTD-interface accounts for the high-efficacy of GluN1/GluN3A/GluN3B receptors. The homophilic GluN3-NTD interface is required for the inhibitory effect of the GluN3-NTDs and we suggest that the GluN3-NTD-LBD linker is involved in transmitting this inhibitory effect from the NTDs to the subjacent LBDs. How this inhibitory signal is then transmitted to the TMDs is currently not known. We reasoned that the LBD heterodimer interface is involved but in our experiments we did not find indications to verify this hypothesis. Further examination of the structure and properties of the NTD-LBD, as well as, LBD-TMD interactions will be required to fully understand the molecular mechanism of GluN3-NTD mediated low efficacy.

Auto-inhibition is a general mechanism to control protein function - Auto-inhibitory domains have already been described in various signaling proteins like AMP-activated protein kinase (AMPK), endosomal sorting complexes required for transport-III (ESCRT-III) or Crk-II type adaptor proteins (Chen et al., 2009, Bajorek et al., 2009, Cho et al., 2011). Crystallization and *in silico* analyses suggest that an auto-inhibitory domain (AID) either reduces the mobility of other subdomains until a

ligand binds (e.g. AMPK) or the AID occludes the binding site for ligands in a thermodynamic manner (e.g. Crk-II) or the AID prevents protomers to assemble to higher-order oligomers (e.g. ESCRT-III)(Chen et al., 2009, Bajorek et al., 2009, Cho et al., 2011). The equilibrium between auto-inhibited and activated conformations of signaling proteins is believed to play a key role in preventing uncontrolled activation to cellular stimuli (Yao et al., 2008, Li et al., 2008). Thus, the interdomain interfaces responsible for auto-inhibition must be stable enough to prevent constitutive activation but also labile to allow for prompt response to external or internal triggers.

To our knowledge this is the first time that an AID has been described for a ligand-gated ion channel. Under physiological conditions conventional NMDARs are blocked by extracellular Mg^{2+} and upon depolarization this Mg^{2+}-block is abolished, rendering conventional NMDARs so-called 'co-incidence detectors' (Madden, 2002). In contrast, GluN1/GluN3 receptors are not blocked by extracellular Mg^{2+} and thus they are constitutively inducible (Chatterton et al., 2002) but due to their low-efficacies this might not have detrimental consequences. However, the role of the GluN3-NTDs as AIDs might play a similar role as the Mg^{2+}-block in GluN2-containing receptors, i.e. fine tuning of receptor activation. Despite these similarities, the molecular mechanisms of AIDs seem to vary. We conclude that auto-inhibition is a common tool to control protein function but the underlying mechanism is not conserved.

Apart from endogenous GluN1 binding site antagonists (e.g. kynurenic acid) that might potentiate glycine-induced currents, also other molecules might exist that bind to the GluN3-NTD like it was described for Zn^{2+} and the GluN2A-NTD (Choi and Lipton, 1999, Fayyazuddin et al., 2000, Low et al., 2000, Paoletti et al., 1997, Paoletti et al., 2000). The functional consequence of the binding of a ligand to the GluN3A-NTD is currently not foreseeable. A relief from auto-inhibition is as reasonable as a reinforced inhibition.

Conclusions - The present study establishes a prominent role of the GluN3-NTD as an auto-inhibitory domain (AID) in GluN1/GluN3A receptor function. In contrast to the GluN1-NTD, deletion of the GluN3A-NTD resulted in a strong increase in channel efficacy. Apart from deleting the GluN3A-NTD, it is possible to increase efficacy by introducing mutations in the homophilic GluN3A-NTD interface or the GluN3A NTD-LBD linker region. Taken together, these results underline the differential roles of

NTDs in determining NMDA receptor efficacy and we also identified critical intersubunit and interdomain residues that account for the auto-inhibitory effect of the GluN3A-NTDs.

REFERENCES

Ahmed AH, Thompson MD, Fenwick MK, Romero B, Loh AP, Jane DE, Sondermann H, Oswald RE. Mechanisms of antagonism of the GluR2 AMPA receptor: structure and dynamics of the complex of two willardiine antagonists with the glutamate binding domain. *Biochemistry* 48: 3894-3903, 2009.

Armstrong N, Gouaux E. Mechanisms for activation and antagonism of an AMPA-sensitive glutamate receptor: crystal structures of the GluR2 ligand binding core. *Neuron* 28: 165-181, 2000.

Armstrong N, Jasti J, Beich-Frandsen M, Gouaux E. Measurement of conformational changes accompanying desensitization in an ionotropic glutamate receptor. *Cell* 127: 85-97, 2006.

Awobuluyi M, Yang J, Ye Y, Chatterton JE, Godzik A, Lipton SA, Zhang D. Subunit-specific roles of glycine-binding domains in activation of NR1/NR3 N-methyl-D-aspartate receptors. *Mol Pharmacol* 71: 112-122, 2007.

Bajorek M, Schubert HL, McCullough J, Langelier C, Eckert DM, Stubblefield WM, Uter NT, Myszka DG, Hill CP, Sundquist WI. Structural basis for ESCRT-III protein autoinhibition. *Nat Struct Mol Biol* 16: 754-762, 2009.

Borschel WF, Murthy SE, Kasperek EM, Popescu GK. NMDA receptor activation requires remodelling of intersubunit contacts within ligand-binding heterodimers. *Nat Commun* 2: 498, 2011.

Chatterton JE, Awobuluyi M, Premkumar LS, Takahashi H, Talantova M, Shin Y, Cui J, Tu S, Sevarino KA, Nakanishi N, Tong G, Lipton SA, Zhang D. Excitatory glycine receptors containing the NR3 family of NMDA receptor subunits. *Nature* 415: 793-798, 2002.

Chen L, Jiao ZH, Zheng LS, Zhang YY, Xie ST, Wang ZX, Wu JW. Structural insight into the autoinhibition mechanism of AMP-activated protein kinase. *Nature* 459: 1146-1149, 2009.

Cho JH, Muralidharan V, Vila-Perello M, Raleigh DP, Muir TW, Palmer AGr. Tuning protein autoinhibition by domain destabilization. *Nat Struct Mol Biol* 18: 550-555, 2011.

Choi YB, Lipton SA. Identification and mechanism of action of two histidine residues underlying high-affinity Zn2+ inhibition of the NMDA receptor. *Neuron* 23: 171-180, 1999.

Dingledine R, Borges K, Bowie D, Traynelis SF. The glutamate receptor ion channels. *Pharmacol Rev* 51: 7-61, 1999.

Farina AN, Blain KY, Maruo T, Kwiatkowski W, Choe S, Nakagawa T. Separation of domain contacts is required for heterotetrameric assembly of functional NMDA receptors. *J Neurosci* 31: 3565-3579, 2011.

Fayyazuddin A, Villarroel A, Le Goff A, Lerma J, Neyton J. Four residues of the

extracellular N-terminal domain of the NR2A subunit control high-affinity Zn2+ binding to NMDA receptors. *Neuron* 25: 683-694, 2000.

Fiser A, Sali A. Modeller: generation and refinement of homology-based protein structure models. *Methods Enzymol* 374: 461-491, 2003.

Furukawa H, Gouaux E. Mechanisms of activation, inhibition and specificity: crystal structures of the NMDA receptor NR1 ligand-binding core. *EMBO J* 22: 2873-2885, 2003.

Furukawa H, Singh SK, Mancusso R, Gouaux E. Subunit arrangement and function in NMDA receptors. *Nature* 438: 185-192, 2005.

Gielen M, Retchless BS, Mony L, Johnson JW, Paoletti P. Mechanism of differential control of NMDA receptor activity by NR2 subunits. *Nature* 2009.

Hansen KB, Furukawa H, Traynelis SF. Control of assembly and function of glutamate receptors by the amino-terminal domain. *Mol Pharmacol* 78: 535-549, 2010.

Hess, B., Kutzner, C., van der Spoel, D. and Lindahl, E. GROMACS 4: Algorithms for Highly Efficient, Load-Balanced, and Scalable Molecular Simulation*, J. Chem. Theory Comput.,* 4, 435-447, 2008.

Hu B, Zheng F. Molecular determinants of glycine-independent desensitization of NR1/NR2A receptors. *J Pharmacol Exp Ther* 313: 563-569, 2005.

Inanobe A, Furukawa H, Gouaux E. Mechanism of partial agonist action at the NR1 subunit of NMDA receptors. *Neuron* 47: 71-84, 2005.

Karakas E, Simorowski N, Furukawa H. Structure of the zinc-bound amino-terminal domain of the NMDA receptor NR2B subunit. *EMBO J* 2009.

Kleywegt GJ. Use of non-crystallographic symmetry in protein structure refinement. *Acta Crystallogr D Biol Crystallogr* 52: 842-857, 1996.

Kuryatov A, Laube B, Betz H, Kuhse J. Mutational analysis of the glycine-binding site of the NMDA receptor: structural similarity with bacterial amino acid-binding proteins. *Neuron* 12: 1291-1300, 1994.

Laube B, Hirai H, Sturgess M, Betz H, Kuhse J. Molecular determinants of agonist discrimination by NMDA receptor subunits: analysis of the glutamate binding site on the NR2B subunit. *Neuron* 18: 493-503, 1997.

Li P, Martins IR, Amarasinghe GK, Rosen MK. Internal dynamics control activation and activity of the autoinhibited Vav DH domain. *Nat Struct Mol Biol* 15: 613-618, 2008.

Low CM, Zheng F, Lyuboslavsky P, Traynelis SF. Molecular determinants of coordinated proton and zinc inhibition of N-methyl-D-aspartate NR1/NR2A receptors. *Proc Natl Acad Sci U S A* 97: 11062-11067, 2000.

Madden DR. The structure and function of glutamate receptor ion channels. *Nat Rev Neurosci* 3: 91-101, 2002.

Madry C BH, Geiger JRP, Laube B. Supralinear potentiation of NR1/NR3A excitatory glycine receptors by Zn^{2+} and NR1 antagonist. *PNAS* 2008.

Madry C, Mesic I, Bartholomaus I, Nicke A, Betz H, Laube B. Principal role of NR3 subunits in NR1/NR3 excitatory glycine receptor function. *Biochem Biophys Res Commun* 354: 102-108, 2007.

Madry C, Mesic I, Betz H, Laube B. The N-terminal domains of both NR1 and NR2 subunits determine allosteric Zn2+ inhibition and glycine affinity of N-methyl-D-aspartate receptors. *Mol Pharmacol* 72: 1535-1544, 2007.

Mayer ML. Glutamate receptors at atomic resolution. *Nature* 440: 456-462, 2006.

Paoletti P, Ascher P, Neyton J. High-affinity zinc inhibition of NMDA NR1-NR2A receptors. *J Neurosci* 17: 5711-5725, 1997.

Paoletti P, Perin-Dureau F, Fayyazuddin A, Le Goff A, Callebaut I, Neyton J. Molecular organization of a zinc binding n-terminal modulatory domain in a NMDA receptor subunit. *Neuron* 28: 911-925, 2000.

Paoletti P, Neyton J. NMDA receptor subunits: function and pharmacology. *Curr Opin Pharmacol* 7: 39-47, 2007.

Papadakis M, Hawkins LM, Stephenson FA. Appropriate NR1-NR1 disulfide-linked homodimer formation is requisite for efficient expression of functional, cell surface N-methyl-D-aspartate NR1/NR2 receptors. *J Biol Chem* 279: 14703-14712, 2004.

Pettersen EF, Goddard TD, Huang CC, Couch GS, Greenblatt DM, Meng EC, Ferrin TE. UCSF Chimera--a visualization system for exploratory research and analysis. *J Comput Chem* 25: 1605-1612, 2004.

Qiu S, Zhang XM, Cao JY, Yang W, Yan YG, Shan L, Zheng J, Luo JH. An endoplasmic reticulum retention signal located in the extracellular amino-terminal domain of the NR2A subunit of N-Methyl-D-aspartate receptors. *J Biol Chem* 284: 20285-20298, 2009.

Smothers CT, Woodward JJ. Pharmacological characterization of glycine-activated currents in HEK 293 cells expressing N-methyl-D-aspartate NR1 and NR3 subunits. *J Pharmacol Exp Ther* 322: 739-748, 2007.

Sobolevsky AI, Rosconi MP, Gouaux E. X-ray structure, symmetry and mechanism of an AMPA-subtype glutamate receptor. *Nature* 2009.

Stern-Bach Y, Russo S, Neuman M, Rosenmund C. A point mutation in the glutamate binding site blocks desensitization of AMPA receptors. *Neuron* 21: 907-918, 1998.

Sucher NJ, Akbarian S, Chi CL, Leclerc CL, Awobuluyi M, Deitcher DL, Wu MK,

Yuan JP, Jones EG, Lipton SA. Developmental and regional expression pattern of a novel NMDA receptor-like subunit (NMDAR-L) in the rodent brain. *J Neurosci* 15: 6509-6520, 1995.

Sun Y, Olson R, Horning M, Armstrong N, Mayer M, Gouaux E. Mechanism of glutamate receptor desensitization. *Nature* 417: 245-253, 2002.

Yao Y, Harrison CB, Freddolino PL, Schulten K, Mayer ML. Molecular mechanism of ligand recognition by NR3 subtype glutamate receptors. *EMBO J* 27: 2158-2170, 2008.

Yao X, Rosen MK, Gardner KH. Estimation of the available free energy in a LOV2-J alpha photoswitch. *Nat Chem Biol* 4: 491-497, 2008.

Yuan H, Hansen KB, Vance KM, Ogden KK, Traynelis SF. Control of NMDA receptor function by the NR2 subunit amino-terminal domain. *J Neurosci* 29: 12045-12058, 2009.

FOOTNOTES

*This study was supported by the Max-Planck Gesellschaft, Deutsche Forschungsgemeinschaft (B.L., LA 1086/4-2), Gemeinnützige Hertie-Stiftung (B.L.) and Fonds der Chemischen Industrie (H.B.).

CHAPTER 5
INTERSUBUNIT CONTACTS IN THE TRANSMEMBRANE DOMAIN INVOLVING TM4 DETERMINE RECEPTOR FUNCTION BUT NOT ASSEMBLY OF NMDA RECEPTORS

Ceyhun Tamer, Adriana Längle and Bodo Laube
Department of Molecular and Cellular Neurophysiology, TU-Darmstadt, Schnittspahnstrasse 3, 64287 Darmstadt, Germany

***N*-Methyl-D-Aspartic acid (NMDA) receptors are tetrameric complexes that belong to the family of ionotropic glutamate receptors (iGluRs). NMDA receptors are composed of two glycine binding GluN1 and glutamate binding GluN2 and/or glycine binding GluN3 subunits. The subunits consist of two large extracellular domains that are homologous to bacterial, periplasmic amino acid binding proteins. Furthermore, the transmembrane domain (TMD) of iGluRs is homologous to potassium channels (K^+ channels). Despite this, iGluRs require one membrane spanning segment (TM4) more than K^+ channels for proper receptor function. However, the exact role of this TM4 segment is not well understood but crystallization of the GluA2-subtype AMPA receptor complex allows further structural analysis. Based on experimental findings in our lab (by Dipl. Biol. Adriana Längle) the TM4 is implicated in receptor function but not the assembly, trafficking or stoichiometry of NMDARs composed of GluN1 and GluN3A subunits. Here, we analyzed a model of the GluN1/GluN2A TMD and introduced single amino acid substitutions in the GluN1-TM4 and GluN2A-TM3. We identified two mutations that render GluN1/GluN2A receptors non-functional. One glycine residue (GluN1-G828) being part of a GxxxG motif and one glutamate residue (GluN1-E835) that forms a polar connection to the GluN2A-TM3. Additionally we performed a bioinformatics approach to identify residues that are evolutionary dependent on either GluN1-G828 or -E835. We found correlations to residues mainly located in the TM1 and TM4 facing the TMD intersubunit contact between GluN1 and GluN2A. Thereby we conclude, GluN1-G828 and -E835 are involved in maintaining the stability of the TMDs but are not directly involved in gating or ion permeation.**

Introduction

Ionotropic glutamate receptors (iGluRs) are ligand-gated ion channels that are present at excitatory synapses in the central nervous system and mediate fast information transfer (Dingledine et al., 1999). These tetrameric complexes can be activated by subtype specific ligands, such as (RS)-2-amino-3-(3-hydroxy-5-methyl-4-isoxazolyl)propionic acid (AMPA), kainate and *N*-methyl-D-aspartic acid (NMDA) thus being classified as AMPA receptors (subunits GluA1-4), kainate receptors (subunits GluK1-4) and NMDA receptors (subunits GluN1, GluN2A-D and GluN3A-B). Each subunit has a modular structure with two large extracellular domains, i.e. N-terminal domain (NTD) and ligand-binding domain (LBD) that show sequence homology to bacterial, periplasmic amino acid binding proteins, i.e. Leucine-Isoleucine-Valine-binding protein (LIVBP) and Lysine-Arginine-Ornithine-binding protein (LAOBP) respectively (Masuko et al., 1999, Paoletti et al., 2000, Madden, 2002, Paoletti and Neyton, 2007). The transmembrane domain (TMD) is formed by three transmembrane segments (TM1, TM3 and TM4) and one M2 re-entrant loop. The C-terminal domain (CTD) is located intracellular and has been implicated to interact with scaffolding proteins (Dingledine et al., 1999).

The overall tetrameric structure of the TMDs and the presence of a re-entrant loop closely resembles the composition of an inverted K^+ channel (KcsA) except for the TM4 that is absent in KcsA channels (Wollmuth et al., 2004). The crystallization of the tetrameric GluA2-subtype of AMPA receptors by Sobolevsky et al. (2009) further confirmed this observation. Although the TMD of the AMPA receptors shares only ~20% sequence identity with the KcsA channel, the structures of TM1, M2 and TM3 of the AMPA receptor superimpose very well on the structure of the KcsA channel (Doyle et al., 1998) yielding a RMSD (root mean squared deviation) of 2.2Å (Sobolevsky et al., 2009). Due to the close homology between NMDARs and AMPARs it is suggested that the NMDAR TMDs are arranged in a similar fashion (Sobolevsky et al., 2009). However, the lack of a fourth membrane domain in the KcsA channel suggests that the TM4 in iGluRs was an evolutionary addition and as such the role of the TM4 is a matter of debate (Wollmuth et al., 2004). The TM4 is not a dispensable domain, Schorge and Colquhoun (2003) analyzed TM4 truncated constructs and found that TM4-lacking subunits are not functional, however, co-expression of the respective TM4 fragment recovers receptor function. The reason why TM4 is required for channel function is unknown. It has been suggested that the

TM4 contributes to the channel pore and mutations in it affect ion channel gating (Beck et al., 1999, Ren et al. 2003). Despite this finding, the AMPA receptor crystal structure shows that the TM4 does not directly contribute to the ion channel, it is located close to TM1 and TM3 of the neighboring subunit and thus engages in intersubunit contacts (Sobolevsky et al., 2009). In a study by Horak et al. (2008) it was reported that endoplasmic reticulum (ER) retention signals in the TM1 and TM3 of GluN1 and GluN2B subunits are present and TM4 truncation results in the intracellular accumulation of the subunits. Furthermore, it is shown that TM4 is required to mask the ER retention signals and thus facilitate surface trafficking of the receptors. It is though that ER retention is a quality assurance system and as such it prevents misfolded proteins to reach cell-surface. Misfolded proteins are retained in the ER and are subsequently degraded.

A study by Haeger et al. (2010) analyzed TMD interactions in another family of ligand-gated ion channels, the Cys-loop receptors. Cys-loop receptors are pentameric complexes in contrast to iGluRs, which are tetramers. Haeger et al (2010) studied the inhibitory glycine receptors (GlyRs) and serotonine receptors (5HT3 receptors) that are members of this class. Each subunit consists of an extracellular ligand-binding domain (ECD), four transmembrane helices (TM1-TM4) and an extracellular C-terminal domain. The TMDs of Cys-loop receptors are not homologous to the TMDs of iGluRs. However, Haeger et al. (2010) found that the truncation of TM4 impairs the subunit stoichiometry and thus, subunits assemble uncontrolled into higher oligomeric states. The co-expression of the TM4 recovers proper subunit stoichiometry and receptor function and it is further shown that an aromatic network of residues determines the pentameric assembly (Haeger et al., 2010).

Experimental findings in our lab indicate that the TM4 is not required for the assembly, stoichiometry or cell surface trafficking of GluN1/GluN3A receptors. Therefore, we suggest that the TM4 might not only be essential for masking ER retention signals but plays an important role in the overall stability of the TMD. Based on these results and our model of the GluN1-GluN2A TMD we aimed at identifying residues in the TMD intersubunit interface of GluN1/GluN2A receptors that determine the stability and function of the receptor complex. For this, we introduced single amino acid substitutions in the TM4 of GluN1 and TM3 of GluN2A and characterized

the resulting receptors by means of recording whole cell currents from cRNA injected *Xenopus* oocytes using two-electrode voltage-clamp.

EXPERIMENTAL PROCEDURES

cDNA constructs, heterologous expression and electrophysiology - The cDNA constructs of GluN1-1a (rat), C-terminal hexahistidyl-tagged GluN1-1a (rat) and GluN2A (mouse) have been described previously (Madry et al., 2007b). Single point mutations were introduced via site-directed mutagenesis (QuikChange XL Site-Directed Mutagenesis Kit, Stratagene) and confirmed by DNA sequencing (Eurofins MWG Operon). All constructs were linearized and transcribed into cRNA (mCAP mRNA Capping Kit, Ambion) as described (Madry et al., 2010). For biochemical analyzes and electrophysiological recordings, 25 ng of cRNA/oocyte was injected. *Xenopus laevis* oocytes were isolated and maintained as described (Laube et al., 1997). Two-electrode voltage-clamp recording of glutamate- and glycine-induced whole cell currents was performed according to Laube et al., 1997.

Metabolic [^{35}S]-methionine labelling, purification and SDS-PAGE - To detect intracellular expressed receptor complexes the oocytes were labelled after cRNA injection, by incubation in [^{35}S]-methionine solution overnight (>40 TBq/mM, Amersham Biosciences) at ~100 MBq/ml (0.2 MBq per oocyte) (Schuler et al., 2008). The receptor complexes were purified from dodecylmaltoside extracts of the labelled oocytes via a hexahistidyl tag by nickel nitriloacetic acid (Ni^{2+}-NTA) agarose (Qiagen) chromatography as described in Madry et al., 2007b. [^{35}S]-methionine-labelled protein samples were solubilized in SDS sample buffer containing 20 mM dithiothreitol (DTT) and electrophoresed together with molecular mass markers (SeeBlue® Plus2 Pre-Stained Standard, Invitrogen) on 8% tricine- SDS-polyacrylamide gels. After blotting, fixation and drying of the gel, it was exposed to BioMax MR films (Kodak, Stuttgart, Germany) at –80 °C.

Surface labelling with cell impermeable Cy5 dye - Four days after the injection of cRNAs, the injected and non-injected control oocytes were surface labelled with 65 µM of Cy5-NHS-ester dye (Amersham Biosciences) and solubilized for affinity purification as described above. Gels containing Cy5-labelled protein samples were

scanned with a gel imager (*Storm 840*, Molecular dynamics) as described in Madry et al., 2007a.

Glycosylation Assay - To distinguish between intracellular and cell-surface receptor complexes, 10µl of the affinity-purified receptors were incubated in reducing sample buffer (20 mM DTT, 1% (w/v) SDS) containing 1% (w/v) octylglucoside with 5U endoglycosidase H (Endo H) or peptide-N-Glycosidase F (PNGase F; NEB, Frankfurt, Germany) at 37°C for 1 h. Afterwards protein samples were analyzed by SDS-PAGE as described above.

Mutual Information analysis - Sequence alignment of the iGluR-receptor subunits was taken from (Sobolevsky et al., 2009) and supplemented with the sequences of GluA1-4, GluK1-4, GluN1, GluN2A-D and GluN3A-B from different species which gave a total of 249 sequences that were downloaded from NCBI. The alignments were computed using Geneious Software (v.4.8.3, Biomatters Ltd. Auckland, New Zealand) and then the alignment was optimized by hand and trimmed to the TM1, TM3 and TM4 domains only. In the MI analysis interdependencies between pairs of positions in a multiple sequence alignment are calculated. If it is possible to infer the amino acid at a certain position by knowing the amino acid at another position, these two positions will have a high MI value, thus they are interdependent. If it is not possible to infer the amino acid at another position, such a pair will have a low MI value and thus they are not interdependent. The MI is calculated according to the following equation:

$$MI(X;Y) = \sum_{x}\sum_{y} p(x,y)\log_2\left(\frac{p(x,y)}{p(x)p(y)}\right)$$

p(x) and *p(y)* represent the frequencies of each amino acid type at position *X* or *Y*, respectively. The probability to observe the combination of these two amino acids is given by *p(x,y)*. Apart from the 20 standard amino acids, *x* and *y* can have a gap "-" or "X" for non-standard amino acids as their values. The MI calculation results in a *N x N* matrix with *N* being the sequence length of the multiple sequence alignment. Thus the symmetrical MI matrix holds $\frac{N(N+1)}{2}$ values, one for each pair of positions in the alignment. The calculation was performed using the statistical software package R (v.2.10, R Development Core Team 2011) and the BioPhysConnectoR library (Hoffgaard et al., 2010). Based on the sequence alignment the MI matrix was

computed and standardized to a null model with 10,000 randomization steps (White et al., 2007, Weil et al., 2009). The null model consists of the same alignment but the amino acids in each column are shuffled vertically in their position as to remove the sequence correlation. In each randomization step a new null model MI matrix is computed. The expectation value from the null model m_{ij} is the average of the 10,000 *(i,j)* entries and together with the corresponding variances the Z-scores can be calculated. For this, the null model was subtracted from the MI matrix and the resulting matrix was divided by the standard deviation (square root of the variance). The entries in the resulting matrix represent Z-scores, which are normalized onto the standard deviation. Thus each Z-score has the standard deviation as its unit e.g. a value of 10 means that the Z-Score is 10 standard deviations away from the expectation value m_{ij}. Because of its symmetry the diagonal and the lower triangle of the Z-score matrix were set to 0. For subsequent data analyses Microsoft Excel (v.2011) and for visualization purposes PyMOL v.1.3 (Schrödinger Inc., New York, NY, USA) were used.

For statistical data analysis Graphpad Prism v.5.0a (GraphPad Software Inc., San Diego, CA, USA) has been used.
For all analyses, values are given as means ± SEM if not stated otherwise.
Statistical significance was tested with one-way ANOVA and the Dunnett Post-Hoc-Test. For all *p*-values applies (*) $p<0.01$, (**) $p<0.001$ if not stated otherwise.

RESULTS

In this study we aimed at identifying residues in the intersubunit interface in the TMDs of GluN1/GluN2A receptors that are critical for receptor function and thus gain more insight into the role of the fourth membrane domain (TM4).

TM4 truncation does not interfere with receptor assembly, cell-surface expression or subunit stoichiometry (Note, the following experiments were conducted by Dipl Biol. Adriana Längle) - Studies by Schorge and Colquhoun (2003) and Horak et al. (2008), conducted on GluN1/GluN2 NMDARs, pointed out that the TM4 is required for proper receptor function and assembly. However, co-expression of the TM4 fragment recovers receptor function. Furthermore an ER retention signal in the TM3 domains was identified and the TM4 domain is involved in

masking this ER retention (Horak et al., 2008). Thus, TM4 truncation impairs cell-surface trafficking of NMDAR complexes. These experiments were conducted on classical GluN1/GluN2 NMDARs. To further investigate the role of the TM4 domain Dipl. Biol. Adriana Längle conducted experiments on GluN1/GluN3A NMDARs. She generated a TM4-truncated GluN1 construct (GluN1ΔM4) and the respective TM4 fragment (GluN1-M4). Functional and biochemical analyses were carried out on cRNA injected *Xenopus* oocytes. It was found that co-expression of GluN1ΔM4 and GluN3A subunits leads to the formation of GluN1ΔM4/GluN3A receptors. These receptors are not only expressed intracellular but also reach the cell surface, shown by [35S]methionine- or Cy5-labelling and SDS-PAGE (Längle et al., in preparation). Analysis of the band intensities also revealed unaltered subunit stoichiometry and thus it is concluded that the GluN1-TM4 does not interfere with receptor assembly, cell-surface trafficking or subunit stoichiometry. However, functional analysis using two-electrode voltage-clamp showed no detectable responses upon agonist application (Längle et al., in preparation). Therefore it is further concluded that the TM4, although not required for proper receptor assembly and trafficking, is essential for receptor function.

These results define a different role of the TM4 in GluN1/GluN2 and GluN1/GluN3A receptors. In Glun1/GluN2 receptors the GluN1-TM4 is required for surface trafficking (Horakt et al., 2008), whereas in GluN1/GluN3A receptors it is not (Längle et al., in preparation). In order to disclose the functional role of the TM4 in more detail we chose to introduce single amino acid substitutions rather than deleting the whole TM4.

Homology model based analysis of TM4 intersubunit contacts - Here, we analyzed our homology model of the tetrameric GluN1-GluN2A TMD. This homology model is based on the tetrameric GluA2-subtype AMPA receptor crystal structure by Sobolevsky et al. (2009, PDB ID: 3KG2) and has already been published in Endele et al. (2010). Each subunit consists of three membrane-spanning domains, i.e. TM1, TM3 and TM4, whereas the M2 domain is a re-entrant loop and was not included in our analyses. The TM3 helices form the inner core of the ion channel (Fig. 1A), whereas TM1 and TM4 helices are not directly located in the ion permeation pathway. Interestingly, the TM1, TM3 and M2 domains of each subunit are in close proximity to each other whereas the TM4 engages mainly in intersubunit interactions

with the neighboring TM1 and TM3 domains (Fig. 1A-B). The TM4 adopts a remote position with respect to its subunit and thus resembles a hook that seems to tie up the neighboring subunit. Therefore, we were interested in the functional role of the intersubunit interface between the TM4 and the neighboring TM1 and TM3 (Fig. 1B). Based on the homology model and the multiple sequence alignment of NMDAR subunits we chose to introduce four amino acid substitutions in the GluN1-TM4, namely GluN1-F817A, -I824A, -G827V and –E834A. According to the homology model the residues GluN1-F817 and –I824 are facing towards the TM1 of the neighboring subunit, as well the position of GluN1-817 is strictly conserved in the other NMDAR subunits, whereas GluN-I824 is not (Fig. 1B-C). By mutating these two residues we intended to asses the functional implication of this TM4 and TM1 intersubunit interface. Furthermore, the GluN1-G827 and –E834 residues are directed towards the TM3 of the neighboring subunit according to our homology model. According to sequence information (Fig. 1C) GluN1-G827 might be a part of a GxxxG motif, a motif that has been shown to critically determine TMD interactions (Unterreitmeier et al., 2007, Langosch et al., 2009). In contrast to the residues mentioned before the GluN1-E834 residue is hydrophilic. Due to its charged character and observations from the homology model we reasoned that this glutamate might form a hydrogen bond with residues GluN2A-T625 or –T626. The respective Cα-atom distance is 11.4 and 10.9 Å, this is a little too far for hydrogen bonds to form, however, *in vivo* this distance might be shorter and the high level of conservation of this position indicates a pivotal role. The apparent interacting residues in the TM3 are only partially conserved. The homologous residues to GluN2A-T625 are only conserved within GluN2A-D subunits, whereas the homologous position of GluN2A-T626 shows a higher degree of conservation, i.e. only the GluN1 subunit differs as it carries a serine at this position (Fig. 1C). By mutating the GluN1-G827 and –E834 residues we intended to gain insight into the functional implication of the TM4 and TM3 intersubunit interface.

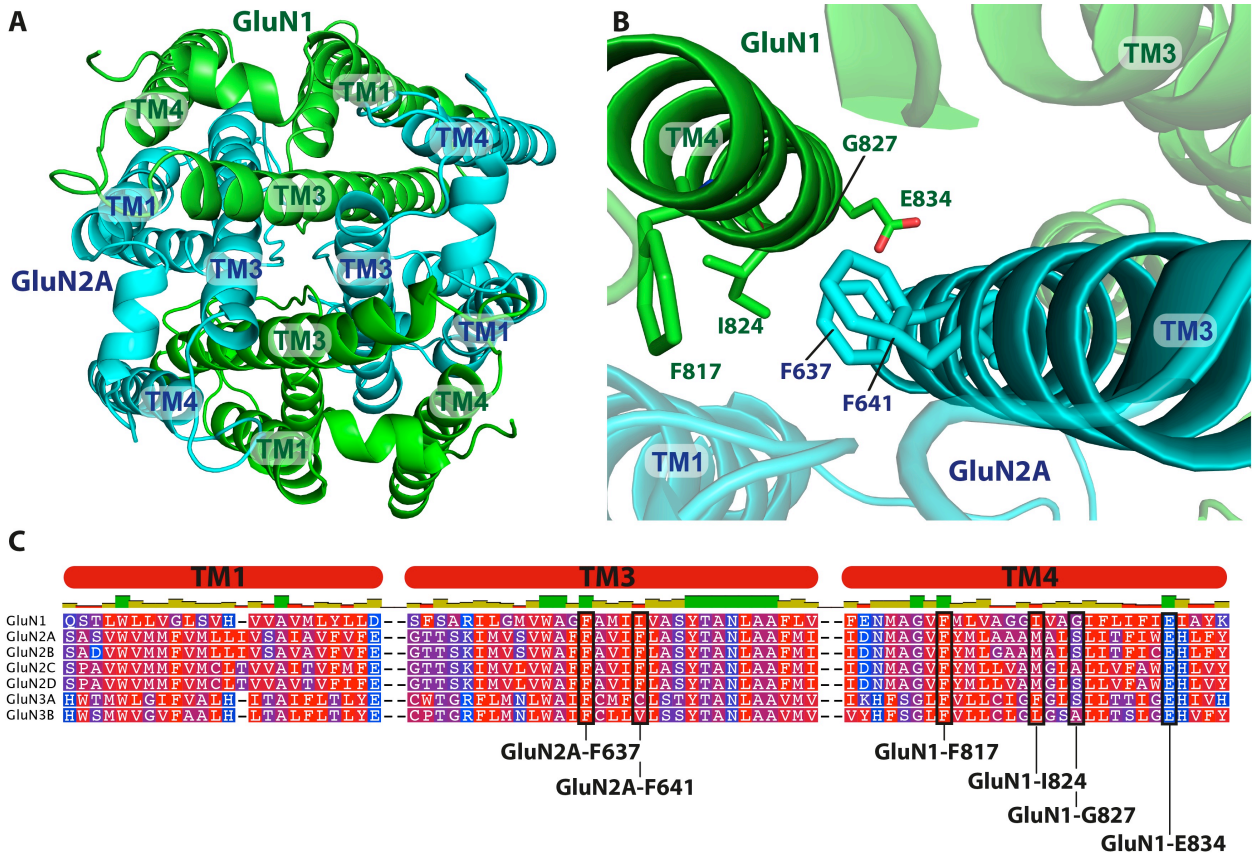

Fig. 1. Homology model based analysis of GluN1-GluN2A TMD interactions. (A) Top view of the 4-fold symmetrical GluN1-GluN2A TMD. The GluN1 subunit is colored in green whereas GluN2A is cyan. **(B)** Magnification of GluN1-GluN2A TMD intersubunit interface. GluN1-TM4 and GluN2A-TM3 are highlighted, amino acids that were selected for site-directed mutagenesis are depicted as sticks. **(C)** Multiple sequence alignment of rat NMDAR subunits. Degree of conservation for each position is shown above the alignment, red horizontal bars indicate TM1, TM3 and TM4 respectively.

Apart from the GluN1-TM4 we decided to mutate two residues in the GluN2A-TM3, which, according to our model, are oriented towards the space between the GluN1-TM4 and TM1 and TM3 of GluN2A. We reasoned that these two residues, GluN2A-F637 and -641, might play a critical role in forming an aromatic network between the TMDs. According to the sequence alignment, GluN2A-F637 and the homologous residues in the other NMDAR subunits are very well conserved (Fig. 1C). GluN2A-F641 and the homologous residues are only conserved within the GluN2 subunits (Fig. 1C). Both residues were mutated to alanine residues, i.e. GluN2A-F637A and –F641A.

Utilizing our homology model of the GluN1-GluN2A TMD and multiple sequence alignment we identified residues that form the TMD intersubunit interface involving the TM4 of GluN1 and TM1 as well as TM3 of GluN2A, thereby assessing the functional implication of the TM4.

Single amino acid substitutions in the TM4 render the NMDA receptor non-functional (Note, the following experiments were conducted by Dipl Biol. Adriana Längle) – In the GluN1 and GluN2A subunits a total of 6 residues were mutated by sited-directed mutagenesis and whole-cell current responses were recorded from *Xenopus* oocytes. The mutations were selected based on the GluN1-GluN2A TMD homology model and sequence alignment, namely these were GluN1-F817A, -I824A, -G827V, -E834A and GluN2A-F637A as well as –F641A. From these GluN1/GluN2A mutant receptor combinations four exhibited robust current responses upon co-application of glycine and glutamate. The GluN1-TM4 mutation G827V resulted in a drastic decrease in the maximal inducible current (I_{Max})(p<0.001), whereas the GluN1-E834A/GluN2A mutant receptors failed to exhibit agonist-induced currents (Fig. 2). The multiple sequence alignment indicates that GluN1-G827 is part of a GxxxG-motif, which was found to be important for TMD interactions and stability (Unterreitmeier et al., 2007, Langosch et al., 2009). The significant reduction in I_{Max} supports the importance of this residue and indicates that indeed a TMD intersubunit ineraction is stabilized by this GxxxG-motif. Even more significant than the GluN1-G827V mutation is the –E834A mutation, as GluN1/GluN2A receptors carrying this mutation did not elicit any measurable currents. The lack of response shows that this highly conserved residue plays an important role in the TMD intersubunit interface. According to our hypothesis, this residue makes a polar connection to the TM3 of the neighboring subunit. As the TM3 domains form the inner core of the ion channel, a functional implication of GluN1-E834 was expected. However, if this effect is caused by a functional effect or a lack of cell-surface expressed receptors in not clear at the moment.

In contrast to these findings, the GluN2A-F641A mutation caused a significant increase in I_{Max} when co-expressed with the GluN1 subunit (Fig. 2)(p<0.001). This finding was surprising as we expected that impairment of the aromatic network between the TMDs would destabilize the receptor. Therefore, we expected to see a decrease in the I_{Max}. The increase in I_{Max} might indicate an increase of the receptor efficacy, which might be due to eased rearrangements in the TMD that lead to the opening of the ion channel.

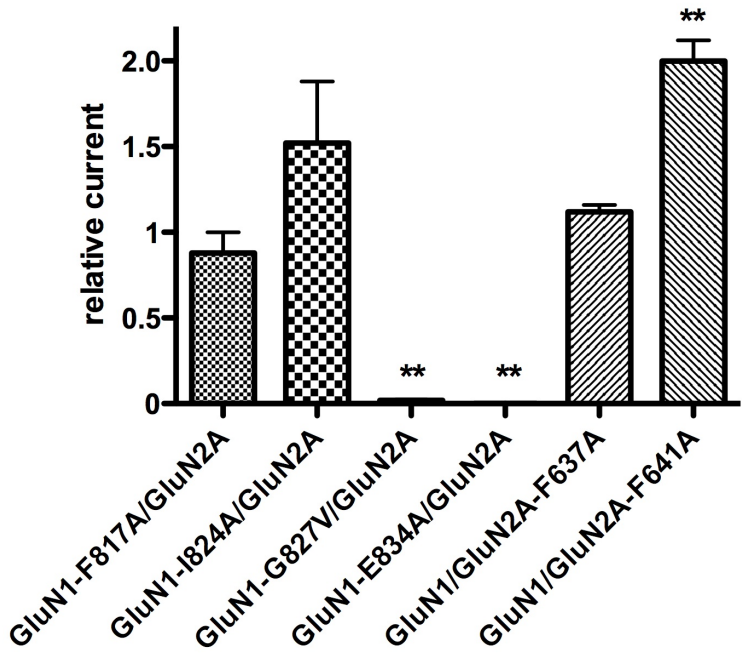

Fig. 2. Maximal inducible currents of mutated GluN1/GluN2A receptors. I_{Max} values were determined in the presence of 100 µM glycine and glutamate.
Data represent means ± SEM, (*) p<0.01, (**) p<0.001
Note: Dipl. Biol. Adriana Längle conducted experiments.

Additionally, the I_{Max}, apparent affinities (EC_{50}) for glycine and glutamate were determined (Table 1). For the mutations that led to non-functional or almost non-functional receptors it was not possible to make dose-response measurements. The other mutant receptor combinations did not alter either glycine or glutamate EC_{50} values significantly (Table 1). These results indicate that the mutations decrease or increase receptor currents specifically by increasing/decreasing receptor efficacy. However, we cannot exclude the possibility that the mutations also affect receptor assembly and/or cell-surface trafficking.

Subunit Composition	EC_{50}		Gly I_{Max}
	Gly	Glu	
	μM		μA
GluN1 / GluN2A	0.6 ± 0.1	1.7 ± 0.3	2.5 ± 0.2
GluN1-F817A / GluN2A	1.5 ± 0.4	1.7 ± 0.2	2.2 ± 0.3
GluN1-I824A / GluN2A	0.8 ± 0.4	1.7 ± 0.3	3.8 ± 0.9
GluN1-G827V / GluN2A	-	-	0.05 ± 0.01**
GluN1-E834A / GluN2A	-	-	nf **
GluN1 / GluN2A-F637A	3.6 ± 2.0	0.7 ± 0.2	2.8 ± 0.1
GluN1 / GluN2A-F641A	0.4 ± 0.1	2.3 ± 0.6	5.0 ± 0.3**

* $P < 0.01$
** $P < 0.001$
n = 6-7

Table 1. Pharmacology of wt and mutated GluN1/GluN2A receptors. Glycine and glutamate EC_{50} values as well as I_{Max} values were determined in the presence of 100 µM glycine and/or glutamate.
Data represent means ± SEM, nf, non-functional
Note: Dipl. Biol. Adriana Längle conducted experiments.

The data presented here show that the mutations in GluN1-TM4 and GluN2A-TM3 either increase or decrease maximal inducible currents but without significantly affecting apparent glycine or glutamate affinities. Note that the mutations in the GluN1-TM4 and GluN2A-TM3 interface, i.e. GluN1-G828V and –E834A, drastically decreased the I_{Max} or led to non-functional receptors, whereas mutations in the GluN1-TM4 and GluN2A-TM1 interface, i.e. GluN1-F817A and –I824A, resulted in currents and apparent affinities comparable to those of wild-type (wt) GluN1/GluN2A receptors.

Using MI analysis for putative functional implications of GluN1-G828V and -E835A – The data presented here establish a prominent role of residues in the GluN1-TM4 and GluN2A-TM3 interface. Whether these residues are involved in receptor function or in receptor assembly or trafficking is unclear. In order to address this question we utilized a bioinformatics approach that is commonly used for the identification of evolutionary interdependent positions in a protein, the so-called mutual information (MI). Using large multiple sequence alignments it is possible to address the question if two positions in the alignment are paired in a way that they

tend to mutate dependently. We already applied this approach successfully in Chapter 2. This approach does not directly reveal putative functions of the residues. Despite this, we reasoned that if two positions are evolutionary connected they might also serve a similar function in the protein. Our hypothesis is that positions that are important for receptor assembly will be evolutionary connected and thus receive a high Z-score in the MI analysis. Vice versa, positions implicated in receptor function will also have a high Z-score in the MI analysis. On the other hand positions that play a role in receptor assembly and those that are crucial for receptor function should receive a lesser Z-score. Based on this hypothesis we were expecting to see significant correlations of either GluN1-G827 or GluN1-E834 with positions in the TM3 that are proximal to the ion permeation pathway, if these residues are involved in receptor function rather than assembly or trafficking. Conversely, if these residues are not directly involved in receptor function but the overall stability of the TMD, we would expect to see significant correlations with residues that putatively stabilize TMD interactions. To test this hypothesis, we selected a position in the highly conserved SYTANLAAF motif in the TM3 of NMDARs. This motif is essential for receptor function and mutations in this motif lead to non-functional receptors (Blanke and VanDongen, 2007). The GluN1-N650 residue is part of the SYTANLAAF motif and we utilized the MI analysis to find positions that are correlated with this position (Fig. 4). According to our hypothesis we would expect to find mainly correlations to positions within TM3 and especially in the SYTANLAAF motif (Table 2). First, we analyzed the Z-score distribution of the MI analysis in order to assess the reliability of the Z-scores. We found a Gaussian-like distribution with its center at Z-score values of 25-30 (Fig. 3). Below a Z-score of 10 an increase the number of data points is visible and we suppose that this increase is generated by a false, i.e. random, signal. Therefore we suggest to focus on Z-scores greater than 5.

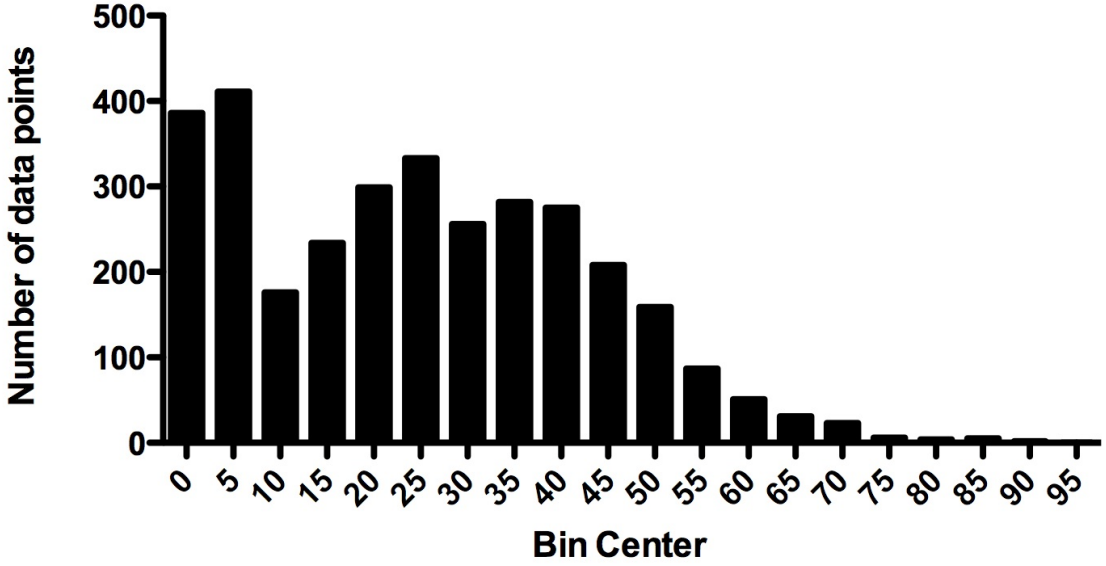

Fig. 3. Histogram of Z-score distribution of MI analysis for TMDs of iGluR subunits. The histogram shows a bimodal distribution of Z-scores. One Gaussian-like distribution with its center at Z-score values of 25-30. The increase of data points at Z-scores 0-5 is presumably caused by random correlations.

Next, we searched for MI correlations for GluN1-N650 with Z-scores greater than 5. We found 10 correlations, which are shown in Table 2.

GluN1-N650 correlations

	GluN1-TM1	Z-score	GluN1-TM3	Z-score	GluN1-TM4	Z-score
1			S585	13.32	F810	7.74
2			A649	12.41		
3			W636	10.78		
4			L651	10.77		
5			A653	10.51		
6			F639	10.34		
7			T648	9.90		
8			Y647	9.69		
9			M634	7.77		

Table 2. Results of MI analysis for GluN1-N650 in TM3. GluN1-N650 is part of the highly conserved SYTANLAAF motif, which is crucial for receptor function. Shown are GluN1 residues that are present at the respective position. MI analysis is based on multiple sequence alignment of TM1, TM3 and TM4 of 249 iGluR subunits.

As expected we found 9 out of 10 correlations within TM3 and 5 correlated positions are within the SYTANLAAF motif and one correlation was found with the GluN1-TM4 residue F810 (Table 2 and Fig. 4). Although not a proof, we take this as an indication for the validity of our hypothesis.

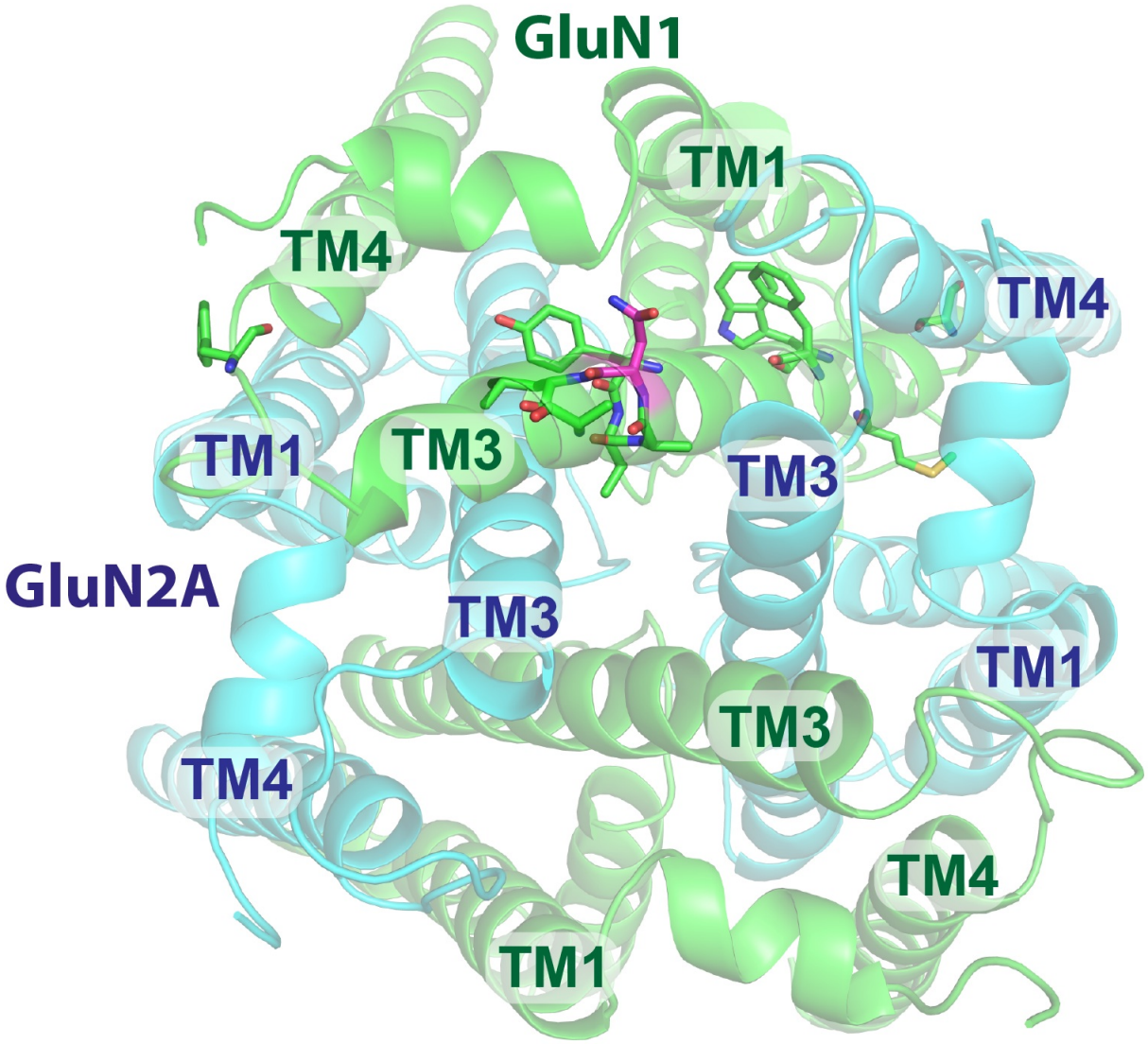

Fig. 4. Homology model of GluN1-GluN2A TMD and MI correlations of GluN1-N650. Top view of the 4-fold symmetrical GluN1-GluN2A TMD. The GluN1 subunit is colored in green whereas GluN2A is cyan. The residue highlighted in magenta is GluN1-N650, an important residue in the SYTANLAAF motif. The other residues depicted as sticks are, according to MI analysis, evolutionary correlated to GluN1-N650.

Next, we applied the MI analysis to the aforementioned GluN1-G827 and GluN1-E834 positions. The MI analysis showed correlations mainly in the TM1 and TM4 domains. As the GluN1-TM4 makes contact to the neighboring subunits' TM1 and TM3 we reasoned that GluN1-G827 and GluN1-E834 are correlated with GluN2A-TM1 and GluN2A-TM3 (Table 3, Fig. 5).

GluN1-G827 correlations

	GluN2A-TM1	Z-score	GluN2A-TM3	Z-score	GluN1-TM4	Z-score
1	S556	43.94			F810	47.28
2	M560	43.47			A821	42.04
3	F576	40.18			G822	39.66
4	V575	38.53			F832	38.41
5					V825	38.25
6					A836	36.17

GluN1-E834 correlations

	GluN2A-TM1	Z-score	GluN2A-TM3	Z-score	GluN1-TM4	Z-score
1	V575	8.22			F817	12.3
2	E577	5.51			M813	6.72
3	M561	5.42			I834	6.48
4	V559	5.35			I824	6.34
5	L566	5.3			G815	5.65

Table 3. Results of MI analysis for GluN1-G827 and GluN1-E834. Identification of positions that are interdependent with GluN1-G827 and GluN-E834. All of the correlations were found either in the TM1 or TM4. MI analysis is based on multiple sequence alignment of TM1, TM3 and TM4 of 249 iGluR subunits.

The correlated positions were only distributed between the GluN1-TM4 and GluN2A-TM1 (Table 3). We observed that preferentially correlations to hydrophobic residues were found. The correlated positions are also distributed along the full length of the TMDs (Fig. 5) indicating that GluN1-G827 and GluN1-E834 are involved in a hydrophobic, not necessarily aromatic, network that stabilizes TMD interactions. We take these observations as an indication that the GluN1-G827 and GluN1-E834 residues are generally involved in stabilizing TMD interactions, which seems to be also important for receptor function as mutations at these positions largely reduced agonist-induced receptor currents.

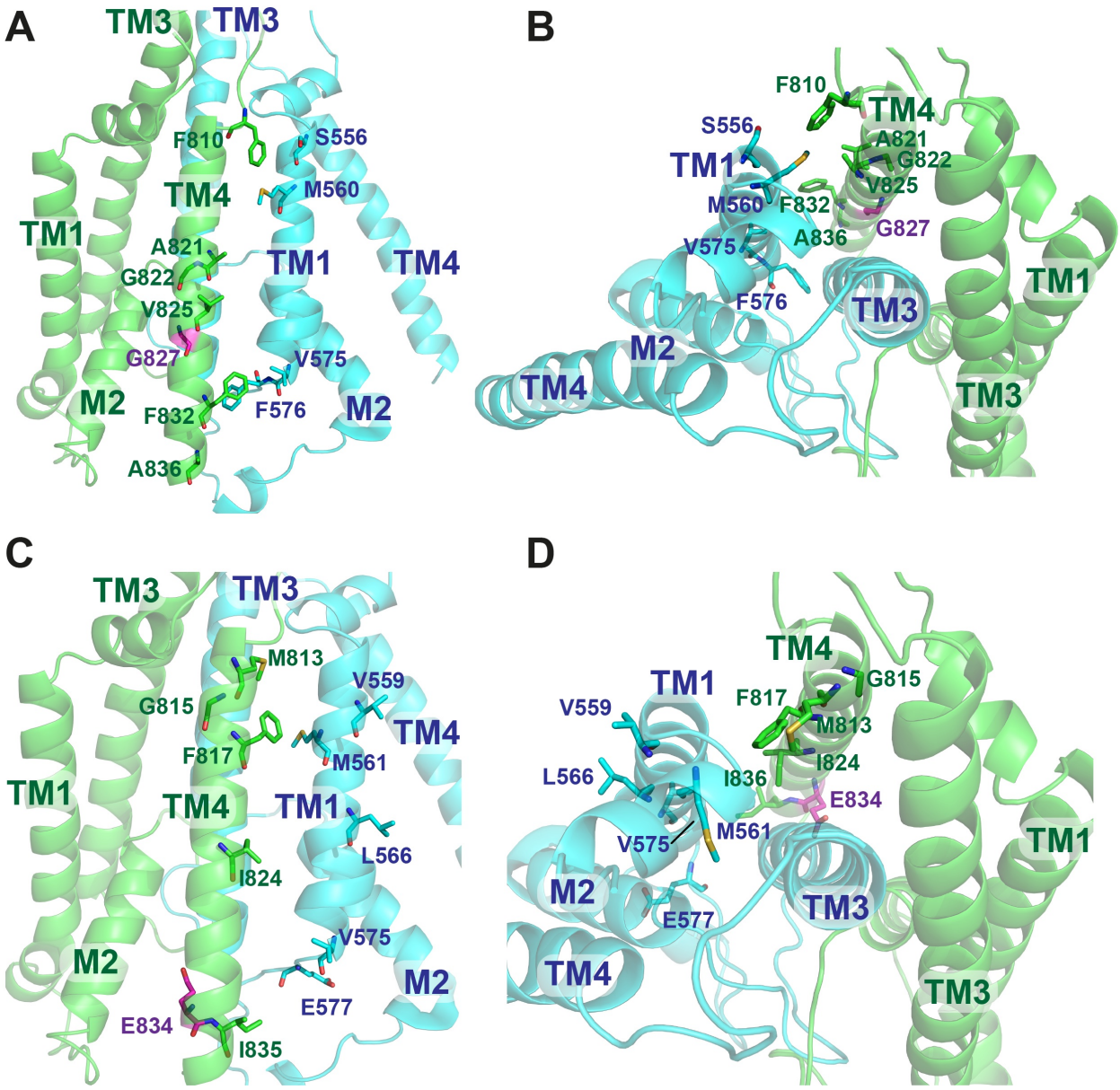

Fig. 5. Homology model based visualization of MI correlations for GluN1-G827 and GluN1-E834. The GluN1 subunit is shown in green and GluN2A is shown in cyan. **(A,B)** Side/Top view of a GluN1-GluN2A TMD dimer. Highlighted in magenta is GluN1-G827 and positions that were found to be interdependent are depicted as sticks. **(C,D)** Side/Top view of a GluN1-GluN2A TMD dimer. Highlighted in magenta is GluN1-E834 and positions that were found to be interdependent are depicted as sticks.

From our MI analysis we conclude that it is possible to draw functional implications for positions that were found to be correlated with each other. Thus, positions with a crucial role in receptor function will most probably tend to have high Z-scores with positions that are also critically involved in receptor function. We hypothesize that the same is true for positions that are important for receptor assembly. The analysis of the GluN1-G827 and GluN1-E834 positions indicates that these positions determine receptor function by stabilizing TMD interactions.

DISCUSSION

In this study we aimed at identifying residues in the intersubunit interface in NMDAR TMDs and thus assess the role of the fourth membrane domain TM4. Our results revealed that the TM4 is not essential in GluN1/GluN3A receptors for receptor expression, assembly, subunit stoichiometry or cell-surface trafficking. These results stand in contrast to findings for GluN1/GluN2B receptors where the TM4 was found to be necessary to mask an ER retention signal for the receptors to reach the cell-surface (Horak et al., 2008). Based on this observation we reasoned that the TM4 is implicated in receptor function. Additionally, Ren et al. (2003) found that a methionine residue (M823) in GluN2A affects functional receptor properties, such as desensitization and channel open probability. Here, we used a homology model of the GluN1-GluN2A TMD to select amino acids in the intersubunit interface between GluN1-TM4 and GluN2A-TM1, as well as GluN1-TM4 and GluN2A-TM3. These residues were mutated and electrophysiological characterized. We also utilized MI analysis to draw conclusions about putative functional implications of these residues. We found that a glycine residue (G827) in a not conserved GxxxG motif in the GluN1-TM4 and the GluN1-E834 residue are critically involved in stabilizing the intersubunit interactions, which seem to be significant for receptor function.

The TM4 is an evolutionary addition responsible for the overall stability of the tetrameric iGluR complex – The crystal structure of the KcsA-type K^+ channel shows that two transmembrane helices are sufficient to ensure ion channel function (Doyle et al., 1998). The crystal structure of the GluA2-type AMPA receptor revealed that despite a relatively low sequence identity of ~20% between the TMDs of AMPARs and the KcsA channel, their structures superimpose pretty well (Sobolevsky et al., 2009). However, all iGluR subunits have a fourth membrane-spanning domain, the TM4. Therefore, the TM4 seems to be indispensable for iGluR function. In a previous study by Horak et al. (2008) it was found that the TM4 masks ER retention signals in GluN1/GluN2B receptors. Our results display a pivotal role of the TM4 in stabilizing TMD intersubunit interactions that are required for receptor function. Combining these findings with the results from Horak et al. (2008) we suggest that masking the ER retention signals is not the essential role of the TM4 but the stabilization of the TMD. We suggest that ER retention developed subsequently as a quality control to prevent non-functional receptors to reach cell-surface. Thus, we

suggest that masking of ER retention signals is a consequence of the significant role of the TM4 in iGluR function. To answer the question why the TM4 is required for the stability of the ion channel we reasoned that size might matter. A KcsA subunit consists of 166 amino acids, hence, the tetrameric complex has 664 amino acids. The GluN1 (rat) and GluN2A (rat) subunits consist of 938 and 1504 amino acids, respectively. Therefore, the tetrameric complex has 4884 amino acids, this is 7.35-times the size of the KcsA channel. We propose that, due to the heavily increased size of iGluRs in general compared to the KcsA channel, a fourth membrane domain was necessary to stabilize the complex.

In contrast, the TM4 in another class of ligand-gated ion channels, the Cys-loop receptors, was found to determine the pentameric subunit stoichiometry (Haeger et al., 2010). Truncation of the TM4 causes the subunits to oligomerize in a non-defined manner. But co-expression of the TM4 fragment recovers the pentameric assembly. The overall organization of the TMD of Cys-loop receptors differs significantly from the KcsA or iGluR TMD. The transmembrane helices of Cys-loop receptors sit straight next to each other, contrary the transmembrane helices in KcsA and iGluR subunits are leaning and twisted (Doyle et al., 1998, Sobolevsky et al., 2009, Haeger et al., 2010). Thus, it seems that the role of the TM4 depends on the receptor class, hence, no underlying general mechanism exists.

MI analysis has the potential to provide functional implications for correlated positions in proteins – The MI analysis is a bioinformatics approach that has originated from telecommunication but was adapted for the identification of positions in proteins that are interdependent in a way that mutations at these positions affect each other. Thus, the MI analysis is a tool to search for positions that mutated in a concerted manner. We utilized the MI analysis to draw conclusions about functional implications of correlated positions and tested this hypothesis by applying the MI analysis to a position in the well-conserved SYTANLAAF motif, which is known to directly determine receptor function. The correlations that were found were mainly located in the SYTANLAAF motif itself and in close vicinity of this motif. This is a good indication that positions that are mainly implicated in receptor function will have a high Z-score with positions that are also implicated in receptor function. The MI analysis of positions in the TM4 found correlations within the TM4 and with TM1 but no positions within the SYTANLAAF motif for example. Hence, we conclude

that the TM4 is not directly involved in determining functional properties. Although these findings are preliminary, we believe that the MI analysis might prove to be a useful utility to predict roles of certain positions and residues in protein complexes. However, this hypothesis should be tested with various proteins and needs to be verified by experiments.

Conclusions – We conclude that the fourth membrane-domain (TM4) is an evolutionary addition to the iGluR subunits to stabilize the TMD and ensure proper channel function. We suggest that this auxiliary stabilizing element was necessary because of the increased size of iGluR subunits compared to KcsA channel subunits. Also we tested the MI analysis for the prediction of identifying functional or other roles of residues in the protein complex. Our results indicate that it is indeed possible to distinguish between positions that determine functional properties and positions that lead to the overall stabilization of the TMD.

REFERENCES

Beck C, Wollmuth LP, Seeburg PH, Sakmann B, Kuner T. NMDAR channel segments forming the extracellular vestibule inferred from the accessibility of substituted cysteines. *Neuron* 22: 559-570, 1999.

Dingledine R, Borges K, Bowie D, Traynelis SF. The glutamate receptor ion channels. *Pharmacol Rev* 51: 7-61, 1999.

Doyle DA, Morais Cabral J, Pfuetzner RA, Kuo A, Gulbis JM, Cohen SL, Chait BT, MacKinnon R. The structure of the potassium channel: molecular basis of K+ conduction and selectivity. *Science* 280: 69-77, 1998.

Endele S, Rosenberger G, Geider K, Popp B, Tamer C, Stefanova I, Milh M, Kortum F, Fritsch A, Pientka FK, Hellenbroich Y, Kalscheuer VM, Kohlhase J, Moog U, Rappold G, Rauch A, Ropers HH, von Spiczak S, Tonnies H, Villeneuve N, Villard L, Zabel B, Zenker M, Laube B, Reis A, Wieczorek D, Van Maldergem L, Kutsche K. Mutations in GRIN2A and GRIN2B encoding regulatory subunits of NMDA receptors cause variable neurodevelopmental phenotypes. *Nat Genet* 42: 1021-1026, 2010.

Haeger S, Kuzmin D, Detro-Dassen S, Lang N, Kilb M, Tsetlin V, Betz H, Laube B, Schmalzing G. An intramembrane aromatic network determines pentameric assembly of Cys-loop receptors. *Nat Struct Mol Biol* 17: 90-98, 2010.

Herrmann JR, Panitz JC, Unterreitmeier S, Fuchs A, Frishman D, Langosch D. Complex patterns of histidine, hydroxylated amino acids and the GxxxG motif mediate high-affinity transmembrane domain interactions. *J Mol Biol* 385: 912-923, 2009.

Horak M, Chang K, Wenthold RJ. Masking of the endoplasmic reticulum retention signals during assembly of the NMDA receptor. *J Neurosci* 28: 3500-3509, 2008.

Laube B, Hirai H, Sturgess M, Betz H, Kuhse J. Molecular determinants of agonist discrimination by NMDA receptor subunits: analysis of the glutamate binding site on the NR2B subunit. *Neuron* 18: 493-503, 1997.

Madden DR. The structure and function of glutamate receptor ion channels. *Nat Rev Neurosci* 3: 91-101, 2002.

Madry C, Betz H, Geiger JR, Laube B. Potentiation of Glycine-Gated NR1/NR3A NMDA Receptors Relieves Ca-Dependent Outward Rectification. *Front Mol Neurosci* 3: 6, 2010.

Madry C, Mesic I, Bartholomaus I, Nicke A, Betz H, Laube B. Principal role of NR3 subunits in NR1/NR3 excitatory glycine receptor function. *Biochem Biophys Res Commun* 354: 102-108, 2007.

Madry C, Mesic I, Betz H, Laube B. The N-terminal domains of both NR1 and NR2 subunits determine allosteric Zn2+ inhibition and glycine affinity of N-methyl-D-aspartate receptors. *Mol Pharmacol* 72: 1535-1544, 2007.

Masuko T, Kashiwagi K, Kuno T, Nguyen ND, Pahk AJ, Fukuchi J, Igarashi K, Williams K. A regulatory domain (R1-R2) in the amino terminus of the N-methyl-D-aspartate receptor: effects of spermine, protons, and ifenprodil, and structural similarity to bacterial leucine/isoleucine/valine binding protein. *Mol Pharmacol* 55: 957-969, 1999.

Paoletti P, Perin-Dureau F, Fayyazuddin A, Le Goff A, Callebaut I, Neyton J. Molecular organization of a zinc binding n-terminal modulatory domain in a NMDA receptor subunit. *Neuron* 28: 911-925, 2000.

Paoletti P, Neyton J. NMDA receptor subunits: function and pharmacology. *Curr Opin Pharmacol* 7: 39-47, 2007.

Ren H, Honse Y, Karp BJ, Lipsky RH, Peoples RW. A site in the fourth membrane-associated domain of the N-methyl-D-aspartate receptor regulates desensitization and ion channel gating. *J Biol Chem* 278: 276-283, 2003.

Schorge S, Colquhoun D. Studies of NMDA receptor function and stoichiometry with truncated and tandem subunits. *J Neurosci* 23: 1151-1158, 2003.

Schuler T, Mesic I, Madry C, Bartholomaus I, Laube B. Formation of NR1/NR2 and NR1/NR3 heterodimers constitutes the initial step in N-methyl-D-aspartate receptor assembly. *J Biol Chem* 283: 37-46, 2008.

Sobolevsky AI, Rosconi MP, Gouaux E. X-ray structure, symmetry and mechanism of an AMPA-subtype glutamate receptor. *Nature* 2009.

Unterreitmeier S, Fuchs A, Schaffler T, Heym RG, Frishman D, Langosch D. Phenylalanine promotes interaction of transmembrane domains via GxxxG motifs. *J Mol Biol* 374: 705-718, 2007.

Wollmuth LP, Sobolevsky AI. Structure and gating of the glutamate receptor ion channel. *Trends Neurosci* 27: 321-328, 2004.

Yuan H, Erreger K, Dravid SM, Traynelis SF. Conserved structural and functional control of N-methyl-D-aspartate receptor gating by transmembrane domain M3. *J Biol Chem* 280: 29708-29716, 2005.

CHAPTER 6
GENERAL DISCUSSION

Molecular mechanism of partial agonism

Crystal structures and nuclear magnetic resonance (NMR) structures are often the only reliable source for structural information on peptides and proteins. We used crystal structures of iGluR LBDs to probe for the molecular mechanism of partial agonists. Crystal structures of GluN1 LBDs with agonists, partial agonists and antagonists suggested that agonists as well as partial agonists could induce a full closure of the clamshell-like LBD structure (Furukawa et al., 2003, Inanobe et al., 2005). However, antagonists stabilize the LBD in an open-conformation (Furukawa et al., 2003). We reasoned that although partial agonists could induce a full closure of the LBDs, the energetic more favorable state would be a partially closed-conformation. Therefore we used crystal structures and homology models of iGluR LBDs with different degrees of clamshell closure and conducted molecular docking experiments. This approach worked well for the GluN1 subunit, using the GluN1 crystal structures it was possible to predict the action of a ligand with 90% accuracy, when using GluN1 homology models the accuracy dropped to 50%. Despite this, docking experiments with GluA2 LBD crystal structures as well as with GluN2A and GluN3A LBD homology models did not give reliable results as most of the ligands docked into the closed-conformation. One possible explanation is that homology models are not suitable for docking experiments. Our results indicate that homology models can be used for docking experiments but one should not expect highly accurate results, though it is possible to identify basic principles or tendencies. Results from GluN1 LBD homology models indicate that the size of the ligand is important for its action but it was not possible to predict ligand actions as accurately as with the GluN1 LBD crystal structures. From our docking analyses we conclude that for the GluN1 subunit the size of the ligand mainly determines its action, thus agonists are small in size whereas partial agonists are generally larger in size. However, this does not seem to be valid for GluA2, Glun2A and GluN3A subunits. In these subunits the ligand binding pocket is larger compared to the ligand binding pocket in the GluN1 subunit. Thus, these subunits have to have another molecular mechanism to distinguish between agonists and partial agonists. We conducted these experiments under the assumption that the molecular mechanism of partial agonism is located within the LBD, however, we cannot exclude the possibility that

other parts of the receptor play an important role in this respect, which would mean that it is not possible to uncover the basic principle of partial agonism on isolated LBDs. We conclude:

I) The size of the ligand mainly determines its action (i.e. agonist, partial agonist, antagonist) in GluN1 but not GluA2, GluN2A or GluN3A subunits.

The LBD heterodimer interface is generally involved in receptor function

We conducted experiments using a reduced GluN1/GluN2 receptor model (i.e. NTD-lacking GluN1/GluN2 receptors) as the NTDs were shown to largely affect functional properties of NMDARs and thus the NTDs might also lead to a misinterpretation of the results. We introduced amino acid substitutions into the LBD heterodimer interface to disclose functional implications of this interface. The interface has been subdivided into three distinct sites (sites I-III) and mutations were introduced at all three sites. Using TEVC we characterized NTD-lacking GluN1/GluN2A and GluN1/GluN2B mutant receptors by determining apparent agonist affinities, extent of desensitization and maximal inducible currents. Our results indicate that the LBD heterodimer interface is generally involved in receptor function as we observed diverse and unspecific effects of the mutations. We were not able to assign specific functional roles to the distinct sites. However, one mutation at site III of the LBD heterodimer interface largely decreased maximal inducible currents in the receptor combinations analyzed. This effect could not be observed when full-length GluN1 subunits carrying the same mutation were expressed together with either full-length or NTD-lacking GluN2 subunits. It is not unclear in which way the GluN1-NTD but not the GluN2-NTD rescues receptor function or if the effect is based on reduced receptor expression, assembly or cell-surface trafficking. This question might be addressed by means of affinity purification of hexahistidyl-tagged subunits and subsequent SDS-PAGE or Blue Native PAGE. If the effect was truly based on e.g. assembly deficiency, this would indicate that the LBD heterodimer interface is involved in receptor assembly rather than receptor function. We conclude:

II) The LBD heterodimer interface in NMDARs is generally involved in receptor function but might also be significant for receptor assembly.

Identification of an autoinhibitory domain in NMDARs

GluN1/GluN3A receptors are glycine-gated NMDARs with very low efficacy. In previous studies it was found that GluN1 antagonists or mutations within the GluN1 ligand-binding pocket potentiate glycine-induced currents ~25-fold (Madry et al., 2007a). These findings indicate that this receptor combination is constitutively inhibited. We constructed a model of the full-length GluN1/GluN3A receptor based on the GluA2-type AMPA receptor crystal structure by Sobolevsky et al. (2009) and we introduced amino acid mutations in the GluN1-GluN3A LBD heterodimer interface because we reasoned that interactions in this interface might account for the observed low efficacy. However, none of the LBD heterodimer mutations increased glycine-induced receptor currents. Thus, we focused on the NTDs and findings by Dr. Ivana Mesic from our lab showed that truncation of the GluN3A-NTD largely increase glycine-induced receptor currents. Hence, we analyzed homodimeric GluN3A-NTD-NTD interactions in our homology model, as it was shown for the GluA2-NTDs by Sobolevsky et al. (2009), and we selected residues in this NTD-NTD interface for amino acid substitutions. Previous studies also mentioned that the NTD-LBD linker in GluN1/GluN2 receptors is involved in receptor function (Yuan et al., 2009, Gielen et al., 2009). Therefore, we also selected residues in the GluN3A-NTD-LBD linker for amino acid substitutions. Further, we used secondary structure prediction algorithms implemented in online servers and also molecular dynamics simulation, which indicate that the NTD-LBD linker might adopt a α-helical conformation. The functional characterization of the aforementioned mutations showed that mutations in the GluN3A-NTD-NTD interface as well as in the GluN3A-NTD-LBD linker increase GluN1/GluN3A receptor efficacy. However, the greatest increase was observed for a GluN3A-NTD-LBD linker mutation. Because of its strategical position we reckon that the NTD-LBD linker and its secondary structure directly convey the modulatory action of the NTDs to the LBDs. In the case of GluN3A this modulatory action is inhibitory, thus representing an autoinhibitory domain (AID). We conclude:

III) The GluN3A-NTD represents an AID and the NTD-LBD linker adopts a α-helical secondary structure, which is pivotal for conveying modulatory signals from the NTD to the LBD.

The TM4 is an evolutionary addition to ensure ion channel function

Earlier reports have indicated that the TMDs of iGluRs are homologous to the KcsA-type potassium channel (Doyle et al., 1998, Wollmuth et al., 2004, Sobolevsky

et al., 2009). But a major difference between these two structures, i.e. KcsA channel and iGluR TMDs, is that the iGluR TMDs have a fourth membrane domain (TM4), which is not present in the KcsA channel (Wollmuth et al., 2004, Sobolevsky et al., 2009). We were interested in the functional implications of this additional membrane domain. Previously it was found, that the TM4 is required to mask ER retention signals present in the TM3s of GluN1 and GluN2B (Horak et al., 2008). Also it was found that coexpression of TM4-lacking subunits together with the TM4 fragment recovers receptor function as shown with GluN1/GluN2A receptors (Schorge and Colquhoun, 2003). Experimental data from Dip.Biol. Adriana Längle showed that the TM4 in GluN1/GluN3A receptors is not required for assembly, subunit stoichiometry or trafficking. Thus, we intended to specifically analyze TM4 interactions with the TM1 and TM3 of the neighboring subunit. Using a homology model of the tetrameric TMD of GluN1/GluN2A receptors, site-directed mutagenesis, TEVC and MI analysis we found that the TM4 is implicated in stabilizing the TMDs, which is required for proper ion channel function. We hypothesize that the TM4 was added to the TMD because of the ~7.35-fold increase in amino acid count for GluN1/GluN2A receptors compared to the KcsA channel. We conclude:

IV) The TM4 is an evolutionary addition to add stability to the TMDs and thus ensure ion channel function.

REFERENCES

Doyle DA, Morais Cabral J, Pfuetzner RA, Kuo A, Gulbis JM, Cohen SL, Chait BT, MacKinnon R. The structure of the potassium channel: molecular basis of K+ conduction and selectivity. *Science* 280: 69-77, 1998.

Furukawa H, Gouaux E. Mechanisms of activation, inhibition and specificity: crystal structures of the NMDA receptor NR1 ligand-binding core. *EMBO J* 22: 2873-2885, 2003.

Gielen M, Retchless BS, Mony L, Johnson JW, Paoletti P. Mechanism of differential control of NMDA receptor activity by NR2 subunits. *Nature* 2009.

Inanobe A, Furukawa H, Gouaux E. Mechanism of partial agonist action at the NR1 subunit of NMDA receptors. *Neuron* 47: 71-84, 2005.

Madry C, Mesic I, Bartholomaus I, Nicke A, Betz H, Laube B. Principal role of NR3 subunits in NR1/NR3 excitatory glycine receptor function. *Biochem Biophys Res Commun* 354: 102-108, 2007.

Schorge S, Colquhoun D. Studies of NMDA receptor function and stoichiometry with truncated and tandem subunits. *J Neurosci* 23: 1151-1158, 2003.

Wollmuth LP, Sobolevsky AI. Structure and gating of the glutamate receptor ion channel. *Trends Neurosci* 27: 321-328, 2004.

Yuan H, Hansen KB, Vance KM, Ogden KK, Traynelis SF. Control of NMDA receptor function by the NR2 subunit amino-terminal domain. *J Neurosci* 29: 12045-12058, 2009.

SUMMARY

Ionotropic glutamate receptors (iGluRs) are tetrameric ligand-gated ion channels that convey the majority of excitatory neurotransmission in the mammalian central nervous system. Members of the iGluR family are AMPA and kainate receptors as well as NMDA receptors. NMDA receptors are unique among the iGluRs due to the obligate heteromeric assembly and their particular roles for learning and memory formation but on the other hand NMDA receptor mediated excitotoxicity causes cell death in various pathophysiological conditions and neurodegenerative disorders. Conventional NMDA receptors are composed of two glycine binding Glun1 subunits and two glutamate binding GluN2 subunits. These receptors are also referred to as 'coincidence detectors' as for the activation a predepolarization of the postsynaptic membrane and ligand binding is required. Receptors composed of two glycine binding GluN1 and two glycine binding GluN3 subunits are referred to as 'excitatory glycine receptors'. Each iGluR subunit has a modular structure and it is hypothesized that each module/domain originates from a prokaryotic ancestral protein. The extracellular N-terminal domains (NTDs) are thought to form local heterodimers between GluN1 and GluN2 or GluN3 NTDs, additionally the GluN2- or GluN3-NTDs form a homodimeric contact. The ligand-binding domains (LBDs) of GluN1 and GluN2 or GluN3 subunits are arranged in a 'back-to-back' conformation forming the LBD heterodimer interface, which is subdivided into three distinct sites (sites I-III). This heterodimer interface has been previously implicated in receptor desensitization, weak interface interactions increase receptor desensitization. Upon ligand-binding, the S1 and S2 subdomains of the LBDs close in a 'venus-flytrap' like fashion. The transmembrane domains (TMDs) of iGluRs show homology to prokaryotic K^+ channels but iGluR TMDs have one transmembrane domain (TM4) more than the prokaryotic ion channel.

The aim of the work presented here was to analyze intra- and intersubunit interface interactions in the NTDs, LBDs and TMDs to determine their functional implications. To achieve this, *in vitro* and *in silico* methods were combined.

Molecular docking experiments and homology modelling were used to gain insight into the molecular mechanism of agonism, partial agonism and antagonism. The results indicate that for GluN1 subunits it is the size of the ligand that determines its action, i.e. agonists are small, partial agonists are slightly larger and antagonists

are large molecules. However, this could not be validated for GluA2-type AMPA receptor subunits, GluN2A or GluN3A subunits. Thus, the mechanism for partial agonism seems to be not conserved but subunit specific.

In order to gain insight into the role of the GluN1-GluN2 LBD heterodimer interface we analyzed the GluN1-GluN2A LBD crystal structure as well used the mutual information (MI) analysis to select amino acids for site-directed mutagenesis. The respective mutants were functionally characterized by two-electrode voltage-clamp on *Xenopus* oocytes. The results did not show specific effects of the mutations, hence it is not possible to imply one interaction site to one function. We conclude that the interface as a network of interactions is generally involved in receptor function. However, one mutation in site III largely decreased agonist-induced currents from NTD-lacking GluN1/GluN2 receptors. Whether this effect is caused by reduced subunit expression, receptor assembly or trafficking needs to be disclosed in further experiments.

Homology model based analysis and subsequent site-directed mutagenesis and functional characterization of GluN1/GluN3A receptors led to the identification of specific residues in the GluN3A-NTD that selectively increased the receptor efficacy. Thus, the GluN3A-NTD resembles the role of an autoinhibitory domain (AID), to our knowledge no AID has been described so far for ligand-gated ion channels.

In a last set of experiments we assessed interactions between the GluN1 TM4 and the TM1 and TM3 of the neighboring GluN2A subunit. Amino acid substitutions were selected based on our GluN1-GluN2A TMD model and functional characterization by TECV revealed two residues that almost completely abolished receptor function. We further used the MI analysis to probe for positions that are evolutionary interdependent and from the position of these correlations we inferred that the TM4 is mainly involved in stabilizing the TMD and thus ensuring proper ion channel function.

ZUSAMMENFASSUNG

Ionotrope Glutamatrezeptoren (iGluRs) sind tetramere liganden-gesteuerte Ionenkanäle, die im Zentralnervensystem von Säugern für den Großteil der exzitatorischen Signalweiterleitung verantwortlich sind. Zur iGluR Familie gehören die AMPA-, Kainat- und NMDA-Rezeptoren. Den NMDA-Rezeptoren wird eine besondere Rolle zugeschrieben, da sie obligate heteromere Komplexe bilden und eine besondere Rolle für das Lernen und die Gedächtnisbildung spielen. Andererseits sind sie auch an pathophysiologischen Vorgängen und neurodegenerativen Erkrankungen beteiligt, da NMDA-Rezeptor vermittelte Exzitotoxizität zum Zelltod führt. Konventionelle NMDA-Rezeptoren bestehen aus zwei Glyzin-bindenden GluN1-Untereinheiten (UEs) und zwei Glutamat-bindenen GluN2-UEs. Dieser Rezeptortyp wird auch als “Koinzidenz-Detektor” bezeichnet, da zusätzlich zur Ligandierung eine Vordepolarisation der postsynaptischen Membran notwendig ist. Rezeptoren, die aus zwei Glyzin-bindenden GluN1-UEs und zwei Glyzin-bindenden GluN3-UEs bestehen, werden als “exzitatorische Glyzin-Rezeptoren” bezeichnet. Jede iGluR-UE hat einen modularen Aufbau und es wird vermutet, dass jedes Modul bzw. jede Domäne von einem prokaryotischen Vorläuferprotein abstammt. Die extrazellulären N-terminalen Domänen (NTDs) bilden lokale Heterodimere zwischen GluN1- und GluN2- oder GluN3- NTDs, zusätzlich bilden die GluN2- oder GluN3-NTDs untereinander homodimere Kontakte. Die Ligandenbindedomänen (LBDs) der GluN1- und GluN2- oder GluN3-UEs sind in einer “Rücken-an-Rücken” Konformation angeordnet. Die Kontaktfläche zwischen den beiden LBDs wird in drei Kontaktstellen unterteilt (Kontaktstellen I-III). Diese Kontaktfläche wurde zuvor mit der Rezeptordesensitisierung in Verbindung gebracht, schwache Interaktionen an der Kontaktfläche würden demnach die Desensitisierung verstärken. Die Ligandenbindung führt dazu, dass die beiden Subdomänen der LBD, S1 und S2, sich in einem “Venus-Fliegenfallen” artigen Mechanismus schließen. Die Transmembranregionen (TMDs) der iGluRs zeigen Homologien zu prokaryotischen Kalium-Kanälen, aber sie unterscheiden sich vorallem darin, dass die TMDs von iGluRs eine vierte Membrandomäne (TM4) besitzen, die im Kalium-Kanal nicht vorhanden ist.

Das Ziel der vorliegenden Arbeit war es Kontaktflächen innerhalb einer Untereinheit und zwischen Untereinheiten in den NTDs, LBDs und TMDs zu

untersuchen, um die jeweilige Rolle für die Rezeptorfunktion besser zu verstehen. Hierfür wurden *in vitro* und *in silico* Methoden miteinander kombiniert.

Docking-Experimente mit Kristallstrukturen und Homologiemodellen wurden durchgeführt, um den Mechanismus des Agonismus, partiellen Agonismus und Antagonismus an NMDA-Rezeptoren besser zu verstehen. Die Ergebnisse zeigten, dass bei der GluN1-UE vorallem die Größe des Liganden seine Aktivität bestimmt. Demnach sind Agonisten immer kleine Moleküle, partielle Agonisten sind größer als Agonisten und Antagonisten sind große Moleküle. Dieses konnte aber nicht für die GluA2-UE der AMPARs oder für GluN2A- und GluN3A-UEs der NMDARs gezeigt werden. Wir schließen daraus, dass der zugrundeliegende Mechanismus für den partiellen Agonismus untereinheitenspezifisch ist.

Für die Untersuchung der Kontaktfläche zwischen den GluN1-GluN2 LBDs wurde die Kristallstruktur näher betrachtet und mit Hilfe der Transinformations-Analyse (TI) Aminosäuren für Substitutionsexperimente ausgesucht. Die daraus resultierenden mutierten Rezeptorkomplexe wurden funktionell mit der Zwei-Elektroden Spannungsklemme (TEVC) an *Xenopus* Oozyten charakterisiert. Die Ergebnisse ließen nicht auf spezielle Funktionen der drei Kontaktstellen schließen. Es erscheint wahrscheinlicher, dass die Kontaktfläche allgemein in der Rezeptorfunktion eingebunden ist. Eine Mutation jedoch an der Kontaktstelle III zeigte bei NTD-trunkierten GluN1/GluN2 Rezeptoren eine Erniedrigung des Agonisten-induzierten Stromes. Ob diese Mutation die Expression, Assemblierung oder Zelloberflächenexpression stört ist nicht bekannt und muss in zukünftigen Experimenten näher untersucht werden.

Homologiemodell-basierte Analyse gefolgt von Aminosäuresubstitution und funktioneller Charakterisierung von mutierten GluN1/GluN3A Rezeptoren, ermöglichte die Identifizierung von Aminosäureresten in der GluN3A-NTD, die spezifisch für die niedrige Effizienz von Glun1/GluN3A Rezeptoren verantwortlich sind. Daher kann der GluN3A-NTD die Rolle einer autoinhibitorischen Domäne (AID) zugeschrieben werden. Nach unseren Kenntnissen ist bisher noch keine AID für liganden-gesteuerte Ionenkanäle bekannt.

Letztlich wurden die Interaktionen zwischen der GluN1-TM4 und der TM1 und TM3 der GluN2A-UE untersucht. Aminosäurereste wurden aufgrund unseres Homologiemodells für Aminosäuresubstitutionsexperimente ausgewählt und funktionell mit der TEVC untersucht. Hierbei wurden zwei Positionen in der GluN1-

TM4 identifiziert, deren Mutation zu nicht funktionellen Rezeptoren führte. Diese Positionen wurden weiter mit Hilfe der TI untersucht um evolutionär-abhängige Positionen in der TMD zu identifizieren. Anhand der Position dieser gefundenen Korrelationen lässt sich schlußfolgern, dass die TM4 wichtig für die Stabilität der TMD ist und nur durch diese Stabilisierung kann eine normale Funktion des Ionenkanals sichergestellt werden.

APPENDIX

Author contributions

Chapter 1 – General introduction:
- Dipl.Bioinf. Ceyhun Tamer

Chapter 2 – *In silico* approach to determine the molecular action of ligand binding to NMDA receptor subunits:
- Dipl.Bioinf. Ceyhun Tamer

Chapter 3 – Role of heterodimer interface interactions in the ligand binding domain for NMDA receptor function:
- Dipl.Bioinf. Ceyhun Tamer

Chapter 4 – Generation of a high efficacy GluN1/GluN3A NMDA receptor:
- Dipl.Bioinf. Ceyhun Tamer
- Dr. Ivana Mesic (Site-directed mutagenesis of GluN3A-M332A, -H470A, -E498A and -H509D; Metabolic and surface labeling, affinity purification and SDS-PAGE, glycosylation assay and TEVC of GluN1/GluN3A receptors carrying GluN3A-M332A, -H470A, -E498A and -H509D mutations. Dr. Ivana Mesic provided Fig. 5 and data presented in Table 2.)

Chapter 5 - Intersubunit contacts in the transmembrane domain inolving TM4 determine receptor function but not assembly:
- Dipl.Bioinf. Ceyhun Tamer
- Dipl.Biol. Adriana Längle (Site-directed mutagenesis of GluN1-F817A, -I824A, -G827V, -E834 and GluN2A-F637A, -F641A; TEVC of GluN1/GluN2A receptors carrying GluN1-F817A, -I824A, -G827V, -E834 and GluN2A-F637A, -F641A mutations. Dipl.Biol. Adriana Längle provided data presented in Fig. 2 and Table 1.)

Chapter 6 – General discussion:
Dipl.Bioinf. Ceyhun Tamer

DANKSAGUNG

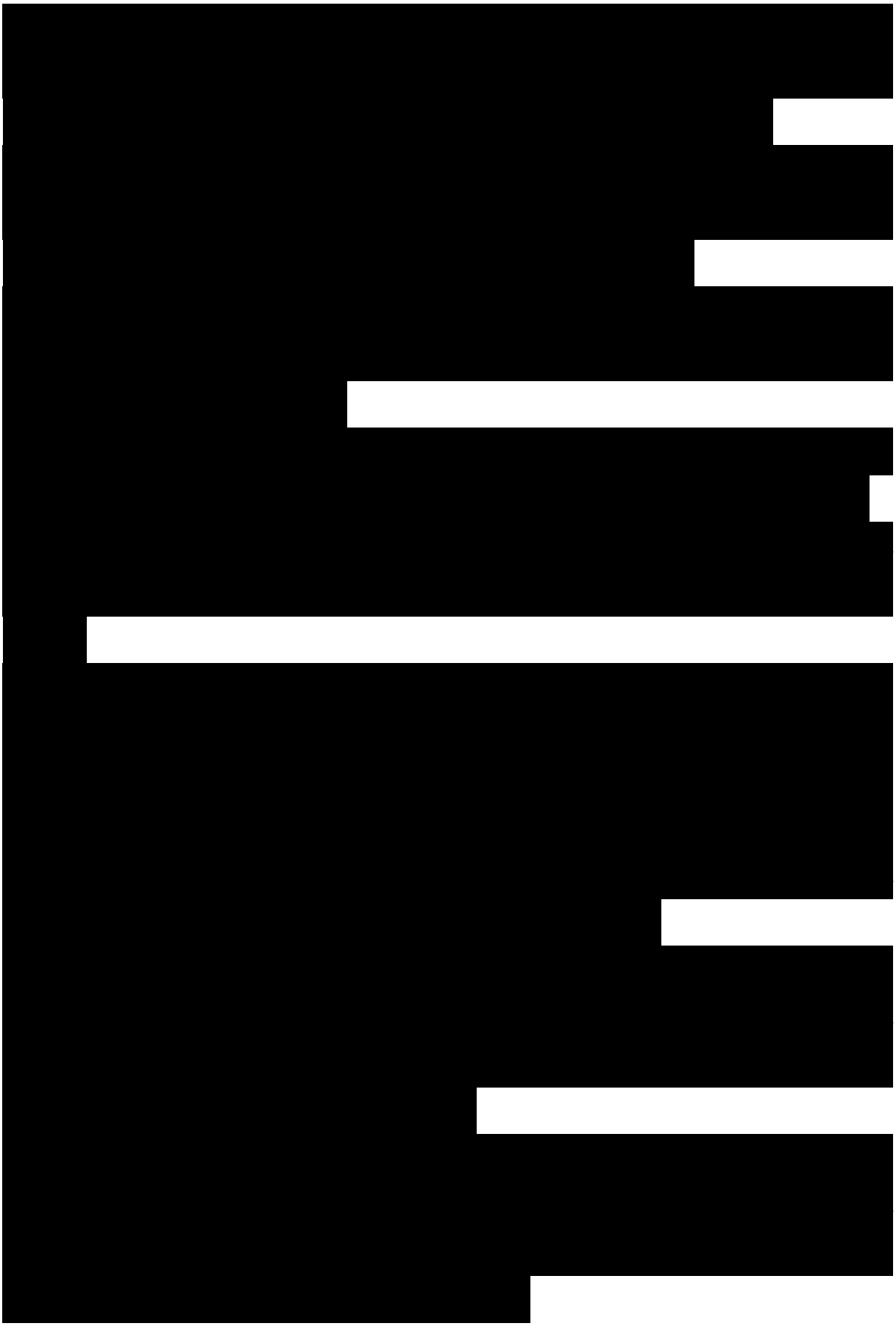

CURRICULUM VITAE

CEYHUN TAMER

,

KEY ACCOMPLISHMENTS

- Award of the very competitive EMBO (European Molecular Biology Organization) short-term fellowship for a 3-month project in the Neuroscience, Physiology and Pharmacology Department of the University College London, UK.
- Co-Authorship on a Nature Genetics Paper

  Endele, S., Rosenberger, G., Geider, K., Popp, B., **Tamer, C.**, Stefanova, I., Milh, M., Kortüm, F., Fritsch, A., Pientka, F.K., et al. (2010). *Mutations in GRIN2A and GRIN2B encoding regulatory subunits of NMDA receptors cause variable neurodevelopmental phenotypes.* (Issue 42, Pages 1021–1026)

ACADEMIC & RESEARCH EXPERIENCE

Goethe University, Frankfurt, Germany. 2005-06

- Teaching assistant for a course on 'discrete modelling' in computer science. Giving classes to students, reviewing papers and running a help-desk.
- Research assistant for the implementation of an online learning environment as well as the preparation of the appropriate topics that are required for the 'discrete modelling' course.

Max-Planck Institute for Brain Research, Frankfurt, Germany. 2006-08

- Intern in the neurochemistry department for 6 months. Induction into state-of-the-art wet-lab and bioinformatics techniques.
- Diploma student in the neurochemistry department for 9 months. Applying the acquired skills from the internship to do research on proteins in the central nervous system.
- Presenting my research findings with a scientific poster at the Max-Planck Institute for Brain Research Symposium.

Technical University of Darmstadt, Darmstadt, Germany. 2008-10

- Presenting my research findings with a scientific poster at the 2nd European Synapse Meeting in Göttingen, Germany.
- Scholar of the German Neurological Society for presenting my research findings with a scientific poster at the annual meeting of the Society for Neuroscience in San Diego, CA, USA.

University College London, London, UK. 2010-11

- EMBO (European Molecular Biology Organization) fellow for a 3-month project in the Neuroscience, Physiology and Pharmacology Department. Learning state-of-the-art electrophysiology techniques for the analysis of single proteins. As well sharing my bioinformatics expertise with colleagues to support their research.

EDUCATION

Goethe University (2002-08) Frankfurt, Germany
- German diploma (1.4), Bioinformatics

Technical University of Darmstadt (2008-12) Darmstadt, Germany
- Doctorate Neuroscience

TRAININGS

- Scientific writing; In-House training at the Technical University of Darmstadt.
- Time- and Self-Management, Training by 'Schmeink Consulting', Darmstadt, Germany.
- Confident presentation; Training by 'uni-support', Düsseldorf, Germany.

PUBLICATIONS

- **Tamer, C.**, Mathias-Costa, B., Mesic, I., Madry, C., Betz, H., Laube, B. (2007).
  Distinct Role of Intersubunit Interaction Sites in NR1-NR2A and NR1-NR2B Subunits Containing NMDA Receptors.
  Scientific poster at the Max-Planck Institute for Brain Research Symposium.
- **Tamer, C.**, Mathias-Costa, B., Kleisinger, P., Mesic, I., Betz, H., Laube, B. (2009).
  Ligand-binding domain interface interactions of NMDAR subunits are crucial for receptor assembly.
  Scientific poster at the 2nd European Synapse Meeting, Göttingen, Germany.
- Laube, B., Betz, H. (2009).
  Die duale Rolle des Neurotransmitters Glyzin im zentralen Nervensystem.
  Preparation of figures for the research report of the Max-Planck Society.
  http://www.mpg.de/312638/forschungsSchwerpunkt1?force_lang=de&l=report
- Endele, S., Rosenberger, G., Geider, K., Popp, B., **Tamer, C.**, Stefanova, I., Milh, M., Kortüm, F., Fritsch, A., Pientka, F.K., et al. (2010).
  Mutations in GRIN2A and GRIN2B encoding regulatory subunits of NMDA receptors cause variable neurodevelopmental phenotypes.
  Scientific paper in Nature Genetics (Issue 42, Pages 1021–1026).
- **Tamer, C.**, Mathias-Costa, B., Binder, E., Betz, H., Laube, B. (2010).
  Assessing the role of N-terminal domains and ligand-binding domain dimer interface mutations for the degree of desensitization in NMDA-receptors.
  Scientific poster at the Society for Neuroscience Meeting 2010 in San Diego, CA, USA.

AFFIDAVIT

Herewith I declare, that I prepared the Doctoral thesis

„ROLE OF INTERDOMAIN AND INTERSUBUNIT CONTACTS FOR NMDA RECEPTOR FUNCTION“

on my own and with no other sources and aids than quoted. This thesis has not been submitted to any other examination authority in its current or an altered form, and it has not been published.

Darmstadt, 29. June 2012

_____

Dipl.Bioinf. Ceyhun Tamer

EIDESSTATTLICHE ERKLÄRUNG

Ich erkläre hiermit an Eides statt, dass ich die vorliegende Dissertation

„ROLE OF INTERDOMAIN AND INTERSUBUNIT CONTACTS FOR NMDA RECEPTOR FUNCTION“

selbständig und nur mit den angegebenen Hilfsmitteln angefertigt habe.
Ich habe bisher noch keinen Promotionsversuch unternommen.

Darmstadt, den 29. Juni 2012

_____

Dipl.Bioinf. Ceyhun Tamer